

**SYNOPTIC SCALE ICE-ATMOSPHERE INTERACTION
OFF THE EAST COAST OF CANADA**

Dennis Matthew Nazarenko

Department of Geography
McGill University, Montreal

A Thesis submitted in partial fulfillment of the
requirements for the degree of M.Sc.

© Dennis Nazarenko, 1990

Abstract

Seasonal ice cover off Canada's east coast was examined in relation to synoptic scale atmospheric events. Ice concentration information derived from Nimbus-7 scanning multichannel microwave radiometer (SMMR) measurements of surface brightness temperatures, supplemented by AES composite ice charts, provided timely coverage of the study area during the 1971/72, 1980/81 and 1984/85 ice seasons, 1971/72 and 1984/85 seasons with high ice concentrations and 1980/81 a season with low concentrations.

Atmospheric variability was monitored using the 850 hPa height at three upper air stations along the western edge of the study region. Additional information was drawn from storm track records, providing an indication of surface variability. Properties of specific storm events were obtained from the storm track data, permitting evaluation of the ice response to passing synoptic disturbances.

Results of this investigation indicate that, 1) passive microwave-derived ice information can be used to monitor high frequency variability in the marginal ice, 2) despite short time series, spectral relationships between ice concentration variability and 850 hPa pressure height indicate a strong association between the two at synoptic frequencies zone, and 3) variability in ice cover extent and concentration can be related to the passage of individual synoptic events.

Résumé

La variabilité saisonnière de la couverture de glace au large de la côte est du Canada a fait l'objet d'un examen par rapport aux mouvements atmosphériques à l'échelle synoptique. Les données sur la concentration des glaces venant des mesures radiométriques (radiomètre multicanal à hyperfréquences à balayage SMMR du Nimbus 7) des températures de brillance en surface, information complétée par les cartes composées des glaces du SEA, décrivent directement les conditions de la région étudiée pendant les saisons glacielles 1971-1972, 1980-1981 et 1984-1985.

Nous avons mesuré la variabilité atmosphérique en élévation 850 hPa en choisissant trois stations en altitude le long de la limite ouest de la zone d'étude. Des informations supplémentaires tirées des données d'observation des orages ont permis de juger de la variabilité en surface. Grâce à ces mêmes données d'observation, nous avons pu étudier les caractéristiques d'orages déterminés et ainsi évaluer la réaction des glaces aux perturbations synoptiques.

Voici ce qu'indiquent les résultats de l'étude : 1) on peut examiner la variabilité fréquentielle de la glace marginale à l'aide de données sur les glaces venant d'un système d'hyperfréquences passives; 2) malgré la brièveté des séries chronologiques, les rapports spectraux entre la variabilité de la concentration des glaces et l'élévation 850 hPa font voir une étroite association des deux éléments à l'échelle synoptique; 3) on peut lier la variabilité de l'étendue et de la concentration de la couverture de glace à des événements synoptiques particuliers.

Acknowledgements

The completion of this thesis came about with the assistance and support of many people to whom I owe many thanks.

I particularly appreciate the assistance of Dr. John E. Lewis, my supervisor, for his advice and guidance in organizing my thinking and directing my effort. Special thanks to David Lapp for providing access to a computer and laser printer. Thanks also to my colleagues, especially Dan Desrochers, Andrew Nadeau and Andrew Heyes, whose friendship was greatly appreciated during my time at McGill.

My good friend John Miller, although he may have questioned my sanity on announcing my academic intentions, made a point of asking for regular status reports and equally regularly reminded me of the dangers in losing one's momentum.

Most important, I appreciate the encouragement and patience of Donna, my wife, and Matthew, who was always confident that a time was coming when dad would finish his thesis. Their accommodation of, and participation in, my personal goals were especially important.

Table of Contents

	<u>Page</u>
Abstract	i
Resumé	ii
Acknowledgements	iii
Table of Contents	iv
List of Tables	vi
List of Figures	vii
Chapter 1 - Introduction	1
1.1 General Background	1
1.2 Present Study	2
1.3 Research Objectives/Hypotheses	4
Chapter 2 - Background Information	6
2.1 Classification of Synoptic Systems	6
2.2 Synoptic Scale Air-Ice Interaction	7
2.2.1 Synoptic Scale Ice Behaviour	8
2.3 Microwave Radiometry	9
2.3.1 Passive Microwave Theory	9
2.3.2 Satellite Systems	13
2.3.3 Applications to Sea Ice Analysis	15
2.4 Eastern Seaboard Environment	17
2.4.1 Atmospheric Conditions	17
2.4.2 Oceanography	22
2.4.3 Ice Regime	26
Chapter 3 - Ice and Meteorological Data Sets	32
3.1 General Background	32
3.2 Data Sources	32
3.2.1 Storm Track Data	32
3.2.2 Upper Air Data	34
3.2.3 SMMR Ice Concentrations	35
3.2.4 AES Ice Charts	37
3.2.5 SMMR/AES Ice Concentration Comparison	39
Chapter 4 - Sea Ice Time Series Analysis	42
4.1 Spectral Analysis	42
4.1.1 Confidence Limits on the Variance Spectrum	43
4.2 Data Preparation	44

4.2.1	Seasonal Adjustment	46
4.2.2	Band Filtering	49
4.3	Data Analysis	55
4.3.1	Ice Concentration Changes	55
4.3.2	Upper Air Dynamics	63
4.3.3	Storm Track Pressure Variability	64
4.3.4	Ice/Atmosphere Cross Spectral Relationships	68
 Chapter 5 - Ice Concentration Variation with Storm Events		76
5.1	Storm Classification	76
5.2	Ice Maps	80
5.3	Evaluation of Ice Cover Response	81
5.3.1	Ice Cover Dynamics	81
5.3.2	Correlation of Ice Cover Dynamics with Storm Events . . .	91
 Chapter 6 - Conclusions		96
 Bibliography		100
 Appendix A - SMMR Concentration Changes		111
Appendix B - SMMR Concentration Changes 60-70°N		118
Appendix C - Selected Synoptic Events and Dates of Corresponding Ice Information		125
Appendix D - Ice Maps		127

List of Tables

<u>No.</u>	<u>Title</u>	<u>Page</u>
3.1	Annual summary of storms passing through the study area (October 1 through July 31)	34
3.2	Deviation between SMMR-derived ice edge and ice reconnaissance observations	40
4.1	Mean seasonal cell counts by change level	46
4.2	Statistical comparison between raw and interpolated storm pressures . . .	66
4.3	Ice Concentration/ 850 hPa Height Cross Spectral Relationship	73
5.1	Storm classification parameters	77
5.2	Distribution of storm events by category	78
5.3	Statistical summary of selected storms	79
5.4	Ice concentration changes and edge movement for selected storms	88
5.5	Results of regression analysis of ice edge movement on concentration change	90
5.6	Multiple regression of storm variables on ice concentration and edge movement	93

List of Figures

<u>No.</u>	<u>Title</u>	<u>Page</u>
2.1	Atmospheric transmission characteristics in the microwave region	12
2.2	Horizontally and vertically polarized emissivities at various frequencies for open water, first year ice and multi-year ice	16
2.3	East coast study area	18
2.4	Seasonal variation in sea level pressure over the eastern Atlantic	20
2.5	Mean east coast storm tracks and storm count for selected months	21
2.6	Monthly variation in Grand Banks water temperature and salinity	23
2.7	Estimated Labrador Sea Sverdrup mass transport	25
2.8	Current regime on the Grand Banks	27
2.9	Extremes in maximum ice extent position (1973-1985)	28
2.10	Typical ice characteristics near the ice margin	30
3.1	Temporal variation in SMMR footprints through the study area	38
4.1	Time series of 1980/81 ice concentration increases and decreases	47
4.2	Time series of 1984/85 ice concentration increases and decreases	48
4.3	Comparison of raw and seasonally adjusted 1980/81 concentration decreases $\geq 3/10$	50
4.4	Unfiltered power spectrum for 1980/81 concentration decreases $\geq 3/10$	51
4.5	Power spectra for footprint counts for the 1980/81 and 1984/85 seasons	52
4.6	Comparison of footprint power spectra before and after band filtering	54
4.7	Autocorrelations for 1980/81 ice concentration increases and decreases	56
4.8	Autocorrelations for 1984/85 ice concentration increases and decreases	57
4.9	Power spectra for 1980/81 ice concentration change time series	59
4.10	Power spectra for 1984/85 ice concentration change time series	60
4.11	Power spectra for ice concentration change time series within the 60-70° latitudinal band	62
4.12	1980/81 and 1984/85 power spectra of 850 hPa height for St. John's, Goose Bay and Iqaluit	65
4.13	Comparison between raw and interpolated surface pressures based on storm data	67
4.14	Autocorrelations and spectra for 1980/81 and 1984/85 surface pressures	69
4.15	Cross spectra, coherence and phase plots comparing region ice concentration change and 850 hPa height at St. John's	70
4.16	Cross spectra, coherence and phase plots comparing region ice concentration change and 850 hPa height at Goose Bay	71
4.17	Cross spectra, coherence and phase plots comparing region ice concentration change and 850 hPa height at Iqaluit	72
5.1	Generalized stages of ice cover development	83
5.2	Example of ice dynamics during early to mid-season - Storm 80-3	84
5.3	Example of ice dynamics during mid-season - Storm 85-2	85
5.4	Example of ice dynamics during late season - Storm 72-5	86
5.5	Scatter plot showing concentration increase vs. edge advance and concentration decrease vs. edge retreat with least squares fit	89

Chapter 1

INTRODUCTION

1.1 General Background

The interaction between atmosphere and ocean is complex - made even more so by the presence of sea ice. On a global scale, sea ice plays a significant role in the climate system as both agent and product of atmospheric and oceanic variability. A key factor influencing the interaction of sea ice with the atmosphere and the oceans is its variation in character and extent over several time scales.

In the Arctic, annual sea ice variations in areal extent range from approximately $8 \cdot 10^6$ km² in summer to $14 \cdot 10^6$ km² in winter (Walsh and Johnson, 1979) at which time the ice cover extent is equivalent to approximately half the area of North America. This virtual twofold variation in the Northern Hemisphere sea ice cover represents a sizeable change in the amount of ocean surface directly exposed to the atmosphere. As an interface between the ocean and the atmosphere, the zone of seasonal ice at the polar ice cap periphery has a major impact on numerous interactive processes which take place between the two media. The ice margins have also been identified as important zones of biological productivity within the ocean.

In addition to the obvious seasonal fluctuations in the ice margin, within-season variations are also considerable. It has been noted by several authors (for example Pease, 1980; Carleton, 1984) that atmospheric events can have considerable influence over short term variations in sea ice character. This is particularly evident at the ice margin where passing storms may affect ice patterns significantly, frequently resulting

in rapid changes in ice conditions.

Furthermore, evidence suggests that in addition to being affected by atmospheric conditions, sea ice can exert a modifying effect on normative climatic patterns (Ackley and Keliher, 1976). McPhee (1983) identified several significant areas in which sea ice influences air-ocean interaction at the ice margin including modifications of momentum transfer from the atmosphere, alteration of the surface albedo and insulation of the ocean surface. In addition, the sea ice, being highly mobile in this region, represents a means by which low salinity, cold water can be advected rapidly over considerable distances in response to passing weather systems. Similarly, the character of the ocean can influence sea ice extent and concentration.

It seems clear that a bidirectional relationship exists between atmospheric conditions and sea ice character. In addition to seasonal variations, the effects of this relationship are evident over much shorter time scales. The Polar Group (1980) indicated that surface-atmosphere feedback processes appear to be accentuated at the ice margins, suggesting the need for further investigation of seasonal ice processes.

1.2 Present Study

The Canadian east coast marine environment is characterized by seasonal ice coverage extending from the northern portion of Baffin Bay to the Grand Banks of Newfoundland, within the Gulf of St. Lawrence and occasionally onto the Scotian Shelf. In many ways this seasonal ice zone typifies ice margins in general, however, ice coverage in this region is unique in that it represents the most extreme southern penetration of sea ice in the northern hemisphere.

The Canadian east coast offshore region, in addition to being an area of considerable seasonal ice development, is strongly influenced by synoptic atmospheric activity during the period when ice is present. The influence of both cyclonic and anticyclonic activity contributes, at least in part, to the extremely dynamic nature of the sea ice cover in this region.

The combination of an extensive seasonal ice zone with a high degree of synoptic-scale atmospheric activity suggests this is an important area for investigation of atmosphere-ice interaction. Previous work in this region (for example Crane, 1978; Jacobs and Newell, 1979) has served to classify synoptic regimes associated with different ice patterns or to focus on variations at seasonal scales. Barry *et al.* (1975) presented a synoptic climatology of the Baffin Bay area while Keen (1977) related ice clearing in the same region to air temperatures and, indirectly, to variations in cyclonic activity. Focusing on the eastern Canadian seaboard as a whole, Walker (1986) presented a climatological analysis of sea ice extent for the years 1973 to 1985, relating ice conditions to the mean position of the Icelandic Low, mean air temperature and sea surface temperature anomalies for the region.

Far less attention has been given to the time-varying dynamics of the relationship on synoptic scales, either temporal or spatial. For other seasonal ice zones, some effort has been made to study the dynamic nature of the ice-atmosphere interaction at these levels. Carleton (1984) investigated the effect of three individual passing synoptic events on sea ice conditions in the Beaufort and Chukchi Seas in 1976, while on an hemispheric scale, LeDrew (1980; 1983) studied cyclonic vorticity variations over the high Arctic in an attempt to identify energy transfer mechanisms

associated with synoptic development.

In the Southern Hemisphere, efforts have been made to relate the monthly ice edge position to latitudinal variations in storm track positioning (Carleton, 1983) and to cyclonic vorticity frequencies (Schwerdtfeger and Kachelhoffer, 1973). Andreas (1985) in analyzing heat and moisture advection over Antarctic sea ice, suggests the existence of a thermodynamic relationship between sea ice extent and synoptic-scale atmospheric conditions. Furthermore, he concludes that monthly mean wind data are insufficient for driving sea ice models in this region and that wind data at shorter time scales are needed.

1.3 Research Objectives/Hypothesis

The objective of this thesis is to investigate the dynamic relationship between synoptic atmospheric conditions and the seasonal sea ice cover along Canada's east coast. A regional study of the area is proposed, using three extreme sea ice seasons - 1971/72, 1980/81 and 1984/85. These three seasons will serve as the basis for investigation of the interaction between storm events and sea ice character. The 1971/72 and 1984/85 ice seasons were characterized by much greater than average areal coverage of sea ice, while in 1980/81, regional ice distributions were well below average (Mysak and Manak, 1989; Walker, 1986). In addition, these three years represent conditions of either early and rapid onset or delayed retreat of the ice season. The use of the three extreme seasons proposed for this thesis offers the possibility for observing ice-atmosphere interaction during seasons of both extensive and light seasonal ice cover.

As a basis for research, it is postulated that significant short-term and finer scale atmosphere-ice interaction occurs within the larger scale variability exhibited over seasonal time periods and hemispheric areas. In an attempt to verify this assertion, the following issues are considered:

- 1) Repeat satellite coverage can be used to investigate time dependent properties of the ice cover variability off Canada's east coast.
- 2) The frequency properties of the ice cover variability can be related to atmospheric variability.
- 3) The passage of a synoptic event over the ice pack results in significant convergence or divergence of the ice pack.
- 4) Pack ice convergence or divergence can be related to the type of synoptic event or to its path of travel relative to the ice pack as a feedback mechanism.

Chapter 2

BACKGROUND INFORMATION

2.1 Classification of Synoptic Systems

Briefly, synoptic climatology is concerned with the relationship between local weather conditions and broader atmospheric circulation (Barry and Perry, 1973). A major focus in this field has been toward the development of synoptic type categories. Traditional methods have utilized subjective classification procedures, however with increasing computing capabilities, there has been a growing move to the use of objective techniques (for example Overland and Heister, 1980; Yarnal, 1984).

Overland and Pease (1982) identify three approaches to the problem of synoptic variability generalization in their efforts to evaluate the interaction between atmospheric conditions and ice extent in the Bering Sea:

- a synoptic climatological approach where weather patterns are described as a function of the static sea level pressure distribution,
- a kinematic approach where weather maps are classified in terms of principal storm tracks, or
- a classification of sea level pressure variation.

In contrast to an area such as the Gulf of Alaska where a large proportion of synoptic features form and/or decay *in situ* or are persistent, the east coast of North America represents an area where storms show no strong locational preference. Based on this, Overland and Heister (1980) suggest the kinematic approach to be most suitable in this area.

The classification of principal storm tracks was the method followed in this

study. This approach has been used by others as well. The work by Howarth (1983) included a classification of storm track distributions. Keen (1977), in a slightly different manner, used the average number of summer days in Baffin Bay experiencing cyclonic or anticyclonic activity for two 9 year periods in analyzing ice variability, principally clearing dates.

2.2 Synoptic Scale Air-Ice Interaction

The analysis of time series or time history records in the atmospheric sciences is common and has proven useful in evaluation of sea ice variability as well. While much of this work has focused on temporal variability at scales on the order of months and years (for example Walsh and Johnson, 1979; Lemke *et al.*, 1980), some work has been directed at higher frequency variability. Notable among this work are studies of Antarctic ice cover fluctuations (Cavalieri and Parkinson, 1981; Cahalan and Chiu, 1986). Cahalan and Chiu in particular were concerned with synoptic-scale atmospheric forcing on sea ice and successfully utilized ESMR (Electrically Scanning Microwave Radiometer) data to evaluate space-time variability of the Antarctic marginal ice zone. Their findings indicate strong correlation between the spatial pattern and advection of sea ice anomalies and atmospheric sea level pressure. Parkinson and Gratz (1983) used three-day averaged ESMR data to monitor the growth and decay of ice cover in the Sea of Okhotsk between 1973 and 1976. Their qualitative evaluation focused on the interaction between an ice cover and the local oceanography in a protected basin but once again demonstrates the utility of satellite microwave-derived ice information in time history analysis. Crane (1983) has shown, using principal component analysis

techniques, for the Beaufort/Chukchi Sea area, ESMR brightness temperature variability can be related to sea level atmospheric pressure and temperature at synoptic scales.

2.2.1 Synoptic Scale Ice Behaviour

The Seasonal Sea Ice Zone is recognized as the most dynamic portion of the sea ice regime in either hemisphere, affected by forcing from a variety of meteorological and oceanographic factors. Investigations of ice-atmosphere interaction at synoptic scales indicate that wind velocity can have an important influence on sea ice limits over time scales of as little as one week (Einarson, 1972 in Barry, 1986; Carleton, 1984a).

Pease (1980) found evidence to indicate that the flux of ice from the Chukchi to Bering Sea could be related to synoptic events of 3-5 days duration. Pease's research indicated that the relationship between the two was especially strong during the ice growth period. In studying the relationship between cyclone variability and sea ice extent in the Antarctic, Howarth (1983), compared variability in cyclone frequency and sea ice extent, finding the interaction to be generally dynamic rather than thermodynamic.

In looking at interannual variability in the Labrador Sea, Ikeda *et al.* (1988) determined important factors to be low air temperature and strong winds. Both were significant in forcing oceanic heat flux, while alongshore wind stress was also important as a mechanical factor. From their modelled results, the correlation between ice and wind velocities exceeded 0.968 with a ratio of ice speed to wind speed of 0.155 at 6° to the right. This compares to Thorndike and Colony's (1982) results of 0.166 and 3°

to the right for free-drifting ice. Ikeda *et al.* suggest that in the Labrador Sea, the internal ice stress is minor beyond 50 km offshore.

Further, Carleton (1981) provides results indicating highly complex Antarctic ice-atmosphere interaction with non-linear feedbacks resulting in a range of synoptic responses. Carleton paid specific attention to the development of a large polynya in the Weddell Sea, the growth of which he concluded promoted regional increases in cyclogenesis.

Whether the strength of these feedback effects is sufficient to modify synoptic-scale atmospheric conditions remains a matter for attention. Howarth (1983) questioned whether the ice-ocean boundary was capable of inducing a baroclinic zone of sufficient strength or persistence to influence cyclonic behaviour. Work by LeDrew (1980;1983) in the Arctic, involves the evaluation of vertical velocities within the atmosphere. He used the total vertical velocity as an index of synoptic activity and by decomposing the total velocity into various contributing components produced results suggesting feedback linkages between the ice and atmosphere through thermal effects.

2.3 Microwave Radiometry

2.3.1 Passive Microwave Theory

As with all objects other than those possessing a temperature of absolute zero, the earth's surface radiates energy. An object that reflects none of the energy striking it, is known as a blackbody. The spectral brightness of a blackbody, according to Planck's radiation law, is described as:

$$B_r = \frac{2hf^3}{c^2} \frac{1}{e^{hf/kT} - 1}$$

where B_f = Blackbody spectral brightness, $\text{Wm}^{-2}\text{sr}^{-1}\text{Hz}^{-1}$

h = Planck's constant = 6.63×10^{-34} joules sec

f = frequency, Hz

k = Boltzmann's constant = 1.38×10^{-23} joule K^{-1}

T = absolute temperature, K

c = velocity of light = 3×10^8 m sec^{-1}

Integrating over all frequencies yields the objects total brightness, B . At a given temperature, T

$$B = T^4/\sigma, \text{ Wm}^{-2}\text{sr}^{-1}$$

which is known as the Stefan-Boltzmann law and where

$$\sigma = 5.673 \times 10^{-8} \text{ Wm}^{-2}\text{K}^{-4}\text{sr}^{-1}$$

is the Stefan-Boltzmann constant.

For low frequency emissions the Rayleigh-Jeans approximation provides a simpler means of calculating the spectral brightness (Ulaby *et al.*, 1981).

If $hf/kT \ll 1$ then

$$B_f = 2kT/\sigma^2.$$

Most objects do not however behave as blackbodies, emitting less energy than a blackbody of the same temperature. The brightness of a greybody relative to that of a blackbody at a given temperature is defined as its emissivity. Since the spectral brightness of a greybody is less than or equal to that of a blackbody by definition, its emissivity will be less than or equal to 1. Thus the brightness temperature, T_B is always less than or equal to its physical temperature.

The relationship of a material's physical temperature, T to its brightness

temperature T_B can be described as

$$\epsilon = T_B/T$$

where ϵ represents the object's emissivity, a measure of its fractional emission as compared to a true black body. The emissive properties of different surfaces vary with the surfaces's composition and physical structure.

An object's thermal emissions occur over a broad frequency spectrum. Numerous sensing devices have been developed to measure various portions of this spectrum in an attempt to monitor the earth's surface remotely. Within the spectrum of commonly sensed frequencies is a portion of radiative energy commonly referred to as microwave radiation. This encompasses emissions within the frequency band from approximately one gigahertz (GHz) to several hundred GHz or alternatively wavelengths from 30 to 0.1 centimetres.

Remote sensing at microwave frequencies has several attractions, stemming primarily from the fact that it offers an all-weather, day/night means of sensing the character of the earth's surface. Microwave signals are relatively free of atmospheric interference from clouds, particularly at the lower frequencies. Transmission characteristics of the atmosphere for the microwave portion of the spectrum are known (Figure 2.1), making it possible to identify optimal frequencies for specific studies. In addition, the availability of multi-channel information allows for the correction of atmospheric interference.

Passive microwave remote sensing implies the detection of radiant energy emitted from the surface of an object. This differs from active radiometry where a

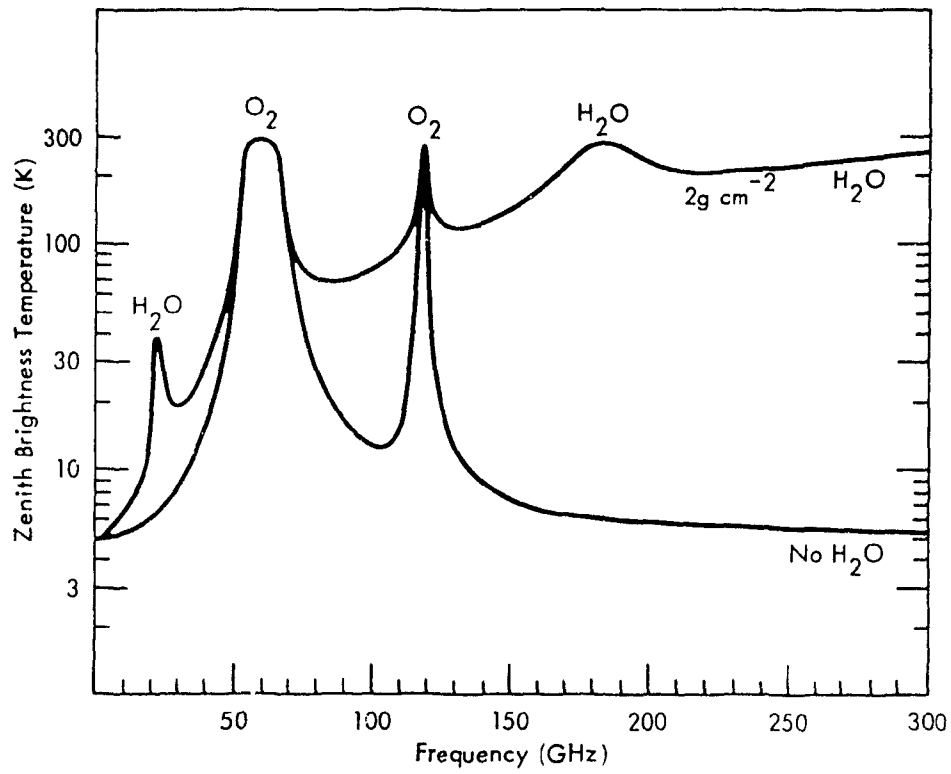


Figure 2.1 Atmospheric Transmission Characteristics in the Microwave Region Showing the Effect of Water Vapor (2g cm^{-2}) on Transmission
 (after Ulaby *et al.*, 1981)

signal is sent from the sensor and the return energy measured to determine frequency variations.

The energy received by a passive microwave sensor from space is a combination of contributions from the earth, atmosphere and space. The radiative transfer equation expresses the relationship of the various contributions to the sensed brightness temperature and can be shown as:

$$T_B = \epsilon T_s e^{-\tau} + T_{UP} + (1-\epsilon) T_{DOWN} e^{-\tau} + (1-\epsilon) T_{SP} e^{-2\tau} \quad (1)$$

where ϵ is the surface emissivity, T_s is the surface temperature, τ is the atmospheric opacity, T_{UP} is the atmospheric upwelling radiation, T_{DOWN} is the atmospheric downwelling and T_{SP} is the cosmic background radiation.

2.3.2 Satellite Systems

One of the past limitations of time-varying studies of this nature has been the lack of ice data on time scales coincident with the movement of synoptic weather events. The availability of passive microwave data within recent years has helped to alleviate this problem. Polar orbiting satellites offer regular coverage of the Canadian east coast. The passive microwave sensor provides more reliable coverage in that it remains an effective tool for obtaining surface information under a variety of weather conditions and does not require solar illumination of the surface. Even though the imagery has a coarser spatial resolution than other common systems (such as LANDSAT), it offers a means of acquiring information at the frequency and with the

reliability needed for a study of this type. In actual fact the 30-50 kilometre resolution may serve to mask some of the local variance which could not be attributed to synoptic-scale events.

Passive microwave sensors provide a measure of the microwave radiation emitted by an object or surface. These radiant emissions vary depending on the physical characteristics of the emitter. The strong radiative contrast between sea water and ice results from the distinction in their respective sensed brightness temperatures. Several algorithms have been developed which take advantage of this contrast and permit the derivation of ice type and concentration information from sensed brightness temperatures values (Cavalieri *et al.*, 1984; Swift *et al.*, 1985). The first satellite passive microwave sensor was part of the 1972 NIMBUS 5 launch. Termed an Electrically Scanning Microwave Radiometer (ESMR), this sensor was capable of detecting microwave radiation at a single 19.5 GHz (1.55 cm) frequency. This was followed by a second ESMR on NIMBUS 6, this time with a 37 GHz channel and dual polarization.

In October, 1978 a new sensor was launched on the NIMBUS 7 satellite which offered multichannel detection capability. The Scanning Multichannel Microwave Radiometer (SMMR) measured microwave emissions at five frequencies (6.7, 10.7, 18.0, 21.0 and 37.0 GHz) and at both vertical and horizontal polarization. At its highest frequency (37 GHz) the SMMR's footprint is 30 km., comparable to that of the ESMR. The multi-channel, dual-polarization was significant, providing the ability to discriminate among first year and multi-year ice and open water.

2.3.3 Applications To Sea Ice Analysis

All objects emit energy at microwave frequencies, their spectral signatures varying according to their emissive properties. The utility of this characteristic in interpreting sea ice conditions arises from the strong thermal microwave emission contrast between open water and ice. Figure 2.2 shows the relationship between emissivity and frequency for open water, first year ice and old ice as used by the NASA experimental team (Comiso, 1983). It can be seen that at a frequency of 19 GHz, the emissivity of first year ice and water are quite distinct with first year ice nearly a blackbody radiator. For low frequencies, the difference in emissive properties between ice types is not as distinct as at higher frequencies although at frequencies approaching 40 GHz the emissivities of multi-year ice and open water are similar. At 19 GHz, with horizontal polarization, the emissivity of sea water is approximately 0.4 while that of ice varies from 0.84 to 0.92 depending on ice type (Carsey, 1982). The differences in emissivity translate into a T_b difference of approximately 80-100 degrees Kelvin (K). This difference makes it possible to distinguish between open water and sea ice from a single frequency microwave signal such as that achieved with the initial ESMR system. Studies have demonstrated the application of scanning microwave radiometers in monitoring seasonal and regional fluctuations in Arctic sea ice extent (Campbell *et al.*, 1980; Comiso, 1983; Parkinson *et al.*, 1987).

While the early ESMR proved useful in determining ice/water boundaries, discrimination of different ice types was not possible. As a result of the ice type variation, accuracy of derived sea ice concentrations was limited to between 15 and 25% (Parkinson *et al.*, 1987). The multichannel SMMR, deployed in 1978 provided

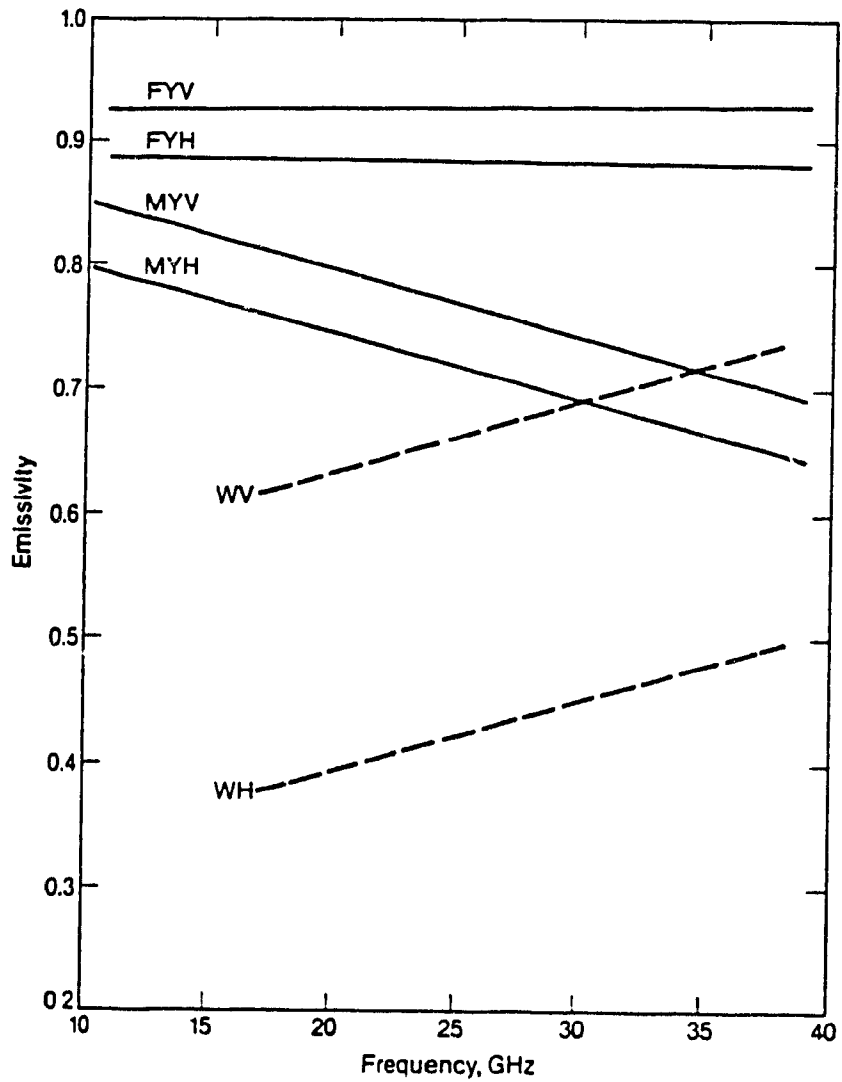


Figure 2.2 Horizontally and Vertically Polarized Emissivities at Various Frequencies for Open Water, First Year Ice and Multi-Year Ice (after Comiso, 1983)

a means for the differentiation of water, first year and multi year ice based on variations in their spectral signatures. It was data from this second generation microwave sensor which was used in this study. A more thorough description of this SMMR ice data is provided in Chapter 3.

2.4 Eastern Seaboard Environment

The portion of the Canadian east coast marine environment of concern in this study is shown in Figure 2.3, encompassing those portions of the eastern continental shelf and slopes from Davis Strait, along the Labrador coast and onto the Grand Banks. This extends from approximately 45°N to 70°N latitude. These regions represent an area of widely varying environmental considerations. The dynamics of this environment are experienced over broad spatial and temporal scales; one product of which is a highly varying ice regime.

The purpose of this section is to describe the environmental conditions most significant to the development and behaviour of the seasonal ice zone. Once presented, a summary of typical ice character and dynamics will be presented.

2.4.1 Atmospheric Conditions

The atmospheric circulation off Canada's east coast is strongly influenced by the seasonal position of the Icelandic Low pressure system. Normally, the low is deepest in winter and centred east of the southern tip of Greenland. Through spring the low weakens until summer when the lowest pressures are found closer to the east coast of Canada. As winter approaches again, the low deepens, the centre shifting

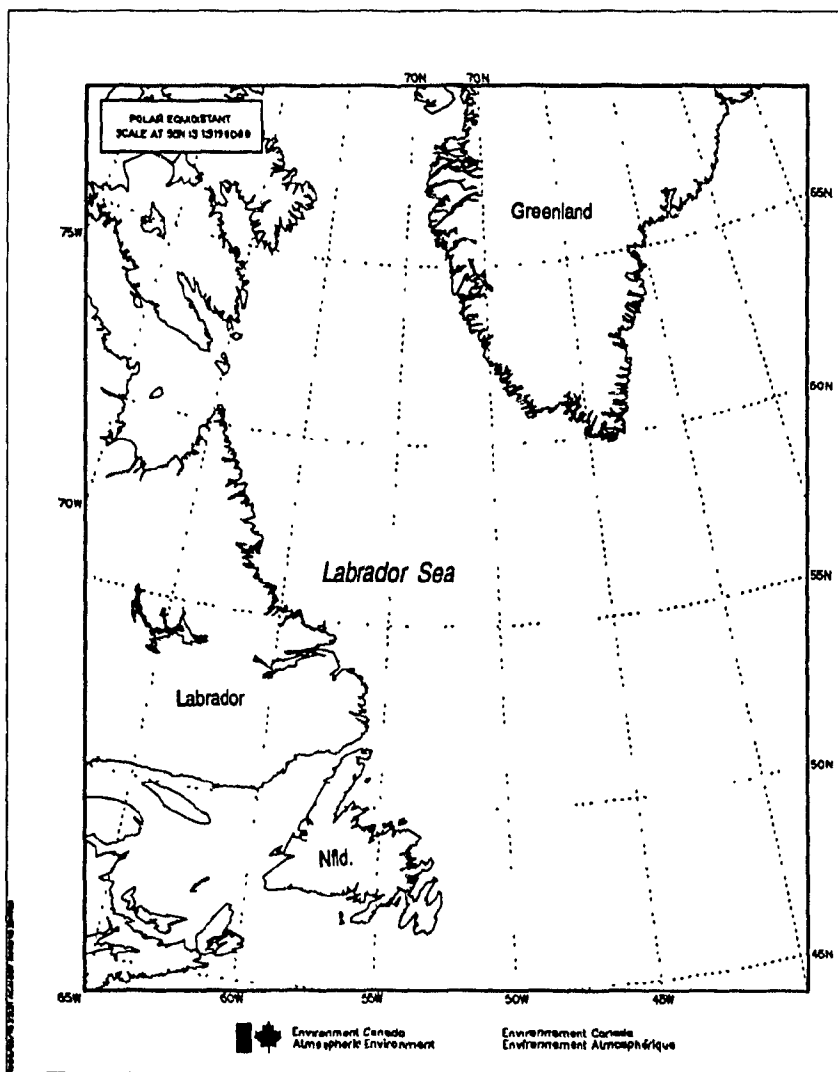


Figure 2.3 East Coast Study Area

eastward to complete the cycle. Figure 2.4 illustrates the seasonal variation in sea level pressure in the North Atlantic.

In response to large scale circulation patterns, synoptic activity through this region exhibits a noticeable summer/winter variation with more intense synoptic activity being felt during the winter months. In winter, systems tend to follow one of two main tracks through the region. One track generally follows a path from the Great Lakes Basin through the Gulf of St. Lawrence and the second, a path along the eastern seaboard coast from Cape Hattaras-Cape Cod area over Newfoundland and into the Labrador Sea. Figure 2.5 provides an indication of mean storm track positions for January, April, July and October as well as highlighting areas of cyclogenesis.

The numbers associated with the 10 degree grid squares in Figure 2.5 indicate the number of storms per square for the period May, 1965 to April, 1974.. During winter an average of approximately seven lows per month affect the Grand Banks area with progressively lower numbers of storms to the north. Many of the lows entering the Grand Banks/Labrador Sea area slow down and can persist in the area for up to two weeks (Burse *et al.*, 1977). Typical areal extent of these lows is on the order of 1000 km.

In summer, the storm tracks tend to pass much further north with an average of 5-6 cyclones per month per 10 degree square over the Labrador Sea. At this time the area of cyclogenesis is much larger, extending from the eastern seaboard through the Labrador Sea as far as the southern edge of Greenland. Despite a wider extent, the storms are generally weaker than those occurring during winter and also tend to exhibit less persistence in the area (Burse *et al.*, 1977).

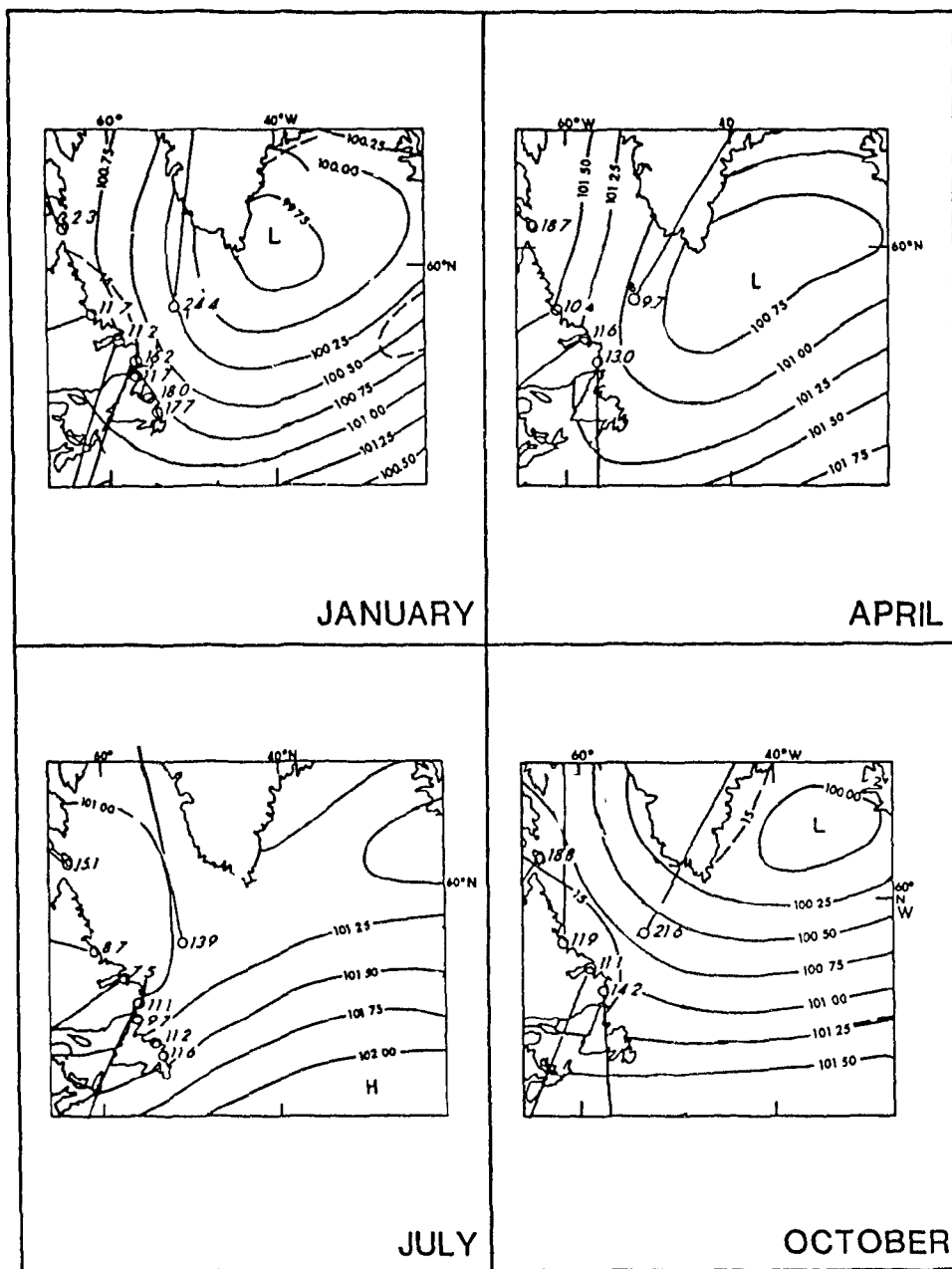


Figure 2.4 Seasonal Variation in Sea Level Pressure over the Eastern Atlantic (after Petro-Canada, 1981)

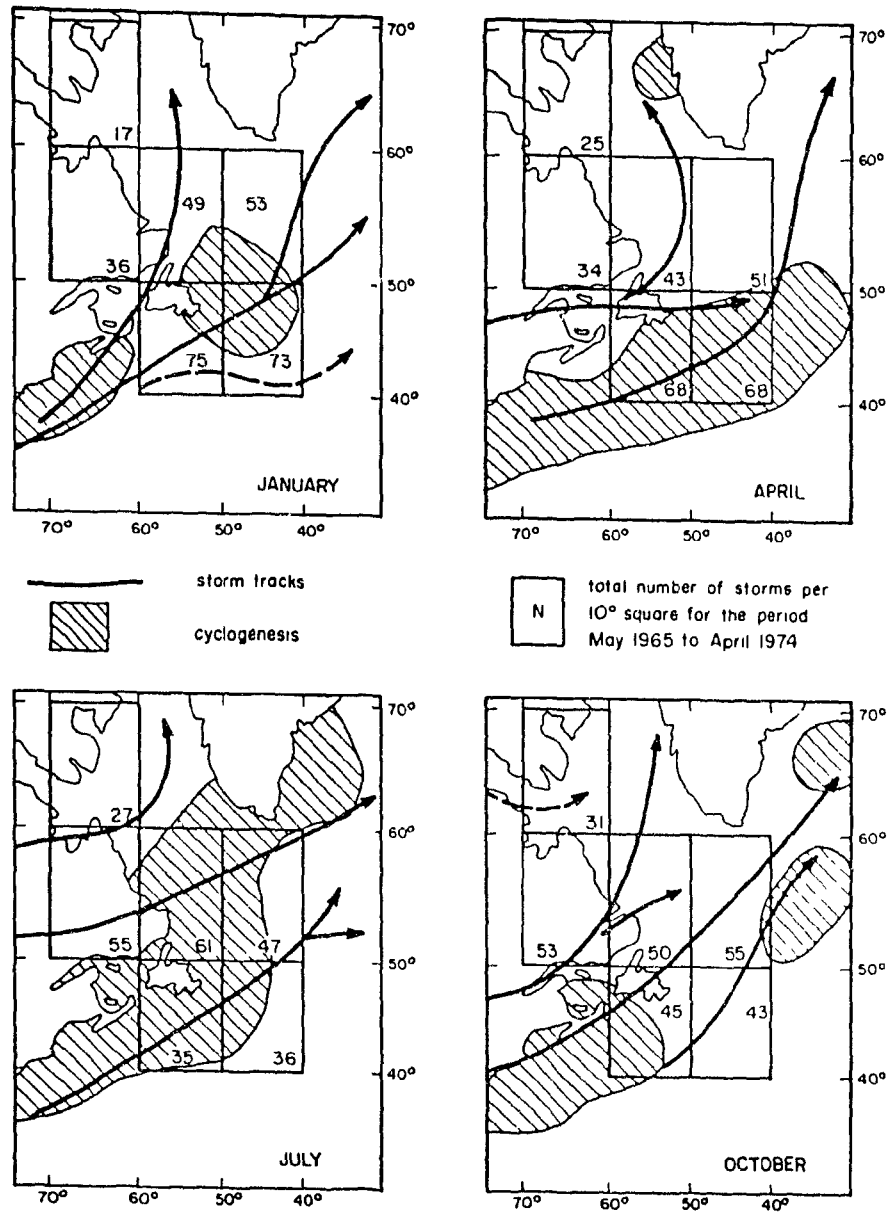


Figure 2.5 Mean East Coast Storm Tracks and Storm Count for Selected Months (after Petro-Canada, 1981)

2.4.2 Oceanography

The dominant feature of the ocean circulation in the Labrador Sea is a large cyclonic gyre, the coastward edge of which is the Labrador Current. The Labrador Current which flows along the coast from northwest to southeast is really two distinct streams which travel approximately on either side of a series of banks along the coastal shelf. The stream flowing along the outer edge of the banks and the continental slope is composed of water from the West Greenland Current while the inner branch comprises water from Hudson Strait and the Baffin Current.

This inner stream tends to flow along the inner portion of the shelf until it reaches the southern tip of Labrador where it divides in two with a portion flowing into the Gulf of St. Lawrence and the other along the coast of Newfoundland to the Grand Banks (Petro-Canada, 1982). On the Newfoundland Shelf, the Labrador Current remains the dominant factor in defining the water mass. As a result, water temperatures on the Grand Banks are colder and salinity lower than the nearby Atlantic Current and the Gulf Stream to the south. Figure 2.6 provides an indication of the seasonal variations in Grand Banks sea surface and 25m depth temperatures and salinity. It can be seen that the annual range in temperature is high. During the months when sea ice is most common the surface temperatures are lowest, near zero degrees and are largely isothermal.

Detailed knowledge of the ocean structure in the Labrador Sea is limited, with virtually no winter and spring data available. On the Grand Banks with the reduced ice severity, it has been possible to monitor ocean currents more extensively with the result that, when compared to the Labrador Sea, more is known of the current regime

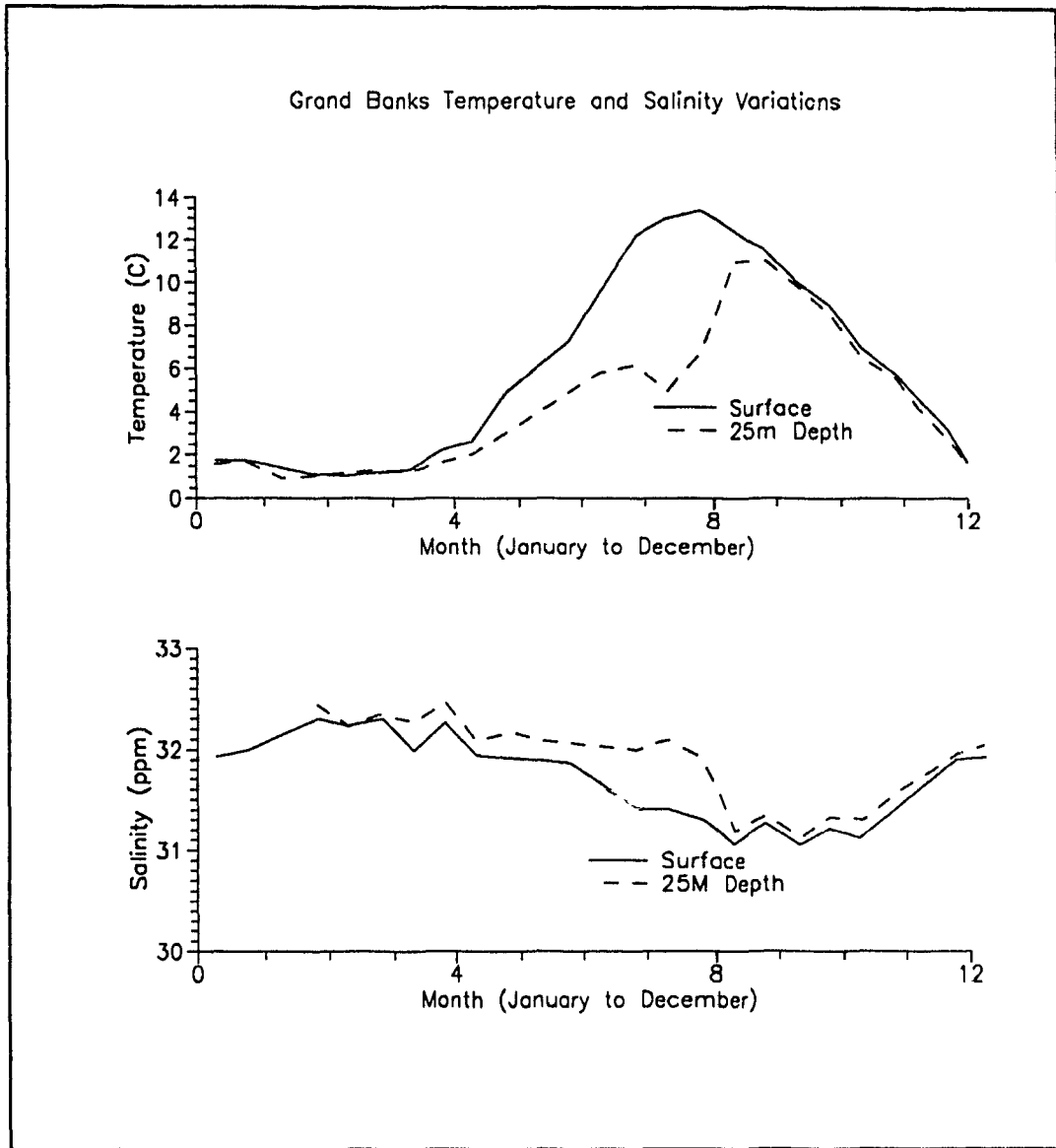


Figure 2.6 Monthly Variation in Grand Banks Water Temperature and Salinity (after Petro-Canada, 1981)

and the physical oceanography in general.

Information concerning the Labrador current structure has been deduced from geostrophic current calculations and inferred from iceberg drift observations. In general, the outer stream in the Labrador Sea is swifter than the inshore branch. Over the banks the currents are significantly weaker and exhibit greater variability. Figure 2.7 provides an estimate of mass transport (units - $10^6\text{m}^3\text{s}^{-1}$) over the shelf based on geostrophic calculations from water density measurements (Keely, 1979). While the numbers are coarse they do indicate that the inner stream transport along the Labrador coast is one quarter to one half that of the outer stream. Direct current measurements have been made since the early 1970's, but as noted earlier, they have a bias towards the ice free season. Based on the available data, Symonds (1986) estimates mean current speeds of 0.30m/sec for the outer branch of the Labrador Current and 0.15m/sec for the inner branch.

While current profile data is limited, it does indicate a distinct shift in current direction, magnitude or both above the thermocline. Seaconsult (1980), as noted by Petro-Canada (1982) postulates that this distinction in current behaviour about the thermocline can be attributed to the effects of the wind and tidal forces above the thermocline while those below are the result of tidal and residual flows.

On the Grand Banks, the current regime is once again dominated by the Labrador Current, with influences of the Gulf Stream felt along the southern and eastern edges of the banks (Figure 2.8). The actual area of interaction between the two currents is highly variable.

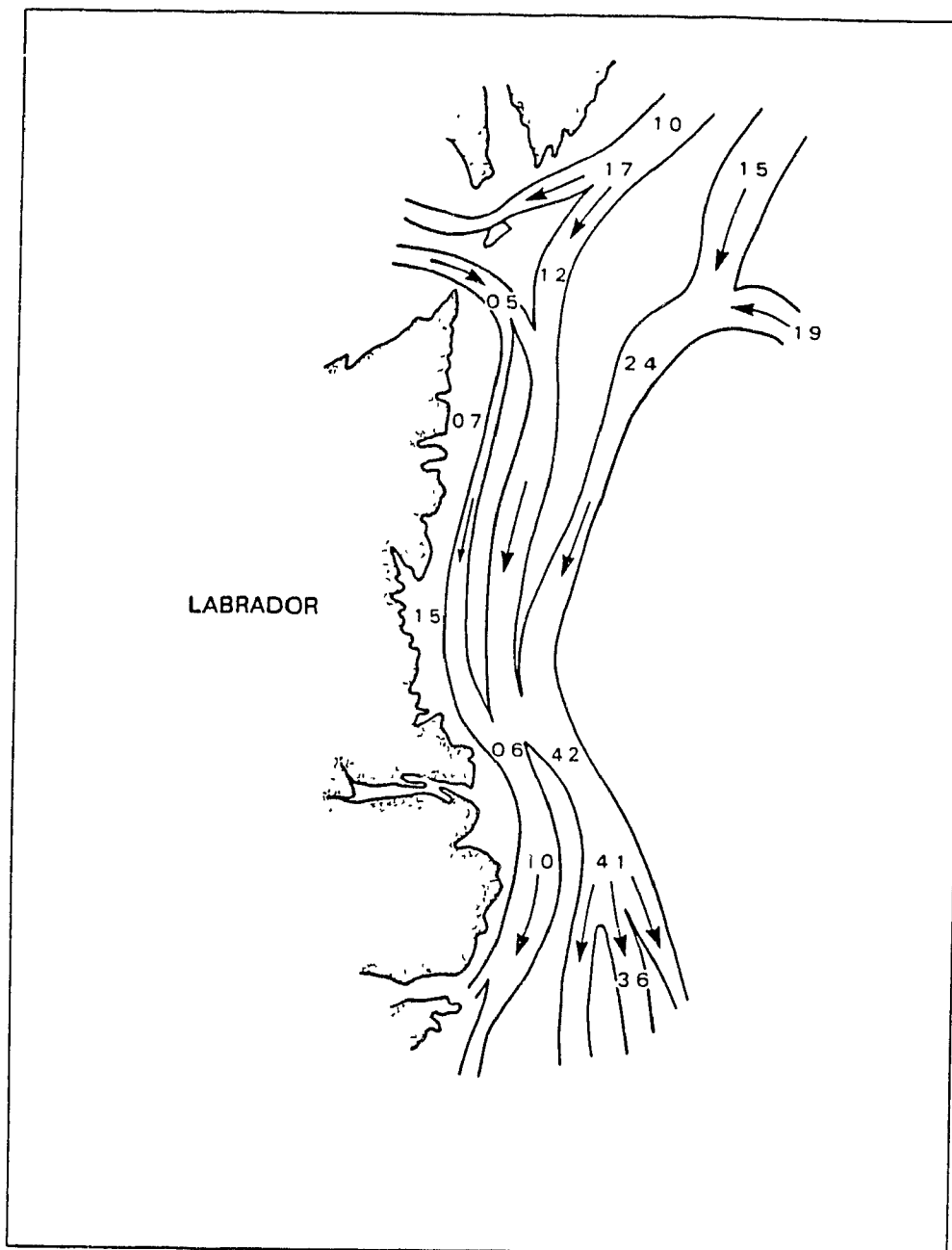


Figure 2.7 Estimated Labrador Sea Sverdrup Mass Transport - units of $10^6 \text{ m}^3 \text{ s}^{-1}$ (after, Petro-Canada, 1981)

As the Labrador Current approaches the Northeastern Newfoundland Shelf it moves into the Avalon Channel where it splits into three main streams. One part closely follows the Newfoundland coast flowing south and then west towards the Gulf of St. Lawrence. A second branch passes over the banks and a third flows along the northern and eastern edges of the banks. As seen in Figure 2.8, the flow over the banks is weaker and more variable than that on either side. It is considered to be primarily wind and tide driven rather than the result of density gradient as is generally the case for the Labrador Current.

2.4.3 Ice Regime

As the term seasonal sea ice zone implies, ice is not a year round phenomenon in the study area. The ice season normally begins in early November with the formation of new ice along the coast of Baffin Island (Crane, 1978). As temperatures drop, ice growth increases and begins to occur at progressively more southern latitudes. The southern limit of the ice edge is reached somewhere off the coast of Newfoundland but exhibits considerable interannual variability as seen in Figure 2.9 which shows the maximum and minimum ice limits observed between 1973 and 1985.

Most of the sea ice occurring near the southern limits (normally at the north edge of the Grand Banks) has its origin at more northerly latitudes (Symonds, 1986), being advected south under the influence of the Labrador Current and the prevailing winds. In general, sea ice occurrence on the Grand Banks is limited to the January to April period. In the median year, the maximum ice extent occurs in March. At that time it reaches south as far as approximately 47°30'N on the Banks proper with

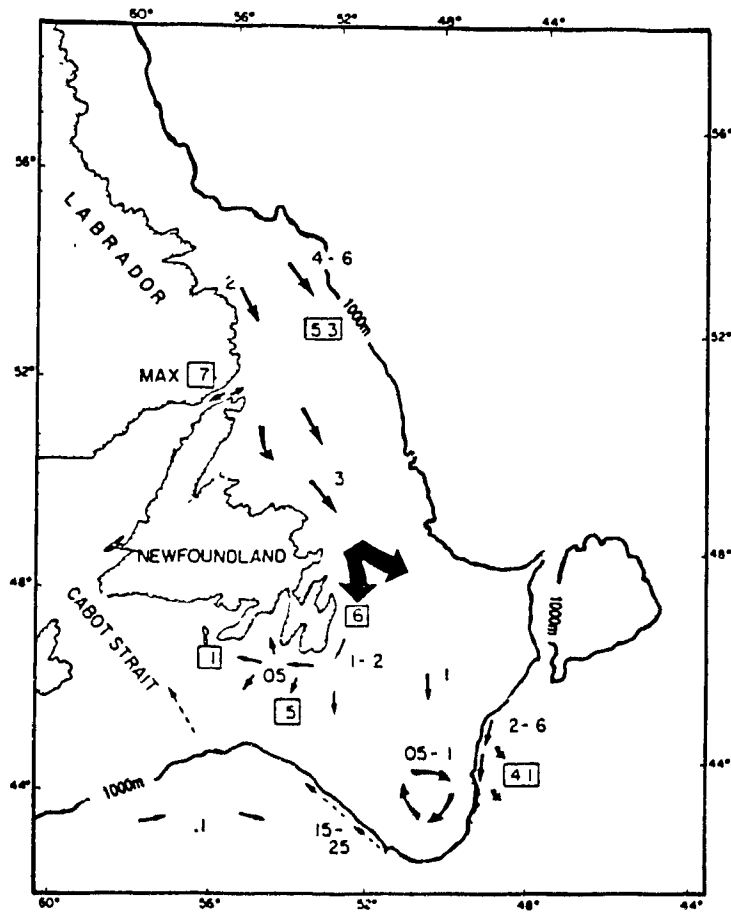


Figure 2.8 Current Regime on the Grand Banks
 Velocity in m/s, Boxes - Transport in units of $10^6 \text{m}^3 \text{s}^{-1}$
 (after Petrie and Anderson, 1983)

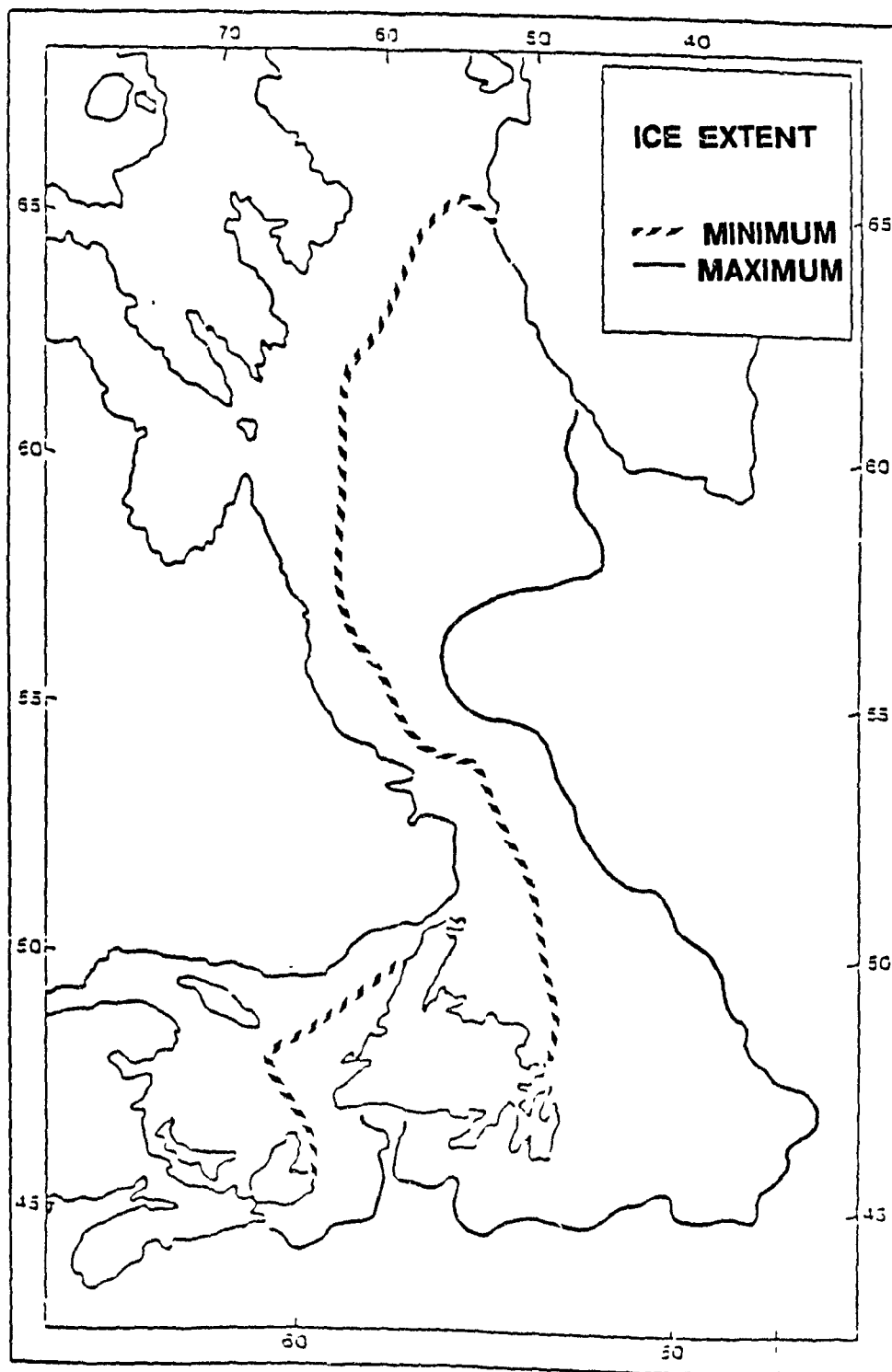


Figure 2.9 Extremes in Maximum Ice Extent Position - 1973-1985
(after Walker, 1986)

a tongue of ice being drawn further south along the eastern edge of the Banks by the Labrador Current (Nazarenko and Miller, 1986).

The physical characteristics of sea ice on the Grand Banks conform closely to typical marginal ice zone conditions (Figure 2.10) particularly in relation to floe size. Ice thicknesses may be higher as the ice advected south from the Labrador Sea has experienced more growth. Figure 2.10 illustrates the influence of mechanical degradation in this zone of the ice pack. Mechanical deterioration is largely attributed to wave energy imparted to the floating ice. During the winter months severe storms are common on the Grand Banks with mean significant wave heights are on the order of 2-4 meters (Petro-Canada, 1981). The resultant energy propagation has been observed for several tens of miles into the ice pack (Digby-Argus *et al.*, 1988).

The wave energy is transferred to the ice, with the large floes that have advected south quickly broken into smaller pieces. As a result, floe sizes near the ice edge are generally small - with an average diameter of 10-20 metres. Progressively greater surface area is exposed to the ocean as the floes are broken, leading to rapid thermal degradation of Grand Banks ice where the water is considerably warmer than the Labrador Current.

With net degradation of sea ice occurring near the ice edge, persistence of the ice pack at the ice limits is largely dependent on prevailing wind conditions (Symonds, 1986) which serve either to carry additional ice southward or force the ice edge north and shoreward.

Under certain climatic conditions *in situ* ice formation can also occur. An example of this was seen in February of 1985 when abnormally low air temperatures resulted in considerable new ice formation over large areas on the Banks. This ice

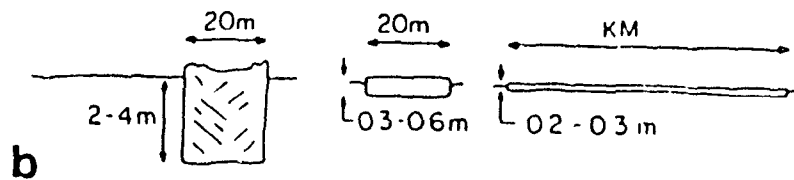
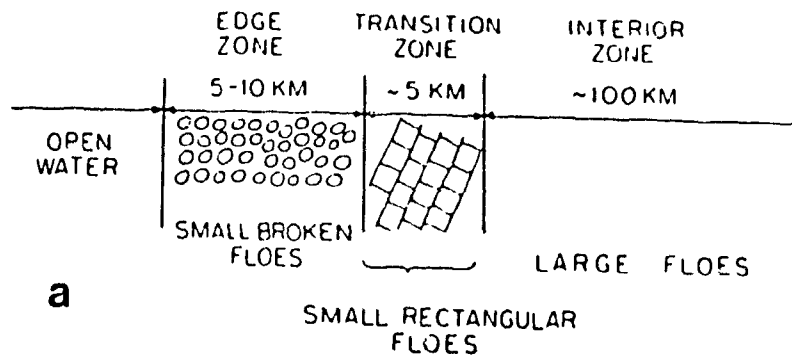


Figure 2.10 Typical Ice Characteristics near the Ice Margin (after Pease, 1980)

a - top view; b - side view

seldom develops beyond 15-30 centimetres in thickness although deformation in the form of local rafting may increase this to approximately one metre in some areas. By comparison, floes advected from more northerly regions generally have a thickness between 100 and 200 centimetres with local ridging and rafting to 3-5 metres (Burse *et al.*, 1977).

The dynamic nature of the ice near the pack edge is also important. As stated previously, ice is advected southward under the influence of the Labrador Current. However, frequent cyclonic disturbances passing through the area can produce significant ice displacements over short periods of time.

In modelling ice extent in the Labrador Sea, Ikeda *et al.* (1988) suggest the critical factors influencing ice extent were air temperature and wind velocity. These efforts are supported by empirical results which indicate a strong correlation between ice velocity variability and wind conditions (Nazarenko and Miller, 1986). Winds can influence both areal extent and near-edge ice pack concentrations, producing a highly concentrated pack with a sharply defined edge when winds are from off ice and the opposite when winds move from the ice to open water.

Chapter 3

ICE AND METEOROLOGICAL DATA SETS

3.1 General Background

The approach in evaluating synoptic-scale atmosphere/ice interaction was based on the empirical interpretation of ice conditions for three ice seasons. This entailed the analysis of coincident atmospheric data in the form of upper air records for coastal stations and storm track position and intensity records against sea ice cover information extracted from two principal sources: Atmospheric Environment Service (AES) ice charts and SMMR-derived ice concentration data.

Based on the questions considered in Chapter 1, the analysis followed two distinct streams. The first was concerned with the frequency analysis of ice cover variations in relation to coincident atmospheric variability. The second dealt with the interaction of unique synoptic events with the ice cover. The following discussion reviews the various data sets used, including comments regarding data errors and manipulation, and highlights the techniques utilized in the subsequent analysis.

3.2 Data Sources

3.2.1 Storm Track Data

AES has compiled pressure system track data from gridded surface pressure data. Storm track data, collected for each of the three ice seasons, were obtained using an AES climate information system known as SPASM (Surface-Pressure Analysis of System Movements) which permitted the tracking of storm centres through a

specified area providing storm centre location and pressure on a six hour basis. Storm tracks were documented for the November 1 to July 31 period, corresponding to the period of SMMR data.

Storm track records were extracted for a region centered on 55°N, 52°W to ensure that data for an area bounded by 40-70°N and 40-70°W could be studied. Using storms which tracked through the study area, basic storm pressure statistics were calculated for each of the three seasons. Additional statistics were calculated including horizontal storm velocity, the latitude and longitude at which the storm entered the study region, and the latitude at which it left and net storm bearing through the study area. The bearing was calculated based on the straight line orientation between the first and last observation within the study area. For each storm a tally was kept of the number of observations within the study area, providing an indication of the storm duration. With the exception of January 1981, the data set provides a continuous record of storms passing through the study area. Monthly variations in spatial distribution of storm centres were examined and found to be consistent with the climatological data described in Chapter 2.

Table 3.1 summarizes seasonal storm statistics. A note is made of the storm count for each season as well as for a subset where the number of observations was greater than one. The statistics generated are based on this subset. The information in Table 3.1 indicates that, on a seasonal basis, the storm regimes for the three seasons were comparable in virtually every respect including the number of storms observed, the average duration and intensity (as implied by the observed pressures) and spatial distribution (storm bearing, starting and ending latitude and starting longitude).

**Table 3.1 Annual Summary of Storms Passing Through
The Study Area (October 1 through July 31)**

Statistic	1971/72		1980/81		1984/85	
	Mean	S.D.	Mean	S.D.	Mean	S.D.
Number of Storms						
Number of Storms with >1 Obs	164		155		167	
	146		146		153	
Duration (Synoptic Obs)	5.8	3.9	6.5	4.3	6.0	4.2
Minimum Pressure (hPa)	993.6	12.9	992.6	12.9	993.8	13.0
Maximum Pressure (hPa)	1002.2	9.5	1001.2	10.2	1001.8	10.4
Mean Pressure (hPa)	997.7	10.6	996.5	11.1	997.6	11.3
Velocity (knots)	47.6	23.4	40.8	19.5	40.8	18.9
Start Latitude (*N)	51.7	9.0	52.8	8.8	52.2	8.7
End Latitude (*N)	55.2	8.1	55.6	8.6	53.5	11.3
Start Longitude (*W)	62.4	8.2	61.2	8.5	61.0	8.5

3.2.2 Upper Air Data

Three coastal principal meteorological stations provided upper air records for the study: St. John's, Newfoundland, Goose Bay, approximately midway along the Labrador coast and Iqaluit at the upper end of Frobisher Bay on Baffin Island. The upper air records provided twice-daily sampling of air pressure, altitude above sea level, temperature, relative humidity, wind direction and wind speed. The parameters of greatest interest were pressure level altitude and temperature. These were relatively

continuous for all stations, however where data gaps were encountered, they were corrected by means of linear interpolation between the last and next available record. Data gaps in the height series were seldom greater than one or two records, however the temperature series had several gaps of considerable length. Wind speed and direction were much less consistent, with data gaps for extended periods excluding the possibility of similar interpolation. From the standard levels included in the upper air record, the 850 hPa pressure level was selected as representative of the geostrophic flow for use in the time series analysis. Since the ice conditions derived from SMMR brightness temperatures were available once every two days, the upper air data were smoothed to provide a similar frequency interval. The resultant time series had 137 events on a two day interval from November 1 through the end of July the following year.

3.2.3 SMMR Ice Concentrations

Ice concentrations derived from the Nimbus 7 SMMR brightness temperature readings provided the basis for regular evaluation of ice conditions through the study area for the 1980/81 and 1984/85 ice seasons. While the SMMR instrument was originally designed to provide daily coverage of upper latitude regions, spacecraft power requirements were such that it was necessary to reduce the SMMR operation to every second day. Ice maps were therefore prepared on a bi-daily basis from November 1 to July 31, providing virtually complete coverage of the ice season within the study area.

Ice concentrations were calculated using an algorithm known as the AES/Phd

algorithm. A detailed description of the algorithm has been provided by others (Phd Associates, 1987; Williams, 1986). Briefly, the algorithm is based on the multispectral capabilities of the SMMR instrument, utilizing the 18 and 37 GHz (both horizontal and vertical polarization) brightness temperatures to calculate total ice concentration and first year and multi-year ice fractions. Since the signal received at the satellite is the product of both the original surface emission and attenuating atmospheric factors, a series of filters are employed to correct for signal contamination. The principle sources of atmospheric contamination are molecular oxygen, water vapour and liquid water droplets. The effect of each is frequency dependent with the latter being the most significant of the three at the frequencies utilized in this algorithm.

In addition to atmospheric effects, the combination of rough seas and atmospheric moisture has been found to yield a signal that can be interpreted as sea ice. As a result, the algorithm employs a series of filters near the ice edge to alleviate this problem.

The ice concentration data were retrieved from AES databases through CRISP (Climate Research in Ice Statistics Program). For each orbit date, the gridded ice concentrations corresponding to SMMR footprints were obtained for the study area. At each grid point total concentration was provided while for some points fractional information was also given indicating composite multi-year and first year ice concentrations. Only the total concentration was utilized in this study.

The polar orbit of the Nimbus-7 satellite affects the extent of overlap and hence coverage at a given latitude. The swath width of the SMMR instrument is 780 km with the result that grid point coverage was not uniform from one orbit to the next.

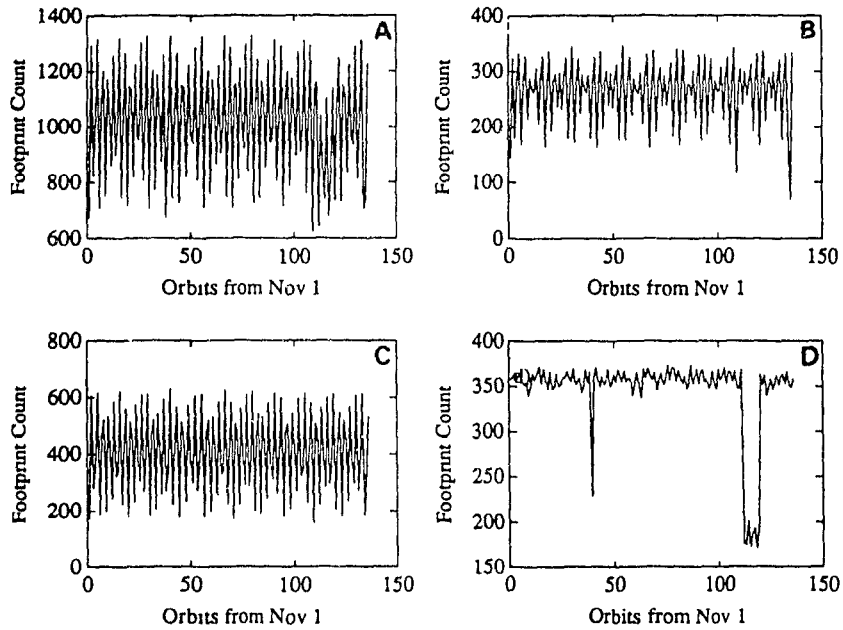
In Figure 3.1a the variability in grid point counts is clearly evident for both seasons. Figures 3.1b-d show the variability by 10 degree latitudinal band. It can be seen that the variability in grid point counts is smallest for the highest latitudinal bands as would be expected given the polar orbit of the Nimbus-7 satellite.

The gridded ice concentration data were used to interpolate a regularly spaced ice concentration grid from which ice distributions were mapped. These were then used for both the time series analysis and for the evaluation of individual storm events.

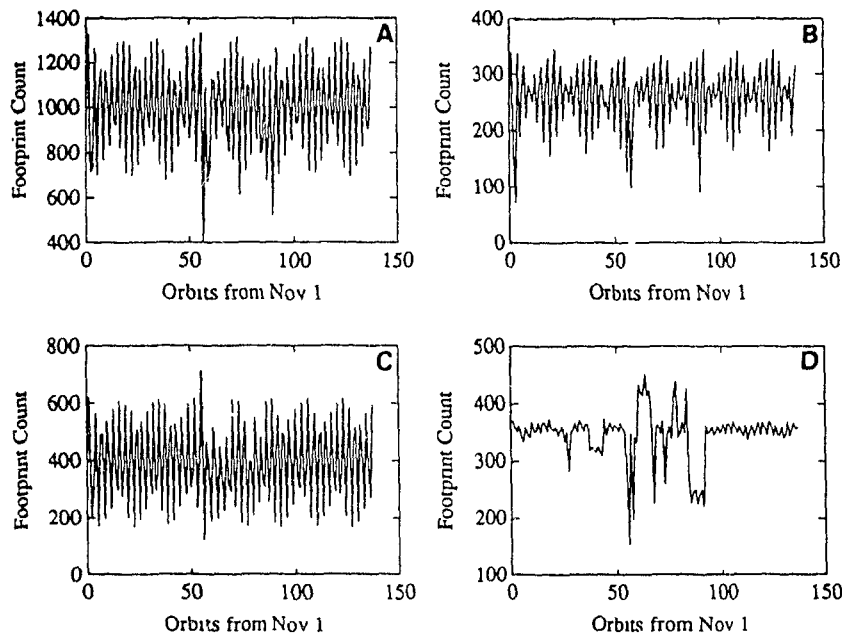
3.2.4 AES Ice Charts

The absence of passive microwave coverage during the 1971/72 ice season necessitated the use of AES composite ice charts produced from a variety of information sources including aircraft observer reconnaissance, satellite imagery, ship and land-based reports and modelled ice drift results. The aerial reconnaissance data is itself a composite of data obtained through visual observation, SLAR imagery interpretation and any other pertinent remote sensing available from the aircraft surveys. An ice forecaster reviews the information available to him, weighs its overall importance and produces the composite ice charts, providing information detailing ice concentration, type and floe size characteristics.

The spatial and temporal coverage of the ice charts is less than that of the SMMR data. From late December, coverage along the Canadian east coast south of about 56°N is available approximately three times per week to the middle of July or until ice conditions ameliorate. This is the most frequent coverage available and in some instances weather limitations mean less coverage.



1980/81



1984/85

Figure 3.1 Temporal Variation in SMMR Footprints through the Study Area (a-complete area, b-50°N, c

The ice information was extracted from ice charts and digitized at a resolution of 1/2 degree latitude by 1/2 degree longitude. The evaluation of ice cover variability was limited to areas south of 56°N as opposed to the entire study area. As a result of the spatial and temporal limitations of the AES data, they were not used in the frequency analysis. However, the data provided reasonable coverage for the evaluation of storm effects on ice cover for several storms.

3.2.5 SMMR/AES Ice Concentration Comparison

The evaluation of satellite-derived ice information is contingent on a reliable data set for comparison. At least two studies have been conducted to evaluate the accuracy of SMMR-derived ice edge positioning (Moreau *et al.*, 1985; Henderson, 1984). Moreau *et al.* (1985) have evaluated the performance of the AES-Phd algorithm in determining the ice edge position, defined as that portion where the ice concentration is greater than or equal to the 10% total concentration. Their evaluation included algorithm performance in the Beaufort Sea against AES Ice charts (the two were not concurrent) and east coast waters for several dates in 1984 where there was concurrent SMMR and SLAR (Side Looking Airborne Radar) or visual data.

Their findings are summarized in Table 3.2, indicating that mean agreement between SMMR and ice chart ice edge in the Beaufort Sea was 7.2km with a root mean square distance (RMSD) of 17.8km. Algorithm over estimation of ice extent was more likely than under estimation in the Beaufort Sea as seen by the maximum and minimum values where positive numbers indicate algorithm estimation of the ice edge beyond the chart position.

On the east coast where the evaluation was against same day SLAR or visual reconnaissance, mean deviation of the 10% contour was -4.4km, with a RMSD of 31.2km. The range of values was much larger than in the comparison using Beaufort Sea data. A comparison of the 35% contour produces better agreement between the algorithm ice edge and the ice reconnaissance observations.

In an earlier study, Henderson (1984) determined there were large mean absolute deviations between the positioning of the SMMR and ice chart ice edge, with the ice charts more accurate in positioning the ice edge and the SMMR product better at positioning the 6/10 contour. The AES ice chart 4/10 and SMMR 3.5/10 concentrations were approximately located at comparable positions.

Table 3.2 Deviation Between SMMR-derived Ice Edge and Ice Reconnaissance Observations (km)

Contour Level	Comparison Source	Location	Mean	RMSD	Max	Min	Obs
10%	AES Ice Charts	Beaufort Sea	7.2	17.8	50	-4	149
10%	SLAR/Visual Observation	Eastcoast	-4.4	31.2	93	-144	223
35%	SLAR/Visual	Eastcoast	3.6	21.2	50	-85	103

Source: Moreau *et al.* 1985

In addition to evaluation of the similarities between the two data sets, Henderson evaluated the two against SLAR and satellite multispectral imagery (NOAA-7 Advanced

of the same area. The results of his evaluation suggest that neither the AES ice charts nor the SMMR ice data set yield statistically similar results to the two imagery sets. Further, the acknowledged problems in georectification of either reference data set (the imagery) means that an absolute standard against which to compare the SMMR-derived concentrations is still lacking. As a result, the absolute reliability of the SMMR in defining ice area and extent remains statistically uncertain (Henderson, 1984). In this study it was felt that while the absolute accuracy of the SMMR ice maps was uncertain, there was sufficient reason to believe that the results were consistent with themselves to justify their use in the manner outlined.

Chapter 4

SEA ICE TIME SERIES ANALYSIS

4.1 Spectral Analysis

Spectral and harmonic analyses have been used successfully in a number of disciplines for the analysis of time series data. The techniques are based on the premise that the time series can be defined in terms of a series of sine and cosine functions. By transforming the time series record in this fashion one is able to conduct an analysis of the periodic versus random components within the time series. It is not the purpose of this study to explain the fundamentals of spectral analysis. Jenkins and Watts (1968), whose techniques were followed here, provide a definitive explanation for those interested.

Suffice it to say, analyses of frequency characteristics have been carried out successfully by many investigators within the climatological and related disciplines. Garrett *et al.* (1985) used spectral and cross spectral analysis to evaluate the frequency dependent relationship between sea level and meteorological forcing off the Labrador coast. Spectra of humidity, temperature and winds near Sable Island have been used to assess boundary layer stability (Smith and Anderson, 1984). Koch and Gohus (1988) followed the techniques described by Jenkins and Watts (1968) to isolate dominant waves within surface pressure and wind data. In looking at Antarctic sea ice variability, Howarth (1983) used harmonic analysis techniques to evaluate the phase relationship between sea ice extent and cyclonic disturbances.

The variance spectrum is defined such that the integral over all positive

frequencies equals the time series variance (Smith and Anderson, 1980). The spectrum can be derived through Fourier transformation of the original data or through transformation of the autocorrelation function.

The autocorrelation function is in itself of interest in that it provides an indication of the correlation between points along the time series. The autocorrelation can be calculated as

$$r_L = \frac{\sum_{i=1}^N x_i x_{i+L}}{N \sum_{i=1}^N x_i^2}$$

where L is the lag between points x along the series. Normalizing r_L as shown forces the autocorrelation to range from 1 to -1 with a value of 1 indicating complete correlation and similarly, a value of -1 perfect correlation but 180 degrees out of phase. A value of 0 indicates no correlation for a given lag. Barry and Perry (1973) point out that in most cases meteorological time series show a tendency toward large autocorrelations for short lags. Both the spectrum and autocorrelation were utilized in this study.

All spectra have been smoothed with a Bartlett window as a means of reducing sampling-related variance (Jenkins and Watts, 1968). In addition to influencing important spectral properties, the choice of spectral window also determines the degrees of freedom and hence confidence limits on the resultant spectrum.

4.1.1 Confidence Limits on the Variance Spectrum

If $C_{xx}(f)$ represents the smoothed spectral estimate of the theoretical variance

spectrum $\Gamma_{xx}(f)$ then $vC_{xx}(f)/\Gamma_{xx}(f)$ can be described by a X_v^2 distribution (Jenkins and Watts, 1968). Further, it can be shown that the $100(1-\alpha)\%$ confidence intervals about $\Gamma_{xx}(f)$ are given by

$$\frac{vC_{xx}(f)}{x_v(1-(\alpha/2))} , \frac{vC_{xx}(f)}{x_v(\alpha/2)}$$

where v is the number of degrees of freedom. The degrees of freedom is dependent on the type and width of the spectral window selected with higher degrees of freedom associated with reduced variance. The confidence intervals calculated in the following sections are based on this approach, with values for the confidence interval multipliers obtained from figures provided by Jenkins and Watts (1968).

4.2 Data Preparation

The objectives of this portion of the thesis were to 1) evaluate the time dependent spectral signatures of ice cover variation, 2) identify significant cycles of variability and 3) relate these to atmospheric variability. This was done for the 1980/81 and 1984/85 ice seasons where the repetitive coverage of the SMMR was available. The atmospheric record was evaluated on the basis of geostrophic flow conditions as well as surface pressure variation inferred from storm track information.

To produce a time series of ice cover variation, the study region was divided into sub-units $1/2^{\circ} \times 1/2^{\circ}$ in size. This yielded 2500 grid cells within the study area, with 2039 free of land. Ice concentrations from the irregularly spaced SMMR were remapped onto the standard grid. The regularly spaced grid was then interpolated using a weighted inverse distance interpolation scheme where:

$$Z = \frac{\sum_{i=1}^n Z_i/d_i^2}{1/d_i^2}$$

with Z_i equal to the value of a neighbouring point and d , the distance between the two points. The weighting factor (in this case 2) controls the influence of surrounding points such that the influence of a given point is inversely proportional to the square of its distance from the point being estimated.

The remapping provided a concentration value ranging from 0/10 to 10/10 for each cell and permitted the comparison of ice coverage from one satellite orbit to the next. Since the SMMR data were available every second day, the time series sample interval was 2 days. Rather than consider individual cells, the number of cells showing a concentration change exceeding some value were summed. This yielded a count of cells experiencing some level of concentration change ranging from zero to a possible maximum of 2039 cells. For the frequency analysis, the count of cells showing increases or decreases $\geq 1/10$ and $\geq 3/10$ were considered.

Once a regular grid had been prepared for each orbit date, the next step was to calculate variation in ice concentration between consecutive orbits. Concentration changes were calculated on a cell by cell basis. Thus for each cell it was possible to determine a time series of concentration variability.

Figures 4.1 and 4.2 show the time series of concentration increases and decreases greater than or equal to 1/10 and 3/10 respectively for each of the two ice seasons. A cursory comparison of the four curves for each season indicates a similar trend with cell counts at or near zero in early November, rising to a peak at approximately 75 to 80 days (mid-January) and then declining gradually to zero in

This seasonal variation is in direct relation to the development and decay of the overall ice cover. With the exception of increases $\geq 1/10$ in 1984/85, cell counts are low for the first 50-60 days before experiencing a rapid increase. The return to zero is more gradual but also quite variable.

The series for the two seasons are noticeably different in the number of cells experiencing changes of a given level. Table 4.1 provides a statistical comparison between the two seasons for each increase and decrease level. It can be seen that for all levels the mean cell counts are lower in 1980/81 than 1984/85, reflecting the less severe ice conditions during the former season. In addition, the standard deviations are lower, indicating less variability in the ice concentration fluctuations.

Table 4.1 Mean Seasonal Cell Counts by Change Level

Change Level	1980/81		1984/85	
	Mean	Std.	Mean	Std.
Increase $\geq 1/10$	92.3	90.1	147.0	123.5
Decrease $\geq 1/10$	93.1	87.0	146.9	122.4
Increase $> 2/10$	32.1	52.1	61.3	73.9
Decrease $\geq 3/10$	33.2	49.7	62.0	72.9

4.2.1 Seasonal Adjustment

The time series in Figures 4.1 and 4.2 exhibit a distinct low frequency fluctuation which can be attributed to the seasonal growth and decay of the ice cover. In order to maintain stationarity in the time series, it was necessary to remove this seasonal effect. Following techniques suggested by Priestley (1981), the seasonal

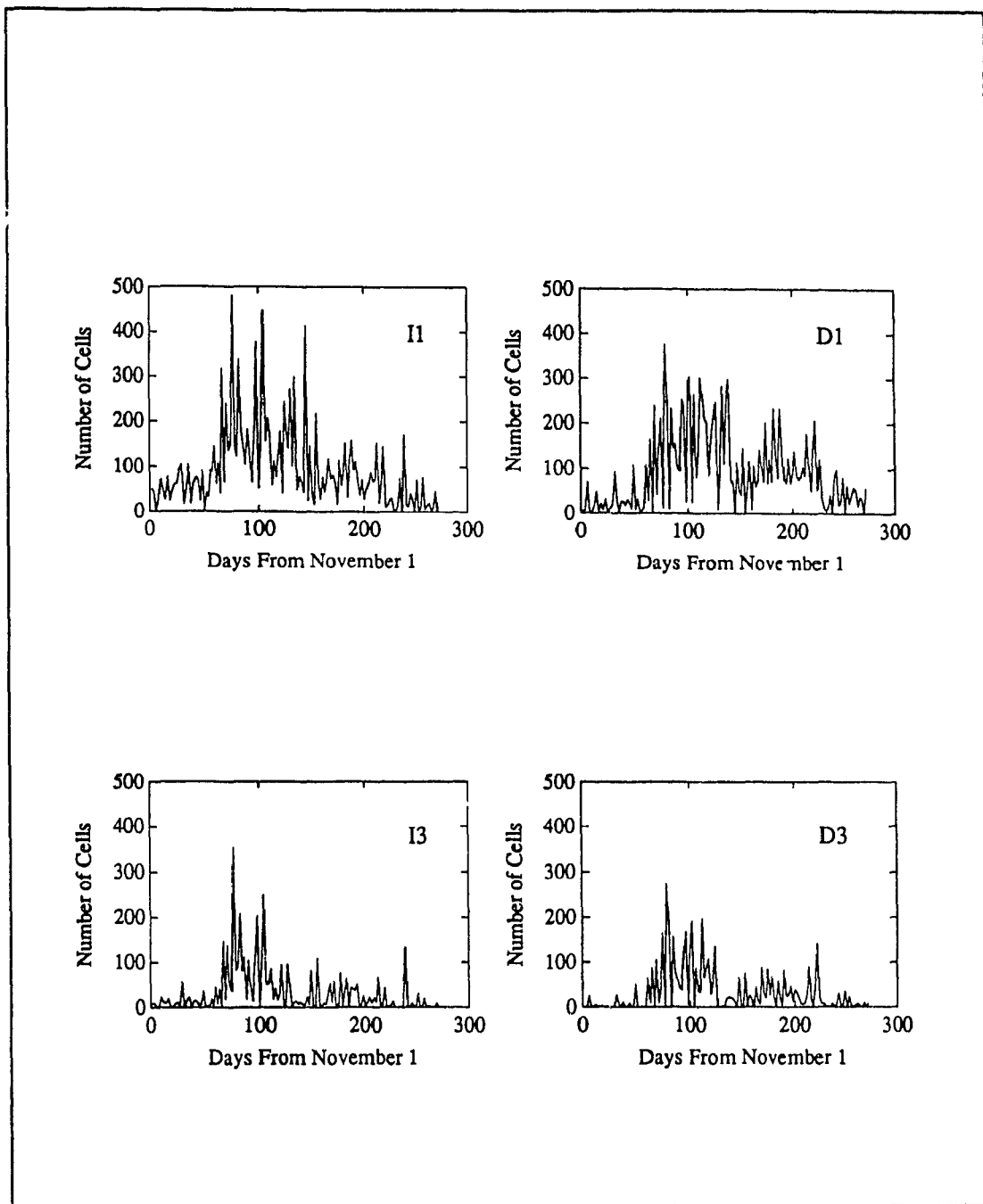


Figure 4.1 Time Series of 1980/81 Ice Concentration Increase and Decreases

I1 - Concentration Increases $\geq 1/10$; I3 - Concentration Increases $\geq 3/10$
 D1 - Concentration Decreases $\geq 1/10$; D3 - Concentration Decreases $\geq 3/10$

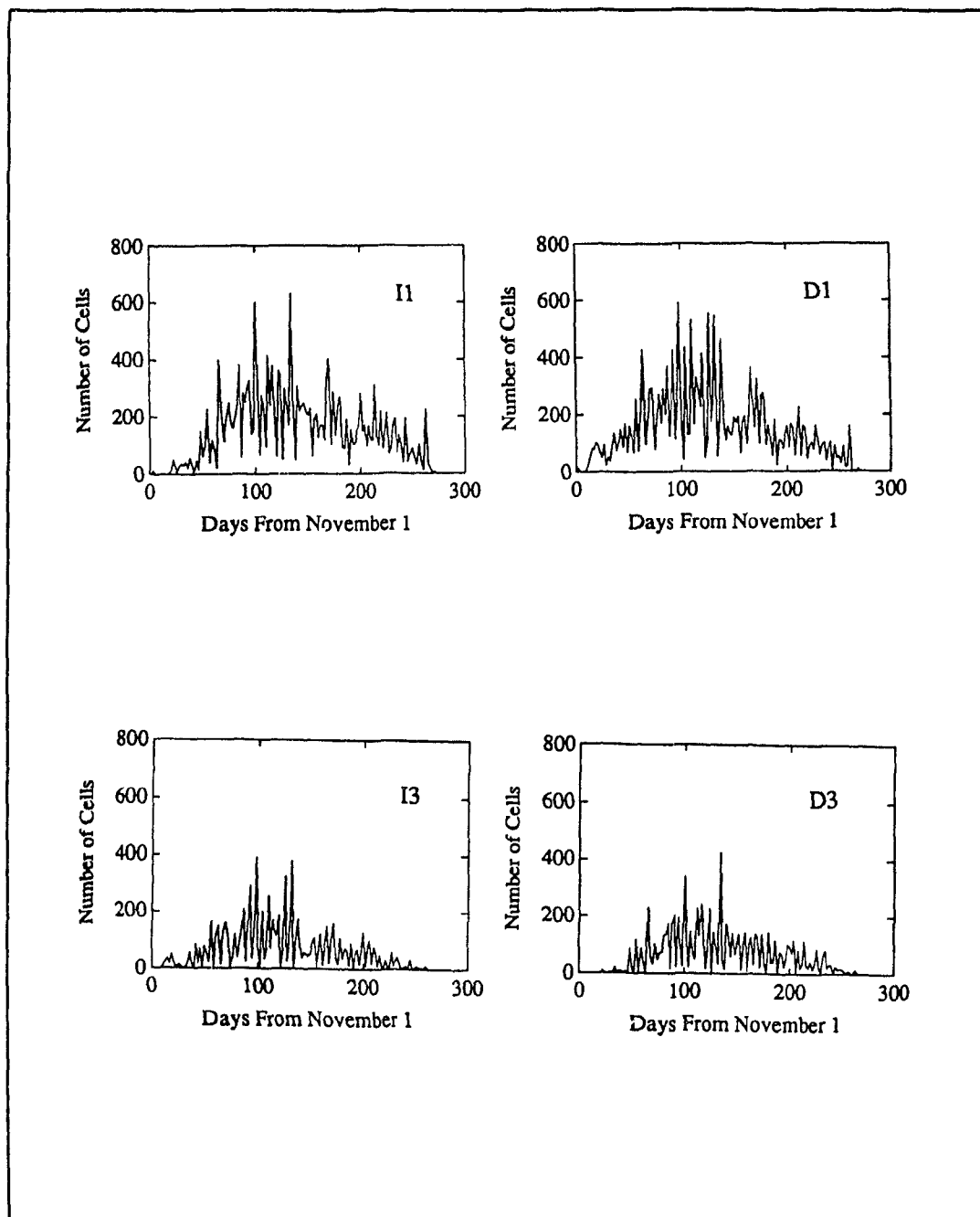


Figure 4.2 Time Series of 1984/85 Ice Concentration Increases and Decreases

I1 - Concentration Increases $\geq 1/10$; I3 - Concentration Increases $\geq 3/10$
 D1 - Concentration Decreases $\geq 1/10$; D3 - Concentration Decreases $\geq 3/10$

effects were filtered by subtracting the 30 day average from the data in a step-wise fashion. Figure 4.3 shows the effect of this filtering on the 1980/81 record for increases $\geq 1/10$ where the filtered time series retains the high frequency variability of the original record while minimizing the seasonal (low frequency) variability. In performing the filtering, the mean was reduced from 91.2 to zero. Similar results were achieved for the other series.

The filtered data were used in the frequency analysis. However initially, variance spectra were calculated for each of the four series using the entire unfiltered record (136 observations in 1980/81 and 137 in 1984/85). As an example, the spectrum for 1980/81 decreases $\geq 3/10$ is shown in Figure 4.4. Major peaks in the spectrum are evident at 0.14 cycles/day (c/d), corresponding to a period of 7.1 days and at 0.18 c/d (5.6 days). With some variation in the amplitude of the peaks, this pattern was repeated for each of the four series, suggesting unique features within the data.

4.2.2 Band Filtering

As noted by Moreau *et al.* (1985), complete SMMR coverage in the study area was incomplete for some orbits as a result of satellite orbit patterns and radiometer swath width. It was suspected that this variability may have been reflected in the interpolated grid of ice concentrations and hence in the periodicities of the concentration change time series.

To investigate this, spectra were calculated for the footprint counts described in Chapter 3. The spectrum for the complete region indicates a dominant peak at 0.18 c/d with a much smaller peak at 0.14 c/d (Figure 4.5). This was seen in both the

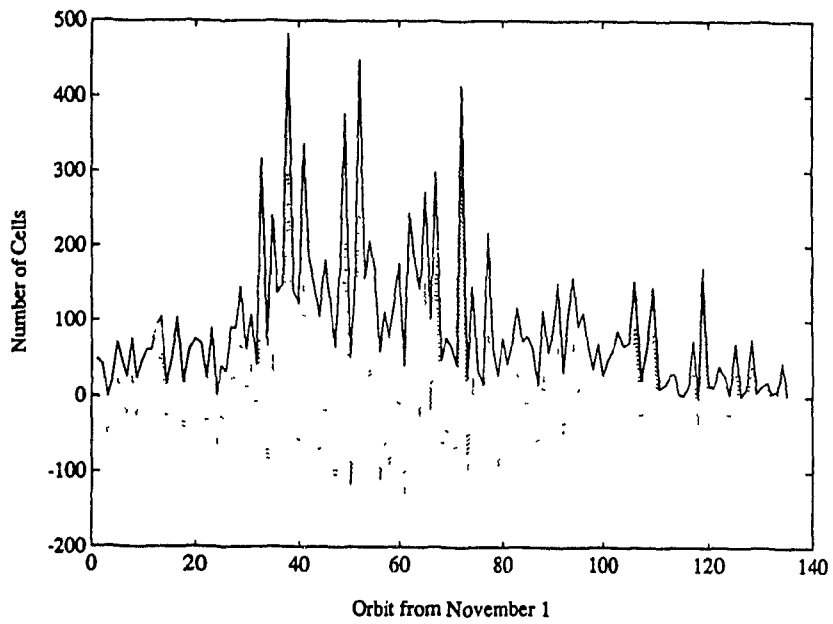


Figure 4.3 Comparison of Raw (solid) and Seasonally Adjusted (dashed) 1980/81 Concentration Increases $\geq 1/10$

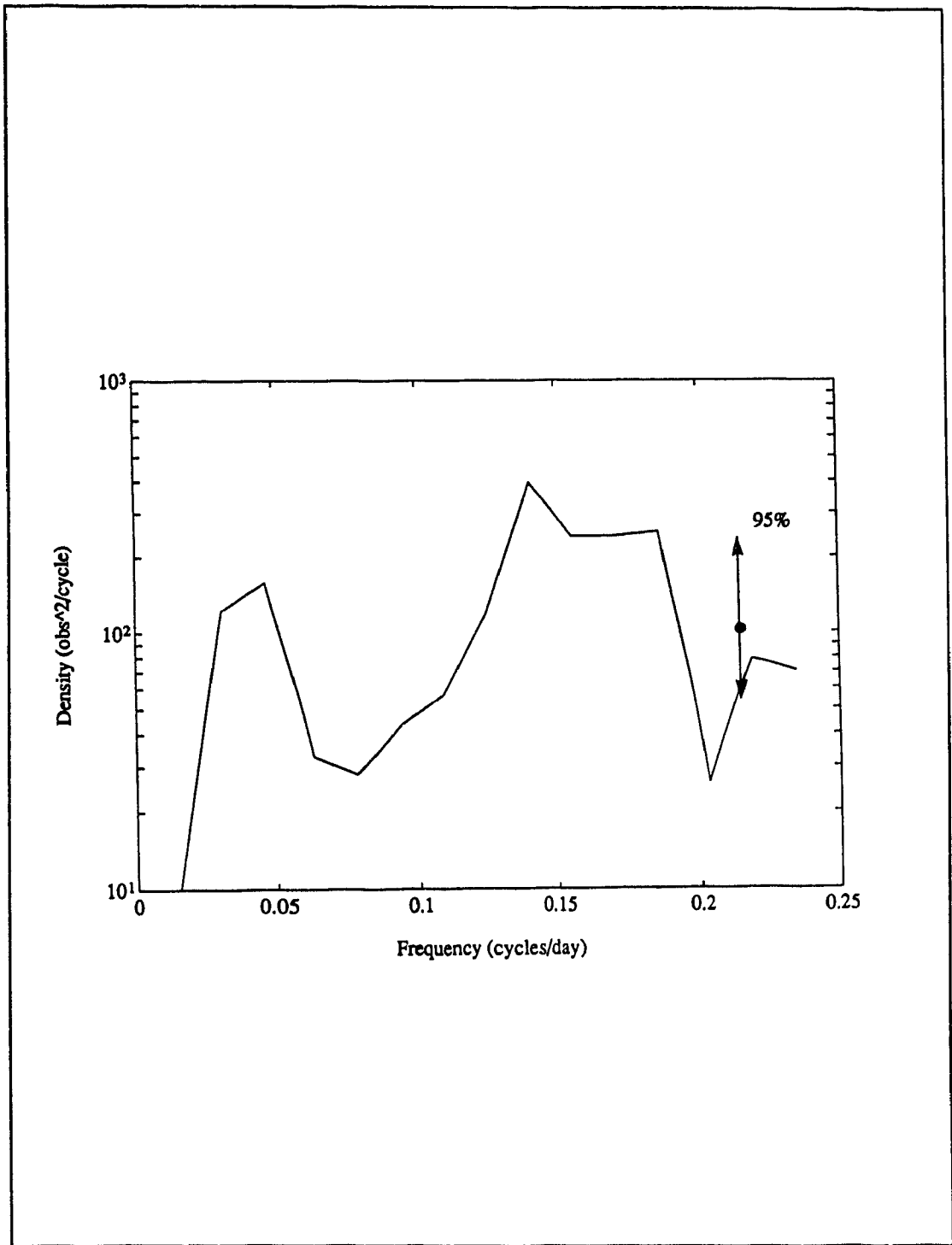


Figure 4.4 Unfiltered Power Spectrum for 1980/81 Concentration Decreases $\geq 3/10$

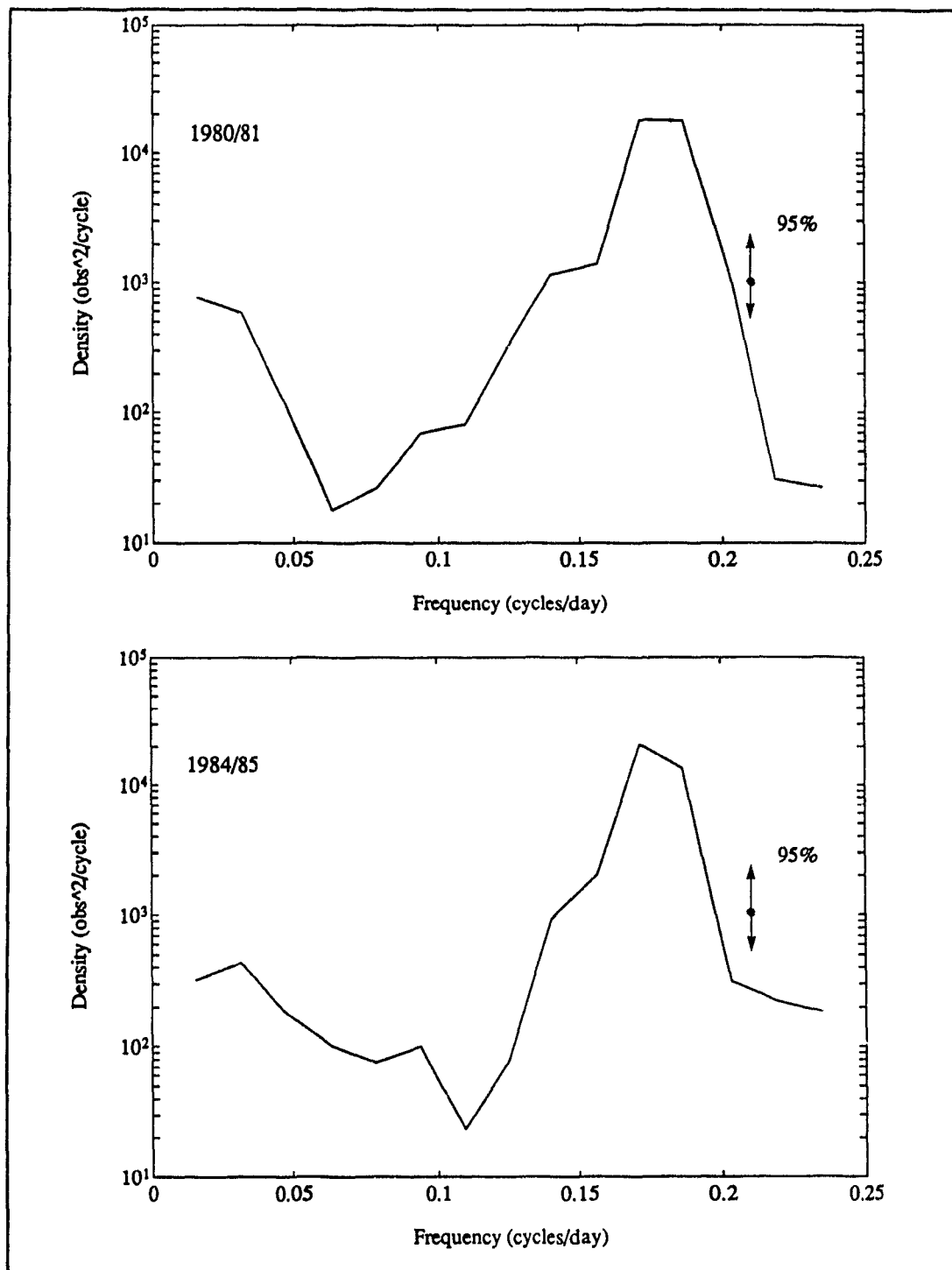


Figure 4.5 Power Spectra for Footprint Counts for the 1980/81 and 1984/85 Seasons

1980/81 and 1984/85 records. It was apparent from this investigation that the high amplitude observed in the concentration change records at 0.18 c/d might in fact be attributed to the irregularity in the SMMR data coverage. This was supported by visual analysis of the SMMR footprints which indicated a major gap in coverage approximately every third orbit (6 days).

In order to effectively evaluate frequency dependent behaviour of the ice cover itself, it was necessary to eliminate the influence of this narrow band of energy. Following techniques commonly used in signal processing (Priestley, 1981), a frequency-specific filter was designed to mask the dominant signal observed at 0.18 c/d in the two footprint time series and which was translated to the ice concentration change records.

Several trials were made to evaluate the behaviour of a frequency impulse response band rejection filter of various widths in minimizing the peak amplitude in the footprint count time series. In the final analysis, a band rejection filter removing frequencies from 0.16 to 0.20 c/d was used.

The performance of the band rejection filter is seen in Figure 4.6 where the spectra for the original and filtered SMMR footprint series are shown for the two seasons. In each plot the solid line represents the unfiltered time series while the dotted line shows the results after implementation of the band rejection filter. It is clear that for both years the high amplitude peak at 0.18 c/d is almost eliminated and the peak at 0.14 c/d reduced substantially.

Since the filtering procedure represents a balance between minimization of the 'noise' and maximization of the true 'signal', it was decided that no further effort

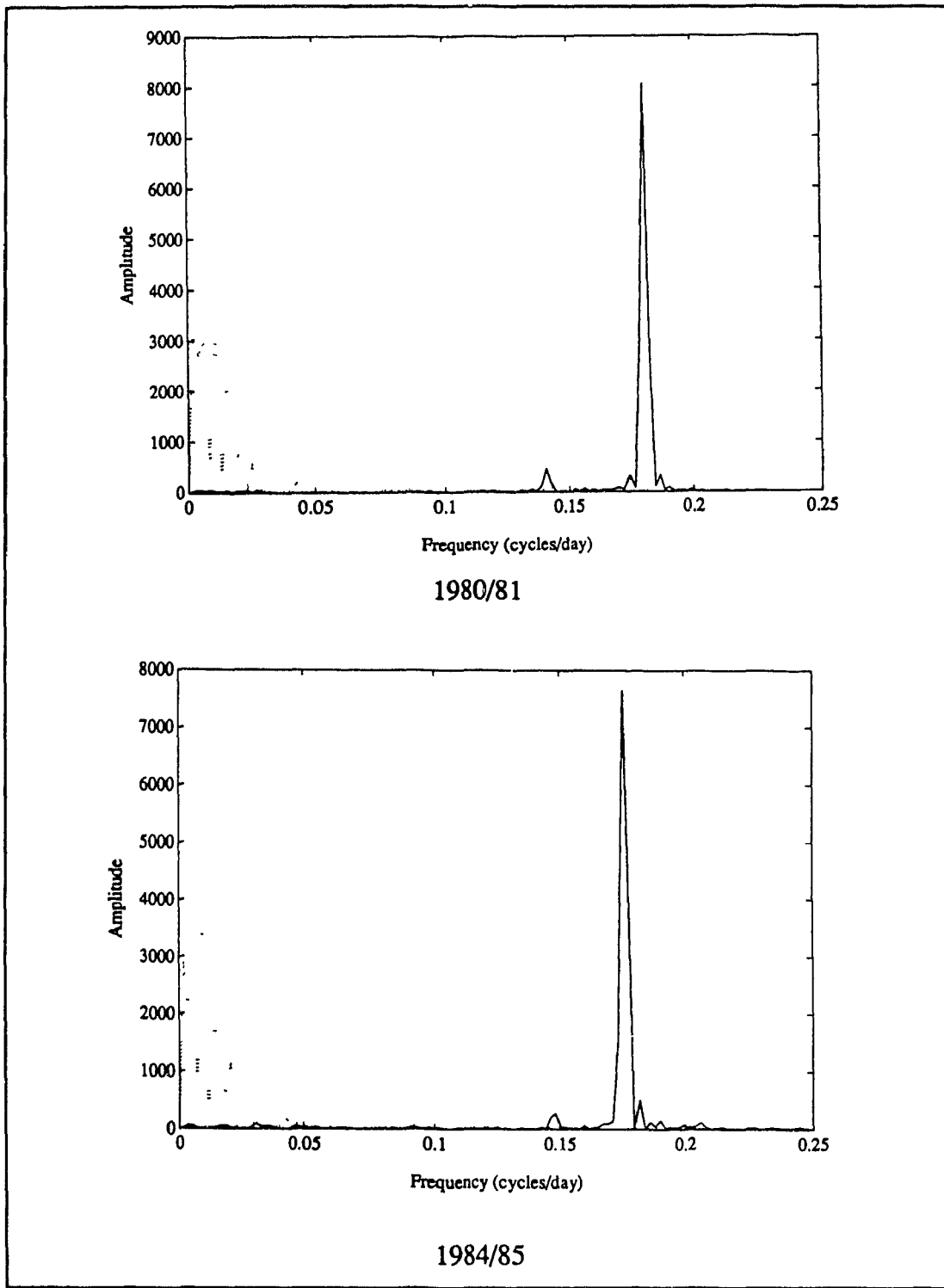


Figure 4.6 Comparison of Footprint Power Spectra Before and After Band Filtering
 (Solid - Unfiltered; Dashed - Filtered)

would be made to reduce the contribution of the 0.14 c/d energy. With the success seen in Figure 4.6 in reducing the key periodicities in the footprint count data, the band rejection filter was applied to each of the ice concentration change time series prior to performing the spectral analysis.

4.3 Data Analysis

4.3.1 Ice Concentration Changes

Once adjustments were made for seasonal effects and the influence of periodic SMMR data gaps reduced through band filtering, the data were ready for analysis. Four time series of 135 observations were used for each year; those of grid cell counts for increases and decreases $\geq 1/10$ concentration and those for increases and decreases $\geq 3/10$. Autocorrelations were calculated for each time series with the results shown in Figures 4.7 and 4.8. The plots extend to 32 lags only since beyond this the autocorrelation tended to zero, fluctuating about the zero axis without any significant peaks.

In all cases other than for ice concentration increases in 1984/85, the autocorrelation falls rapidly from unity at lag 0, suggesting little correlation between changes in ice concentration beyond a few orbits. The 95% confidence limits have been included for each autocorrelation to show that very few of the peaks at later lags are significantly different from zero. For the 1980/81 series, significant autocorrelations are observed at approximately 12, 15 and 26 lags for the concentration increase series. In 1984/85, the concentration decrease series exhibit significant autocorrelations at 5 and 18 days.

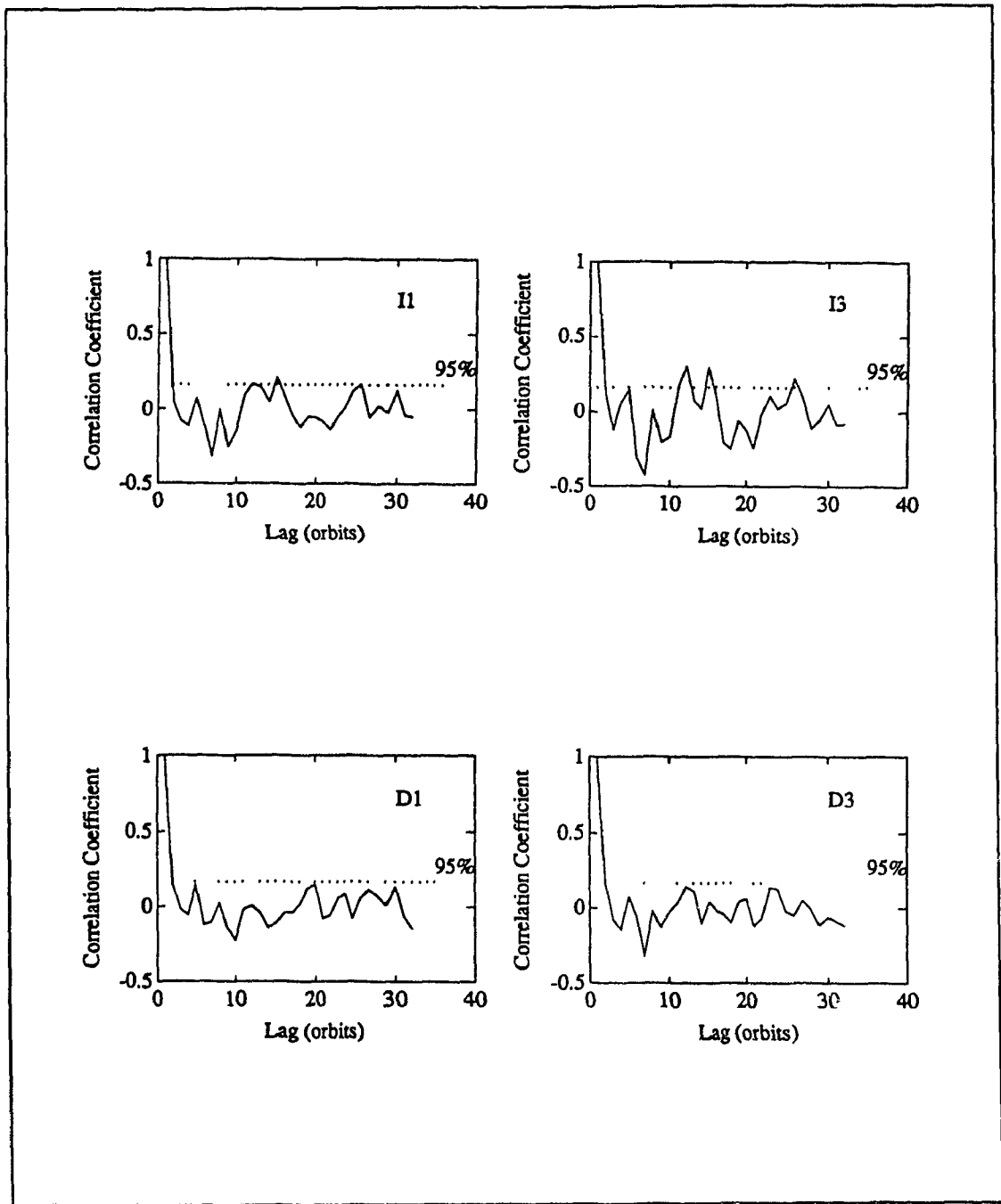


Figure 4.7 Autocorrelations for 1980/81 Ice Concentration Increases and Decreases Showing 95% Confidence Limits

I1 - Concentration Increases $\geq 1/10$; I3 - Concentration Increases $\geq 3/10$
 D1 - Concentration Decreases $\geq 1/10$; D3 - Concentration Decreases $\geq 3/10$

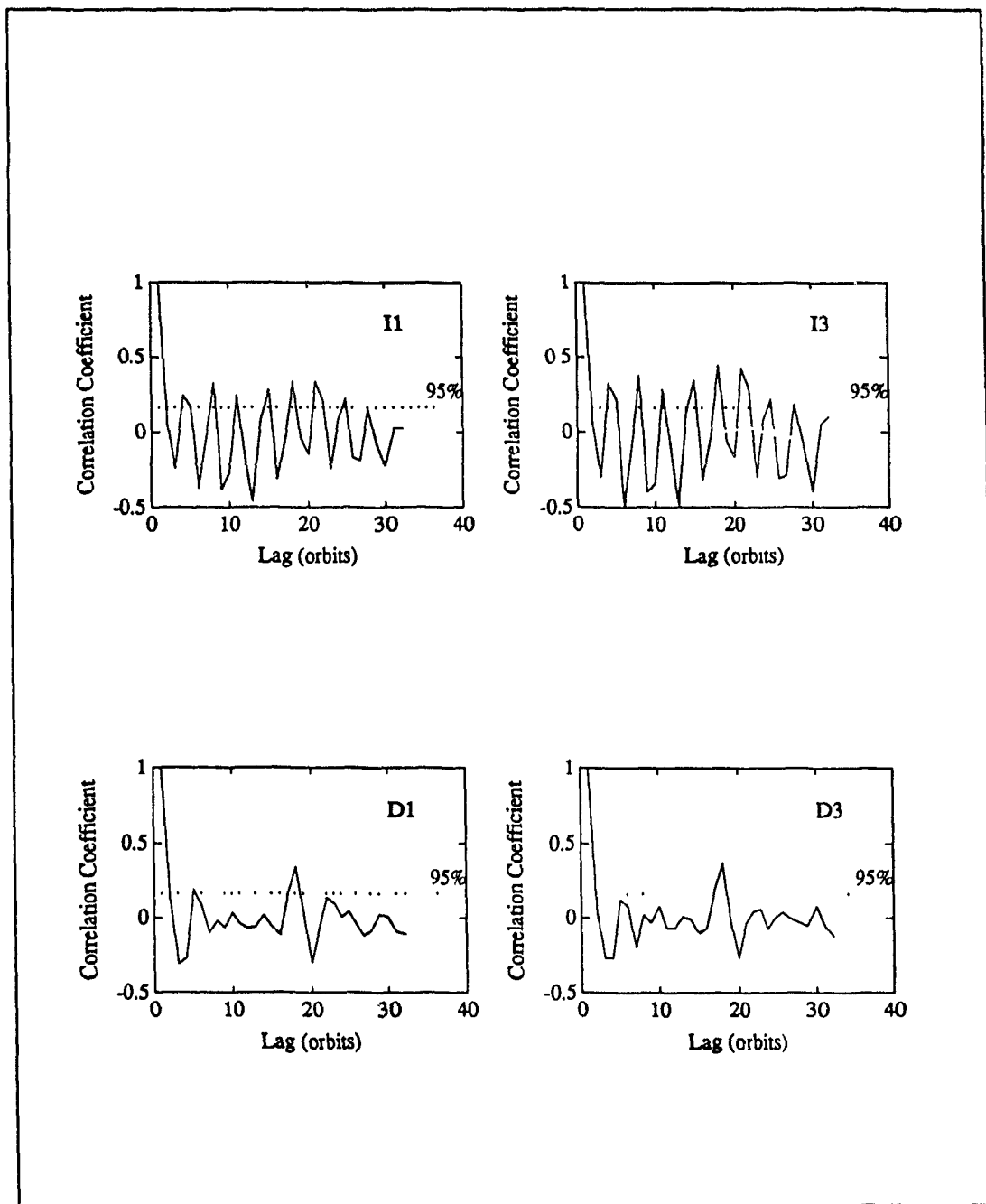


Figure 4.8 Autocorrelations for 1984/85 Ice Concentration Increases and Decreases Showing 95% Confidence Limits

I1 - Concentration Increases $\geq 1/10$; I3 - Concentration Increases $\geq 3/10$
 D1 - Concentration Decreases $\geq 1/10$; D3 - Concentration Decreases $\geq 3/10$

The two 1984/85 autocorrelations for increases $\geq 1/10$ and $\geq 3/10$ (Figure 4.8) exhibit different behaviour from the others in that they continue to oscillate about zero with a fairly regular period of about 4 lags or 8 days, exhibiting more gradual damping tendencies. The explanation for this behaviour is not immediately apparent. The fact that all time series of concentration change were treated similarly with regard to filtering would suggest that the cause is real rather than the result of artificially introduced effects. The regular oscillation indicates the presence of a stationary random process (Bendat and Piersol, 1980). The 1984/85 ice season was heavier than 1980/81 with more extensive ice coverage. It would seem that with a more fully developed ice cover, the variability in ice concentration increase was more regular than in 1980/81 when the ice extent was below average.

Comparison of the autocorrelations for increases $\geq 1/10$ and $\geq 3/10$ show that the two behave similarly, being more or less in phase. The $3/10$ autocorrelation does, however, tend to have more exaggerated maxima and minima. Autocorrelations for concentration decreases behave similarly.

To better understand the frequency dependent variability of the time series, the spectra were calculated. Power spectra for the 1980/81 concentration change time series are shown in Figure 4.9. A general pattern emerges which is consistent in each of the spectra; a peak at approximately 0.03 c/d (33.3 days), a second at 0.14 (7.1 days) and a third at 0.22 (4.5 days). The first two peaks do not differ significantly in amplitude but are larger than the 0.22 c/d peak. The power spectra for the 1984/85 concentration changes (Figure 4.10) show evidence of a low frequency peak at 0.03 c/d, similar to the 1980/81 time series. Differences emerge at the high frequency end of

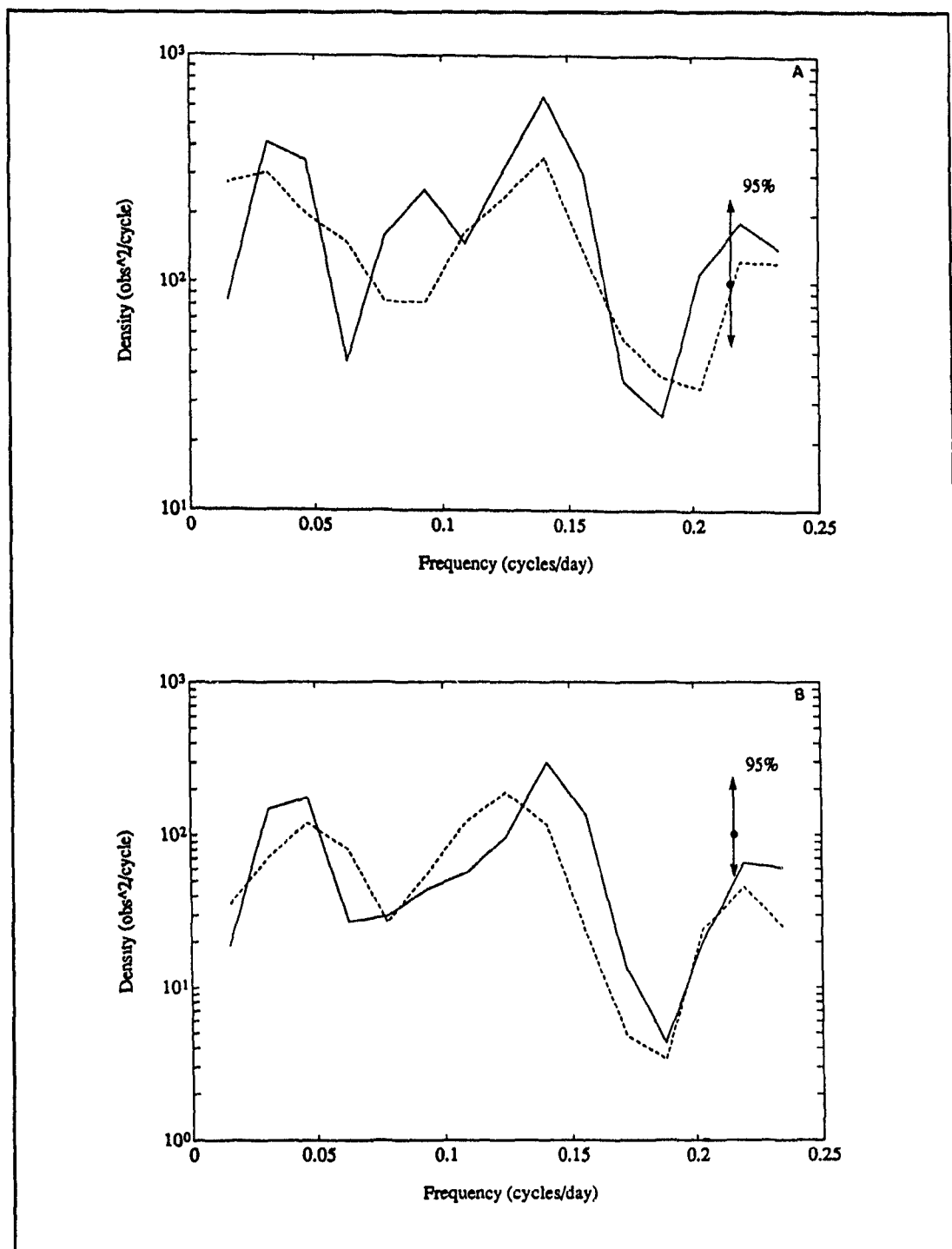


Figure 4.9 Power Spectra for 1980/81 Ice Concentration Change Time Series

- a) Time Series for Ice Concentration Change $\geq 1/10$ Solid - Increase; Dashed - Decrease
- b) Time Series for Ice Concentration Change $\geq 3/10$ Solid - Increase; Dashed - Decrease

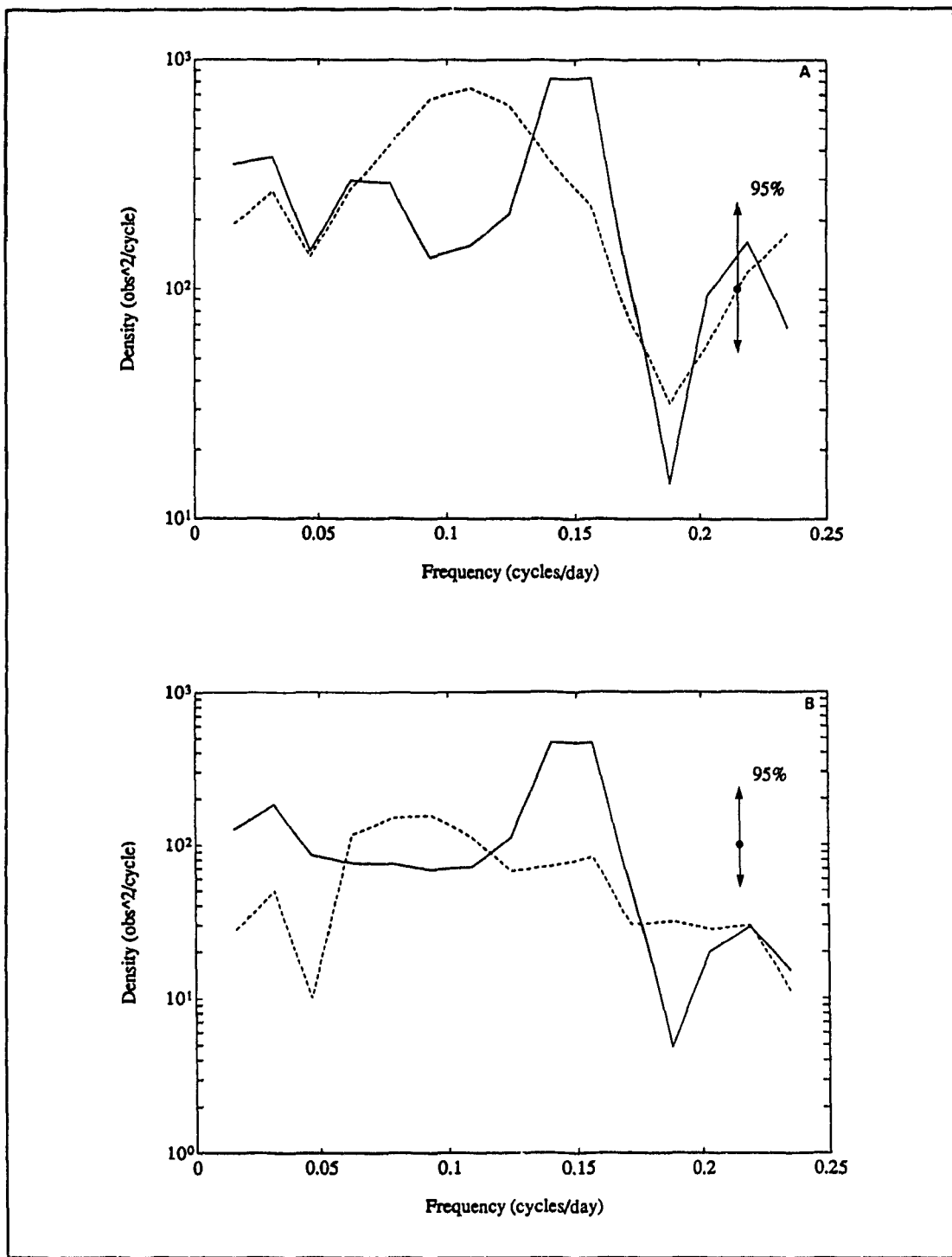


Figure 4.10 Power Spectra for 1984/85 Ice Concentration Change Time Series

- a) Time Series for Ice Concentration Change $\geq 1/10$ Solid - Increase; Dashed - Decrease
- b) Time Series for Ice Concentration Change $\geq 3/10$ Solid - Increase; Dashed - Decrease

the spectra where a single high energy peak replaces the two peaks seen in 1980/81. This peak occurs at a frequency of approximately 0.17 c/d (5.8 days). In both seasons the high frequency peaks are consistent with the synoptic ice variability observed by Pease (1980) in the Bering Sea.

A difficulty that arises in attributing this high frequency energy to synoptic scale atmospheric events is that the peak at 0.14 c/d corresponds to a frequency which was identified earlier as being the lesser of two peaks observed in the variance spectra for the SMMR footprint counts (Figure 4.5). To evaluate the significance of this artificial variability, the spectral properties of the entire study area were compared to those of a spatial window where the variability in footprint counts was minimized. As noted in Figure 3.1, the footprint variability was greatest in the southern regions, declining towards the 70° northern limits in Baffin Bay. Based on this observation, a window was selected to include the area from 60-70°N encompassing Davis Strait and Southern Baffin Bay. Using the same grid network as for the full concentration change time series, a total of 400 1/2 degree square, non-land cells were included in this window. While this approach minimized the influence of system variation, it presented a problem in that this portion of the study region was probably the least dynamic in terms of ice variability. Since the footprint count variability was reduced, no band filtering was applied to the time series, although they were adjusted for seasonal effects.

The power spectra for the 60-70°N band concentration change series are shown in Figure 4.11. The results confirm that energy levels at all frequencies are reduced from those of the entire study area. This is consistent with the generally lower levels

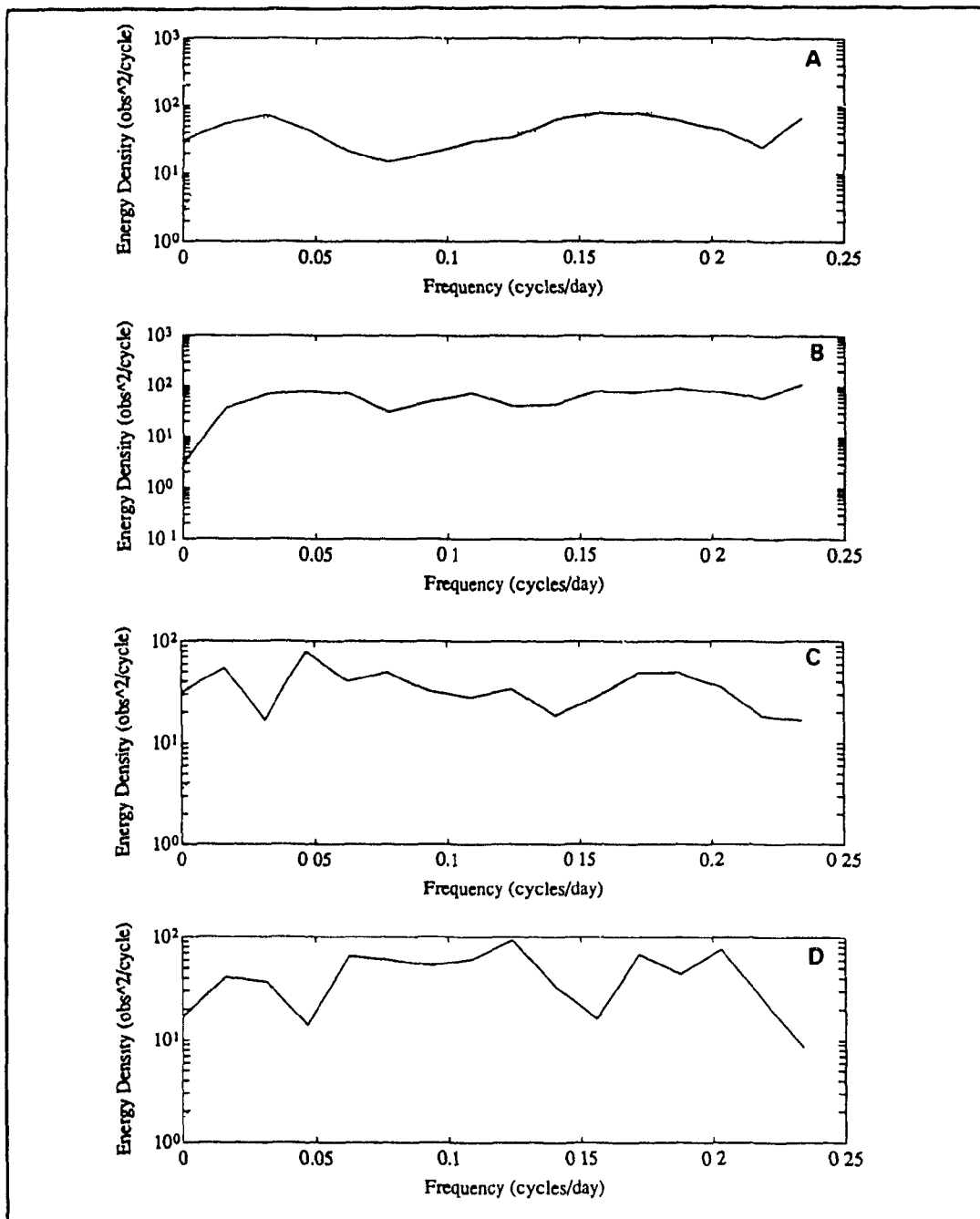


Figure 4.11 Power Spectra for Ice Concentration Change Time Series within the 60-70° Latitudinal Band

- a) Time Series for 1980/81 Concentration Increases - Solid $\geq 1/10$; Dashed $\geq 3/10$
- b) Time Series for 1980/81 Concentration Decreases - Solid $\geq 1/10$; Dashed $\geq 3/10$
- c) Time Series for 1984/85 Concentration Increases - Solid $\geq 1/10$; Dashed $\geq 3/10$
- d) Time Series for 1984/85 Concentration Decreases - Solid $\geq 1/10$; Dashed $\geq 3/10$

of ice dynamics. It is also apparent from the damped curves that there is less variation in spectral energy between frequencies.

The reduced variance and resolution limitations combined, make it difficult to evaluate similarities between the two sets of spectra. Despite this, there does appear to be some correspondence between the 0.03 c/d and 0.14 c/d peaks in Figures 4.9 and 4.10 and those observed for the windowed area in Figure 4.11. In Figure 4.11, the spectrum for increases $\geq 1/10$ have distinct amplitude peaks at 0.03 c/d and approximately 0.15 c/d. The concentration spectrum for increases $\geq 3/10$ exhibits less distinct peaks slightly out of phase, once again in keeping with the patterns seen in Figure 4.9 and 4.10 for increases $\geq 3/10$. In comparing spectra for concentration decreases (Figure 4.9b and 4.10b), the windowed spectra are damped considerably, although some argument could be made that a similar pattern exists.

Comparison of the full area and sub-area spectra suggests that the factors contributing to the frequency events at 0.03, 0.15 and 0.22 c/d could be the result of genuine physical phenomena as opposed to system-induced variability. To evaluate this further, an assessment of meteorological conditions was done using upper air records for three east coast stations and storm track data for the eastern Canadian seaboard.

4.3.2 Upper Air Dynamics

Initially, the time histories of the 850 hPa height for the Iqaluit, Goose Bay and St. John's upper air stations were used as a measure of atmospheric activity in the study area. Twelve hour observations for the November to July period were averaged over two day intervals in conformance with the sampling of the ice data.

results of the spectral analysis for each of the three sites and for the two seasons are shown in Figure 4.12. Energy densities are comparable to those observed for the full area ice time series. The overall similarities in the spectra are readily apparent indicating high variability associated with low frequencies or seasonal periodicities in all spectra, declining towards the higher frequencies. In each case, there is a minimum near 0.20 c/d followed by a rise in energy once again. The positioning of this minimum shows an ordering, occurring at the lowest frequency in the St. John's record followed by Goose Bay and then Iqaluit. This ordering corresponds to a progression from most southerly site to most northerly. In comparing the 1980/81 and 1984/85 spectra it can be seen that, in general, the two seasons are out of phase with the 1980/81 season leading 1984/85.

In addition to the low frequency variability, high variability is observed at approximately 0.10 c/d (10 days), a slightly lower frequency than that for the ice time series. This value is in keeping with the 12 day periodicity presented by Garrett *et al.* (1985) for meteorological conditions off Nain, Labrador.

4.3.3 Storm Track Pressure Variability

Storm track records offered a second means of evaluating the frequency characteristics of atmospheric activity during the ice seasons. For the two ice seasons, storms were tracked through the study area as described in Chapter 3. The minimum observed pressure for each storm while in the study area was used as a measure of storm intensity. These were then plotted against the time of first appearance, providing a time series but with irregular time intervals.

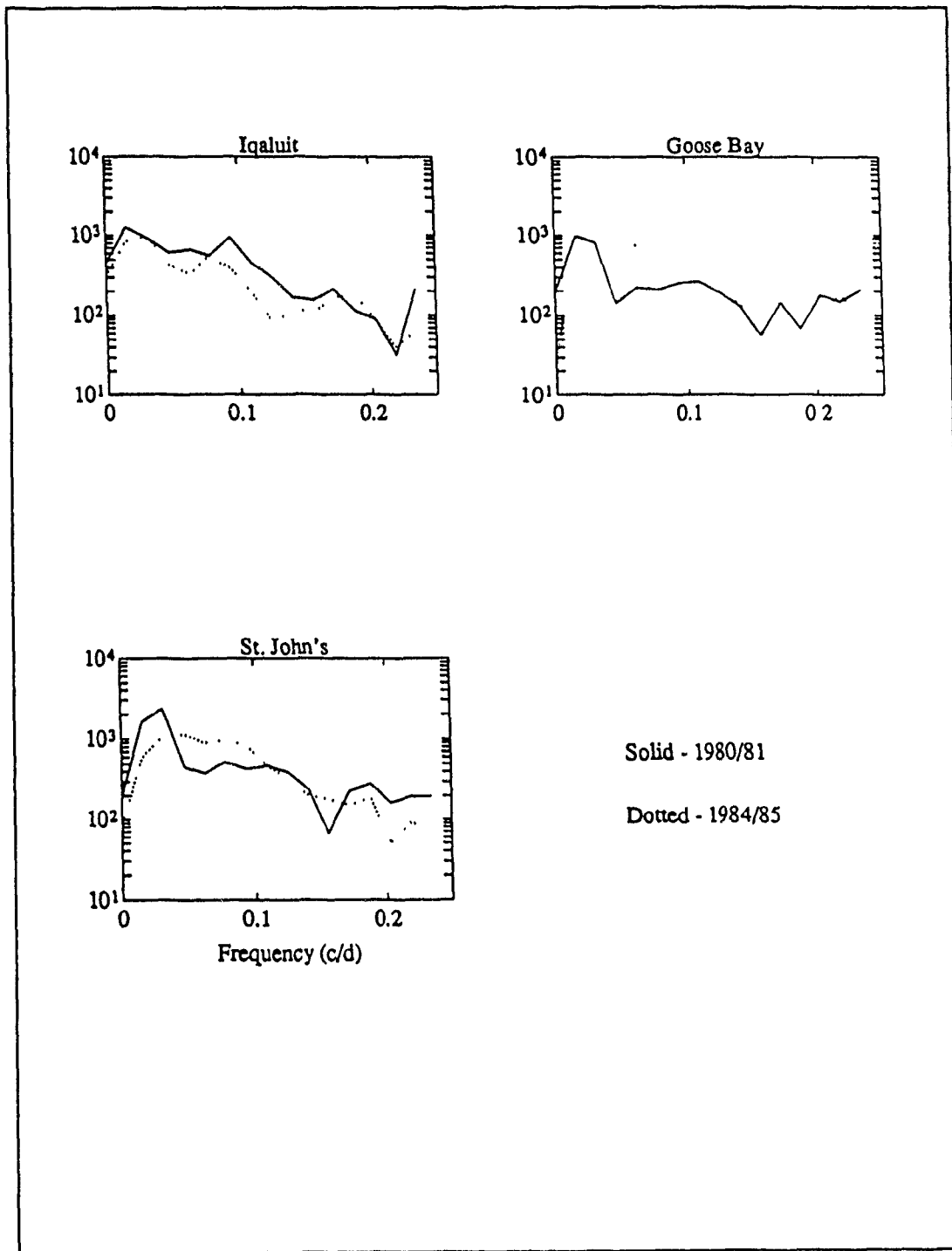


Figure 4.12 1980/81 and 1984/85 Power Spectra of 850 hPa Height for St. John's, Goose Bay and Iqaluit

To facilitate spectral analysis, this time series was interpolated to provide regular one day intervals. A Lagrangian three point interpolation was used following the example of Birch *et al.* (1983) who employed the technique in evaluating drifting surface buoys and iceberg motion off the Labrador coast. The results of the storm intensity interpolation are compared to the original time series in Figure 4.14. The interpolated values fit well although there are some noticeable departures. The large discrepancy between Julian day 1 and Julian day 30 in the 1980/81 series is related to the absence of storm track data for January of 1981. Table 4.2 provides a statistical comparison of the original and interpolated records. In both years, the mean pressure of the interpolated series is within one percent of the original series. Of some concern is the fact that the variance increased with interpolation, particularly in the 1980/81 series. To a large extent this difference was attributed to the interpolation of January pressures. When this portion of the interpolated record was removed, the variance fell to within 10% of the original data. For 1984/85 the difference was approximately 16%. These similarities between raw and interpolated time series were considered sufficient to justify continuation with the frequency analysis however, because of the 1980/81 data gap, the analysis was conducted on the February to July portions of the records only.

Table 4.2 Statistical Comparison Between Raw and Interpolated Storm Pressures

Season	Mean Pressure			Variance		
	Raw	Interpolated	R/I ¹	Raw	Interpolated	R/I ¹
1980/81	99.3	98.7	0.993	153.5	271.0	1.765
(minus Jan)	99.3	99.1	0.998	153.5	170.3	1.109
1984/85	99.3	99.2	0.999	163.6	189.0	1.155

¹ R/I - Raw/Interpolated

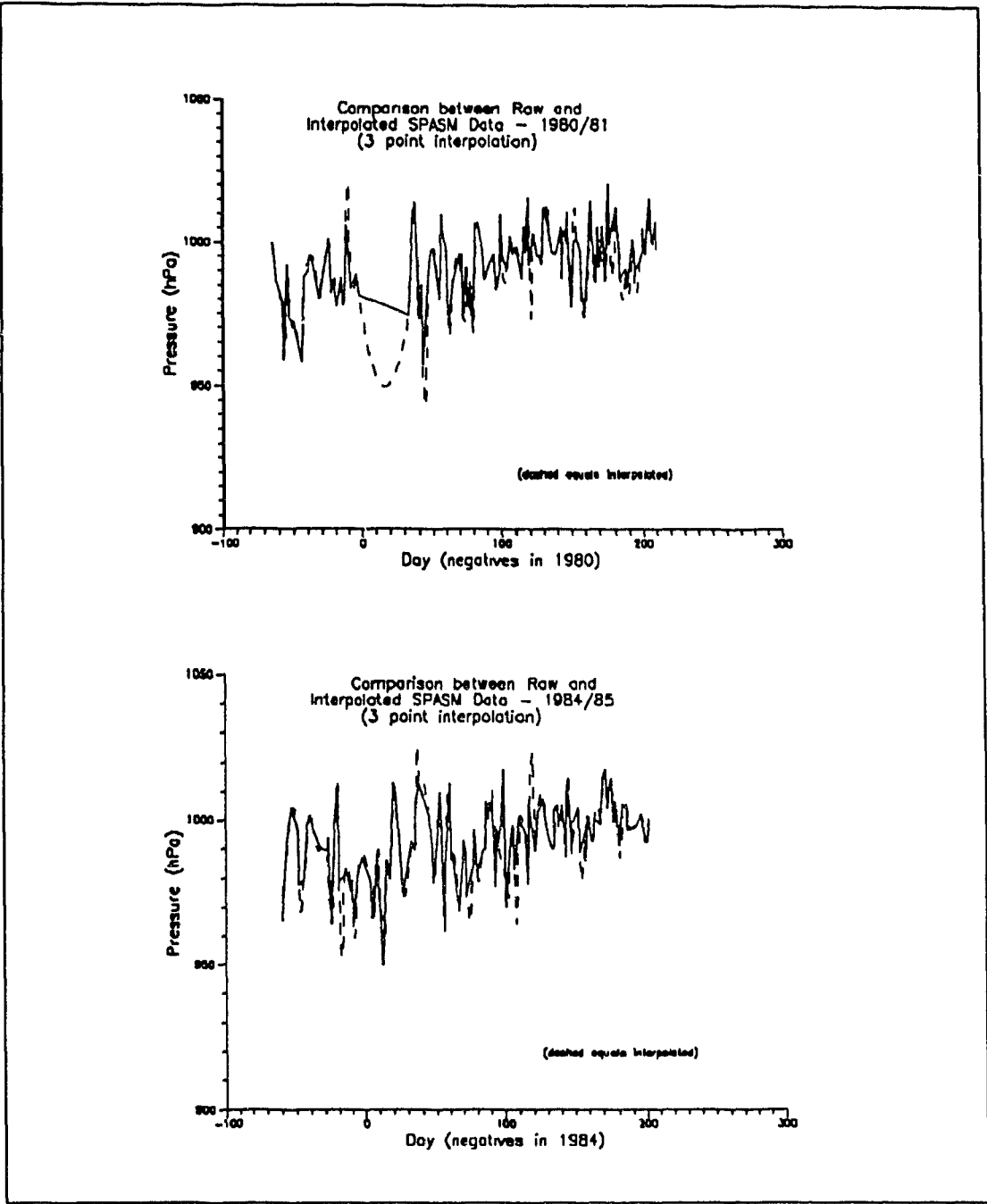


Figure 4.13 Comparison Between Raw and Interpolated Surface Pressures Based on Storm Data

Figure 4.14a shows the autocorrelation for the two February to July periods. Both autocorrelations exhibit a distinct periodicity with peaks spaced at approximately 6 lags. The two are out of phase with 1980/81 leading 1984/85.

In Figure 4.14b, the power spectra indicate a similar out of phase relationship. Both seasons exhibit a low frequency peak with the 1980/81 peak at 0.06 c/d and the 1984/85 peak at 0.13 c/d or periods of 16.7 and 7.7 days respectively.

4.3.4 Ice/Atmosphere Cross Spectral Relationships

One of the objectives in investigating frequency domain properties of the sea ice cover and meteorological data was to relate significant periodicities in one to those in the other. In this respect, the ice time series for the entire study area were compared to the upper air 850 hPa pressure height records for individual stations (St. John's, Goose Bay and Iqaluit). No attempt was made to limit the evaluation to ice conditions within closer proximity of the upper air station because of the data gaps in the satellite coverage at the southern latitudes.

Cross spectra, coherence and phase angles were calculated for each ice time series against each upper air time series. The results are shown in Figures 4.15 through 4.17 with one figure for each station. In each figure, six graphs are shown, the top three describing 1980/81 conditions and the bottom three 1984/85 conditions. The first graph (a) in each set shows the cross spectrum for each of the ice time series against the station's pressure level record for that year; the second graph (b), their associated coherence and the third (c), phase plots for each of the cross spectra. The results are also summarized in Table 4.3. The summary data in Table 4.3 have

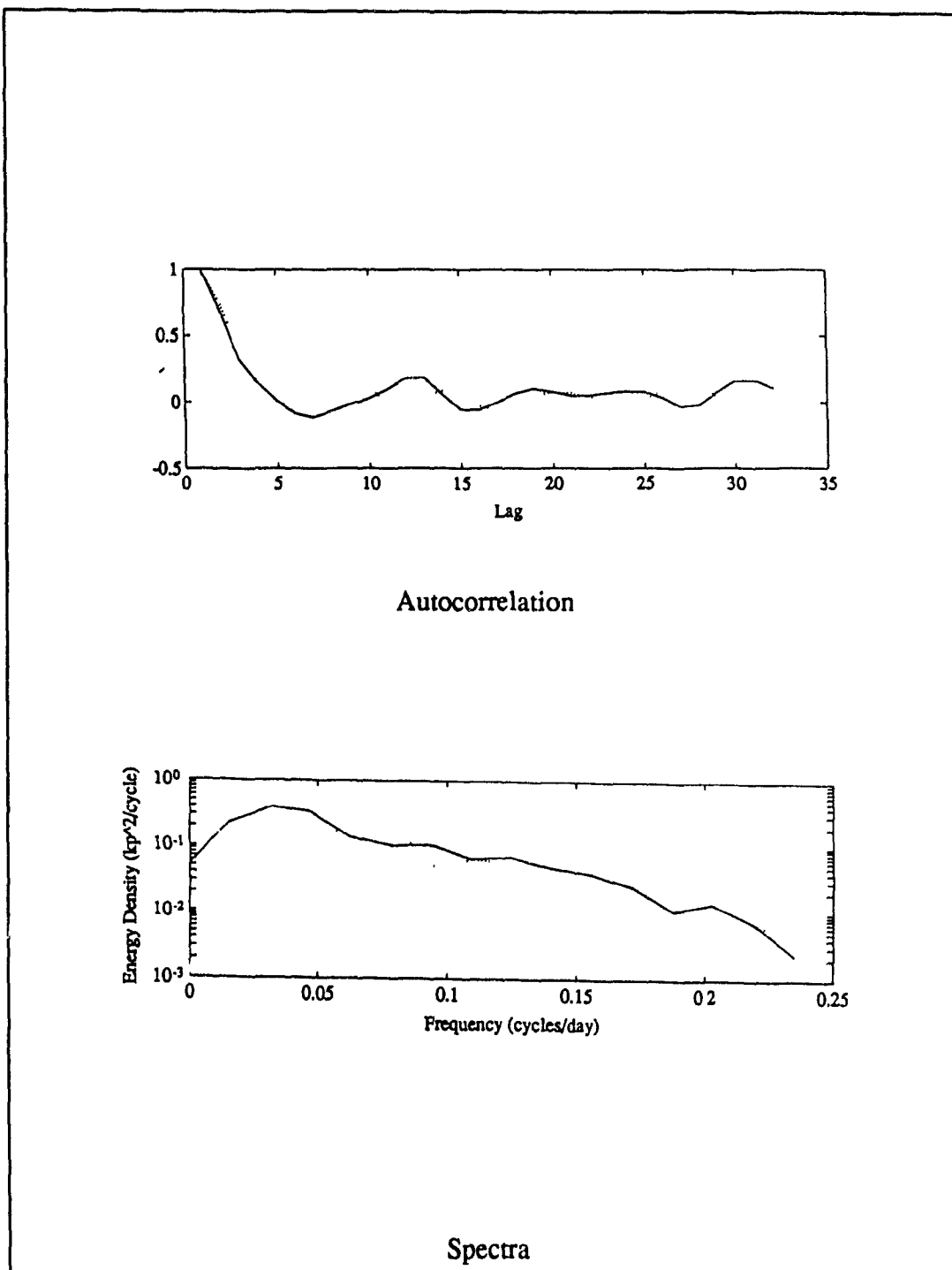


Figure 4.14 Autocorrelation and Spectra for 1980/81 and 1984/85 Surface Pressures
(Solid - 1980/81; Dashed - 1984/85)

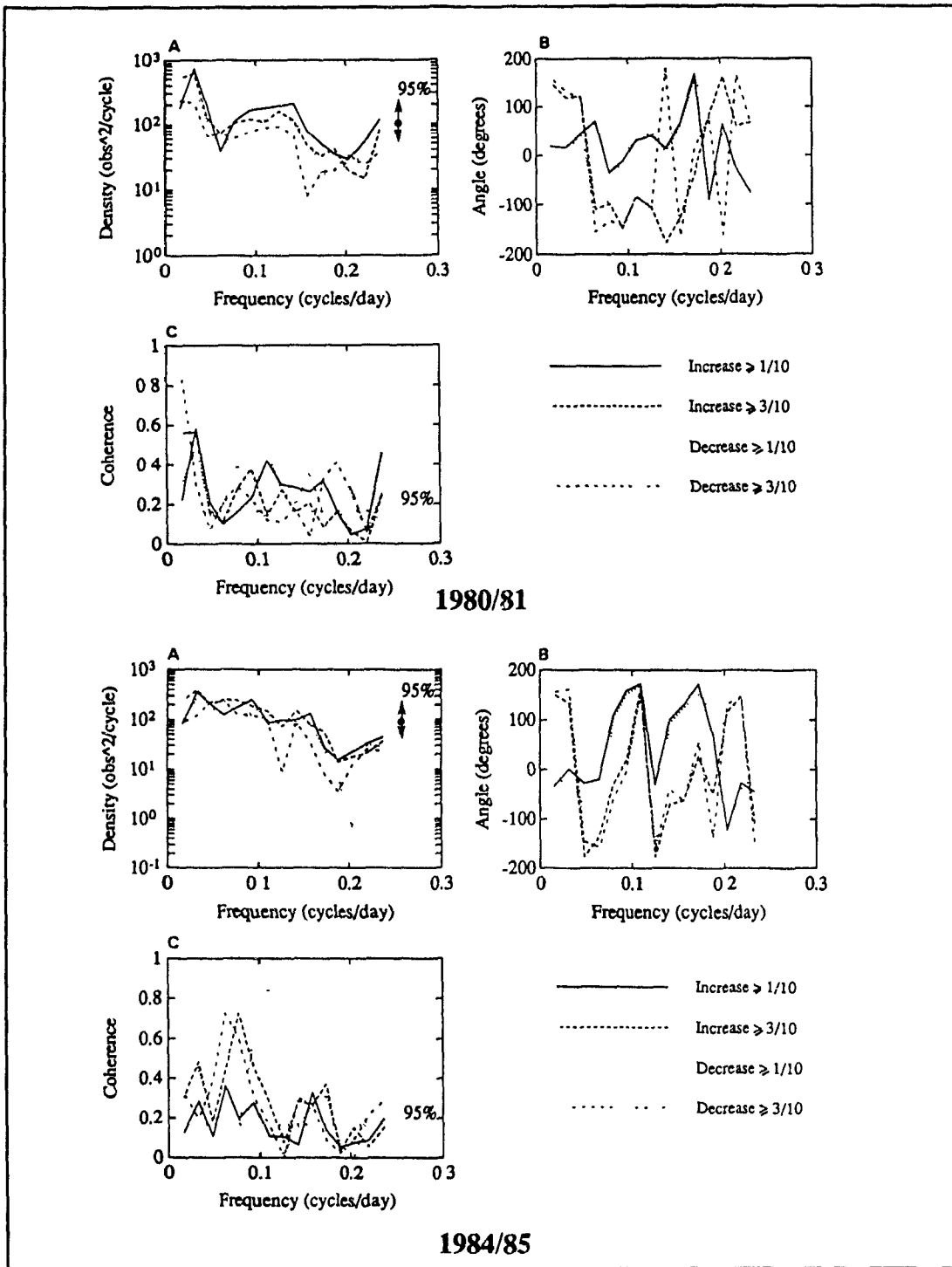


Figure 4.15 Cross Spectra, Coherence and Phase Plots Comparing Region Ice Concentration Change and 850 hPa Height at St.John's (a - cross spectra; b - phase angle; c - coherence)

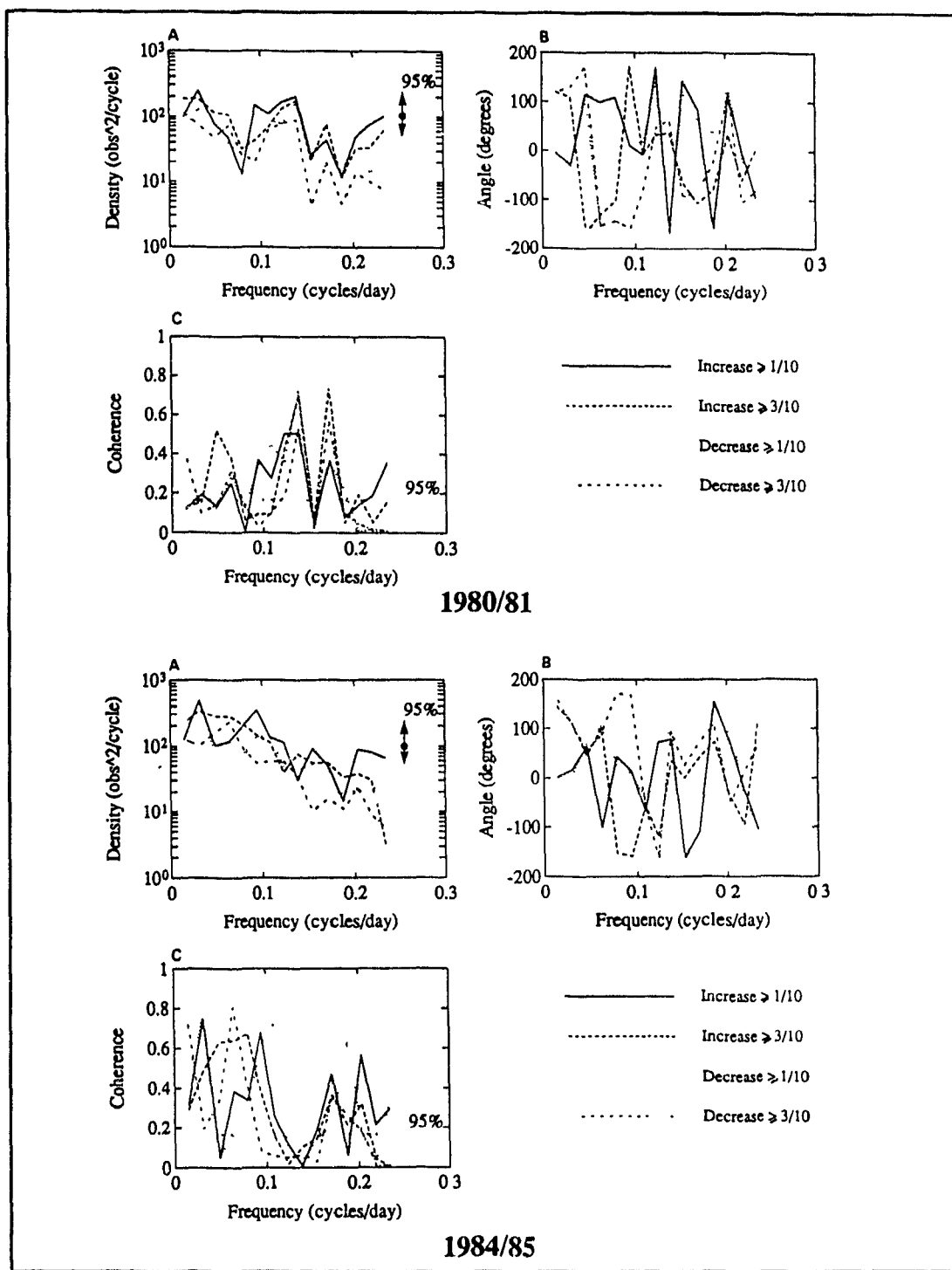


Figure 4.16 Cross Spectra, Coherence and Phase Plots Comparing Region Ice Concentration Change and 850 hPa Height at Goose Bay (a - cross spectra; b - phase angle; c - coherence)

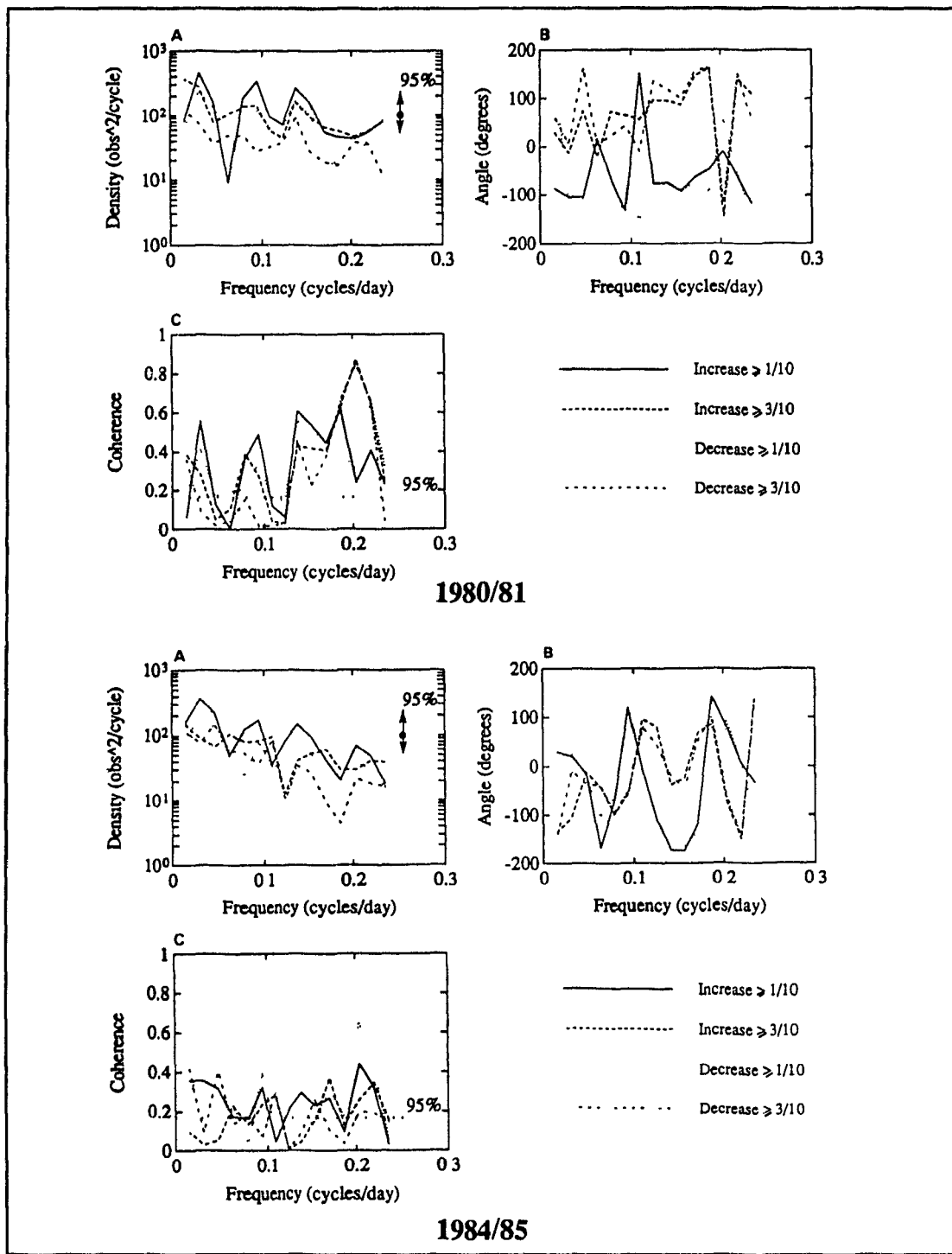


Figure 4.17 Cross Spectra, Coherence and Phase Plots Comparing Region Ice Concentration Change and 850 hPa Height at Iqaluit (a - cross spectra; b - phase angle; c - coherence)

Table 4.3 Ice Concentration/850 hPa Height Cross Spectral Relationship
(Using concentration change cell count time series)

Season/ Station	Spectral Peak (c/d)		Coherence		Phase (°)	
	Concentration Increase	Concentration Decrease	Concentration Increase	Concentration Decrease	Concentration Increase	Concentration Decrease
1980/81						
St. John's	0.14	0.14	0.3	0.2	40	-100
Goose Bay	0.14	0.14	0.6	0.6	-180	50
Iqaluit	0.14	0.14	0.6	0.4	-90	100
1984/85						
St. John's	0.09	0.09	0.5	0.8	-100	0
Goose Bay	0.09	0.09	0.5	0.6	100	-180
Iqaluit	0.09	0.09	0.7	0.5	-90	-90

been presented in a manner that provides one average value for the two concentration increase time series and one for the two decrease time series. A positive phase angle indicates that the ice change leads the upper air variability.

Figure 4.15 shows the relationships between the ice concentration change time series for the entire region and the upper air pressure level records for St. John's. For a given season, the four cross spectra (Figure 4.15a) show consistent behaviour, although interseasonal differences are evident. Similar relationships are observed for the Grand Banks and Iqaluit records (Figures 4.16 and 4.17).

The cross spectral information reveals the existence of subtle differences in the two ice seasons. In 1980/81 a mid-frequency spectral peak can be observed at approximately 0.14 c/d (7.1 days) in each upper air station/concentration time series

comparison. In 1984/85 a similar peak is evident, but at a frequency of approximately 0.09 c/d (11.1 days). The 11 day periodicity in the 1984/85 cross spectra and coherence plots is consistent with the 12 day periodicity in Nain atmospheric pressure and sea level observed by Garrett *et al.* (1985) during the 1971/72 winter season.

Both the coherence and phase information in Figures 4.15-4.17 and in Table 4.3 exhibit considerable variability across frequencies although the coherence is generally more consistent for a given station and season than is the phase angle. In addition, the phase angle exhibits much less consistency between cross spectra for the three upper air stations.

The summary information in Table 4.3 also indicates that coherences at the noted dominant frequencies are generally higher during the 1984/85 season for all stations. The lower coherences in 1980/81, when ice conditions were light, suggest that the meteorological conditions as represented by the 850 hPa height do not have as strong an influence on ice conditions as they do in 1984/85. The higher coherences associated with the Goose Bay and Iqaluit stations may be related to their central location relative to the study area as a whole.

The cross spectral information, although limited by the short data record, provides some insight into within-season ice/atmosphere interaction. It also suggests some important differences exist in this relationship when two contrasting ice seasons are compared.

Each of the cross spectra indicate a high level of energy at synoptic frequencies. Coherences at these frequencies indicate a relatively strong association between the 850 hPa height and ice concentration suggesting that synoptic scale atmospheric variability

has a distinct influence on ice cover dynamics.

The cross spectral information reveals important differences in the two ice seasons. A comparison of the two seasons shows that the dominant synoptic frequency is higher during the less severe ice season (1980/81). At the same time the coherence is somewhat lower. The combination of these two would seem to indicate that the ice cover was subjected to more frequent atmospheric disturbance but that the strength of the influence was somewhat less.

Chapter 5

ICE CONCENTRATION VARIATION WITH STORM EVENTS

The mapping and analysis of ice cover extent and concentration with the passage of individual storms provides a means of testing whether or not, as posed in Chapter 1, ice cover response can be related to storm characteristics.

5.1 Storm Classification

The evaluation of synoptic events in this study was based on storm track characteristics which have been described previously in Chapter 3. In order to relate synoptic atmospheric activity to ice conditions, it was necessary to generalize important synoptic patterns. This was done through the preparation a series of contingency tables. The contingency tables were used solely as a means of grouping the storm track data according to selected parameters. The parameters considered are shown in Table 5.1. Five storm parameters were considered:

- 1) the latitude at which the storm entered the study area,
- 2) its trajectory,
- 3) its duration in terms of the number of 6 hour observations,
- 4) storm intensity as measured by its minimum pressure, and
- 5) the pressure range exhibited by the storm,

all while the storm was in the study area.

Based on the contingency tables, a set of synoptic events were selected to provide a reasonable representation of storms during various stages of ice cover

development. The distribution of storms by category is shown in Table 5.2. A total of 31 storm periods were selected for analysis. While the time series analysis was limited to the 1980/81 and 1984/85 seasons, the evaluation of storm influences also included conditions south of 55°N during 1971/72 for which AES ice charts were available.

Table 5.1 Storm Classification Parameters

Parameter	Levels
Latitude of entry into study area	45-50, 50-60, 60-70°
Duration in study area (number of synoptic observations)	Low, Medium, High <10 10-<20 ≥20
Bearing of mean trajectory through study area	NW, SW, SE, NE
Intensity - minimum observed pressure in study area	Low, Medium, High <980 980-1000 ≥1000
Range in pressure while in study area	<10, 10-<20, 20-<30, 30-<40, ≥40

In general, the storms selected were of medium to high intensity, entered the study region at low to mid latitudes and remained for 10 to 20 synoptic observations. Storms with trajectories to the northeast predominated. Important statistical properties of the 31 storms are presented in Table 5.3. These include minimum observed storm centre pressure, pressure range, duration, entry latitude and longitude, exit latitude and storm trajectory.

Table 5.2 Distribution of Storm Events By Category

		Start Latitude			Duration(Obs)			Bearing (°T)				Pressure Range (hPa)				
		40-<50	50-<60	60-70	High	Med	Low	NW	SW	SE	NE	0-<10	10-<20	20-<30	30-<40	≥40
Storm Intensity	High	9	4	1	0	11	3	3	0	1	10	0	4	5	4	1
	Med	4	6	2	3	7	2	2	1	2	7	2	7	3	0	0
	Low	2	1	2	0	3	2	0	0	1	4	3	2	0	0	0
Start Latitude	40-<50				3	11	1	2	0	1	12	2	4	6	2	1
	50-<60				0	8	3	3	1	2	5	2	5	2	2	0
	60-70				0	2	3	0	0	1	4	1	4	0	0	0
Duration	High							1	0	0	2	0	1	2	0	0
	Med							3	1	4	14	4	8	5	2	1
	Low							1	0	1	5	1	4	0	2	0
Bearing	NW											1	3	0	0	0
	SW											0	1	0	0	0
	SE											0	2	0	1	0
	NE											3	7	7	3	1

Table 5.3 Statistical Summary of Selected Storms

Storm	Sdat	Obs	Minp	Rngp	Trj	Slat	Slong
72-1	02/07	7	975.1	11.2	35	60.3	43.2
72-2	02/26	10	973.2	29.3	61	47.3	68.5
72-3	04/19	17	967.9	45.8	2	43.3	42.8
72-4	04/30	12	980.4	21.0	74	54.9	55.4
72-5	06/06	20	994.6	15.1	352	40.3	55.8
80-1	11/05	12	958.9	33.8	320	54.9	52.3
80-2	11/24	7	1005.1	14.2	74	65.5	69.3
80-3	12/12	11	977.5	25.5	59	48.7	64.9
81-1	02/02	10	974.4	16.3	58	49.8	61.1
81-2	02/24	27	980.3	24.2	58	42.1	67.6
81-3	03/14	12	973.1	22.4	11	43.0	62.5
81-4	04/18	13	996.3	10.4	105	48.8	68.0
81-5	05/14	8	1002.2	11.9	77	52.4	65.5
81-6	06/06	15	984.0	10.1	97	53.3	68.0
81-7	06/13	16	1004.5	5.7	107	64.8	67.1
81-8	06/19	14	991.2	17.7	27	61.8	69.3
81-9	06/26	11	1000.6	4.2	64	47.8	68.5
84-1	11/16	10	979.1	14.2	284	56.7	41.3
84-2	12/03	9	993.8	6.9	360	55.9	68.1
84-3	12/05	9	963.8	36.5	54	42.6	68.3
84-4	12/15	7	980.7	12.5	82	64.4	62.4
85-1	01/17	11	979.3	12.9	298	44.8	42.0
85-2	01/21	19	949.6	36.0	19	47.2	57.3
85-3	02/26	9	978.0	30.7	101	56.3	62.0
85-4	03/14	14	968.6	29.0	65	52.0	62.5
85-5	04/20	11	993.7	15.9	214	50.1	40.9
85-6	05/03	13	977.7	27.7	53	40.2	66.5
85-7	06/02	13	988.5	17.6	52	56.1	66.1
85-8	06/08	24	986.2	22.3	62	40.1	69.8
85-9	07/07	11	1003.5	3.1	69	48.8	67.1
85-10	07/22	12	992.2	6.5	55	52.3	69.6

Sdat - date of entry into study region
 Obs - number of synoptic observations
 Minp - minimum observed pressure, hPa
 Rngp - range in storm centre pressure, hPa
 Trj - trajectory (degrees) from first to last observation, °T
 Slat - entry latitude, °N
 Slong - entry longitude, °W

A list of the storms is also provided in Appendix C complete with documentation of the appropriate SMMR or ice chart coverage available for each storm.

5.2 Ice Maps

Two factors were of interest in assessing storm influence on ice conditions; ice extent variation and concentration change within the ice pack. The former was considered by examining the changes in the ice limit through the storm period by contouring the limits of detected ice. Ice concentration variations were then investigated by plotting the difference in concentration between the first and last appropriate ice maps.

AES reconnaissance flights are irregular with the result that the time interval between ice maps is generally inconsistent. However for all 1972 storms selected, the interval between ice maps was two days with the exception of Storm 72-2 when maps were obtained for February 25 and March 1. In 1980/81 and 1984/85, the SMMR data permitted the generation of ice maps at regular 2 day intervals although in some cases because of gaps in the satellite data, it was necessary to edit the map if ice chart information was available.

The average storm duration was 12.7 synoptic observations or about 3.2 days. This varied from less than 2 days to about 8. Since storms varied in length, the number of snapshots of the ice cover also varied. If the storm start date did not coincide with the satellite or ice chart output, a map from the preceding day was also included to represent pre-storm conditions. For example, Storm 80-1 first appeared on

November 5 but satellite coverage was available on even days so that a map for the 4th was also utilized.

For each storm, the ice edge was calculated every time a set of ice conditions was available. This provided an indication of expansion or contraction of the ice edge. In addition, the difference in concentration from the beginning to end of the storm period was also calculated and plotted, showing internal changes in the ice pack composition. Concentrations changes were also binned at 1/10 intervals. Much of the study area remains ice free so that grid cells showing no change dominated. Map output and histograms were produced for each of the storms and are included in Appendix D.

5.3 Evaluation of Ice Cover Response

5.3.1 Ice Cover Dynamics

An initial analysis of the output in Appendix D indicates that the ice cover is highly dynamic and is apparently responsive to synoptic conditions. For the purpose of further evaluation, three general stages of ice development were considered:

- 1) **Early season** - ice is limited to the northern portion of the study area; generally north of 60°N.
- 2) **Mid-season** - ice pack is fully developed, extending along the Labrador coast to the Grand Banks.
- 3) **Late season** - ice pack is deteriorating and the ice limit retreating northward.

Figure 5.1 depicts the three general scenarios graphically. A selection of

examples from the 31 storms also illustrates the three typical stages of development. In Figure 5.2 it is early to mid-season. The ice pack has developed to a point where the ice edge extends from the northern tip of Labrador, northeast to the Greenland coast by late November. With the passing of a low intensity storm (Storm 80-3) north of the ice edge, the ice limit shows a moderate advance from November 24 to November 28.

Figure 5.3 shows mid-season conditions and the impact of Storm 85-2 (late January 21 to January 25) on ice conditions. The ice edge plot shows variations in the ice edge off the Labrador coast with largely stable edge position along the southeast ice limit. At the same time, concentration changes from just prior to the storm to just after (January 26) indicate areas of concentration increase from approximately 60-50°N. Inshore, concentration increases are as high as 6/10 while in the ice edge region, changes are on the order of 3/10. North of 60°N, ice concentrations decrease eastward to the southern tip of Greenland. This pattern is evident in many of the situations where mid-season ice pack is exposed to a synoptic disturbance.

Figure 5.4 provides an example of late season ice conditions along the southern Labrador and Newfoundland coasts. A storm with an almost due north trajectory has little effect on the ice edge position but at the same time concentration changes within the pack are significant with decreases in concentration as high as 6/10. In this southern area 26% of the grid cells show decreases in concentration with 12% exhibiting increases to 2/10. The increases are along the Labrador coast, suggesting some inshore convergence with the northward movement of the storm.

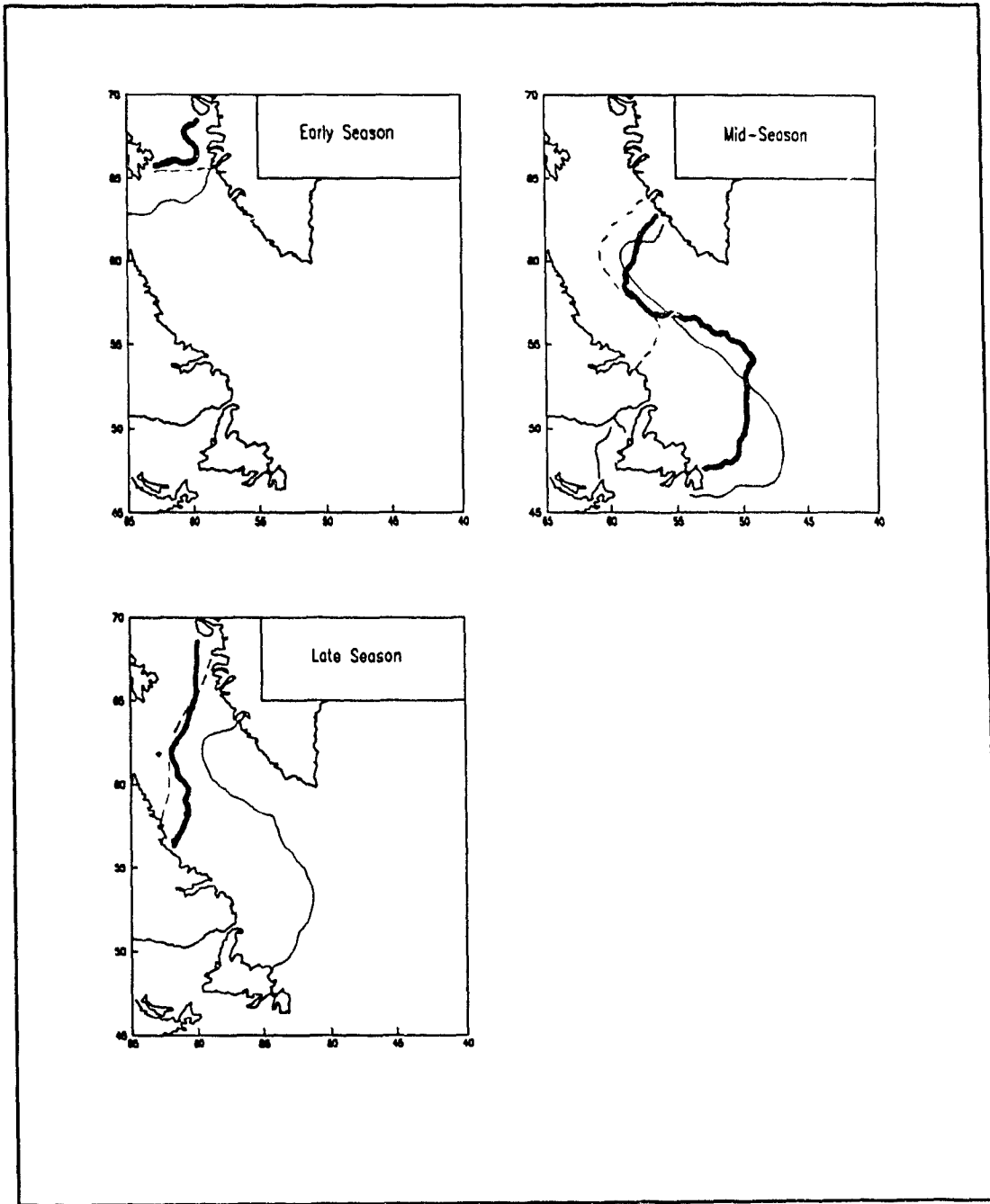
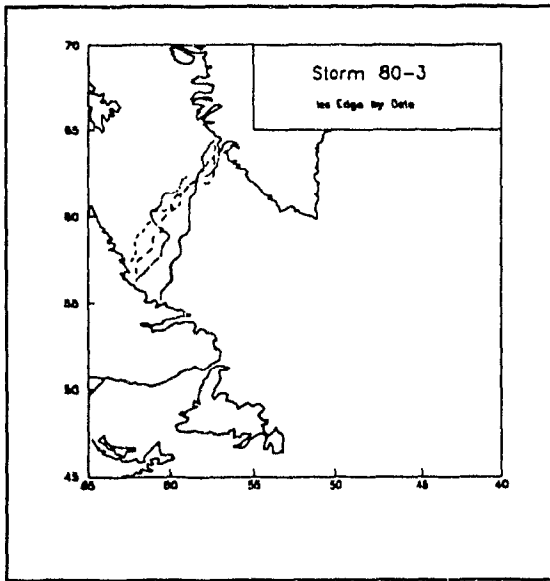


Figure 5.1 Generalized Stages of Ice Cover Development
 (Heavy line - Average; Dashed Line - 1980/81; Solid - 1984/85)



Storm 80-3	
Minimum Pressure.	977.5 hPa
Pressure Range.	25.5 hPa
Storm Bearing:	59.0°T
Entry Latitude:	48.7°N
Entry Longitude:	64.9°W
Duration:	11 Obs
Ice Map/SMMR Dates:	12/12,12/14,11/16,12/18
Cells Increasing in Concentration:	15%
Cells Decreasing in Concentration.	4%

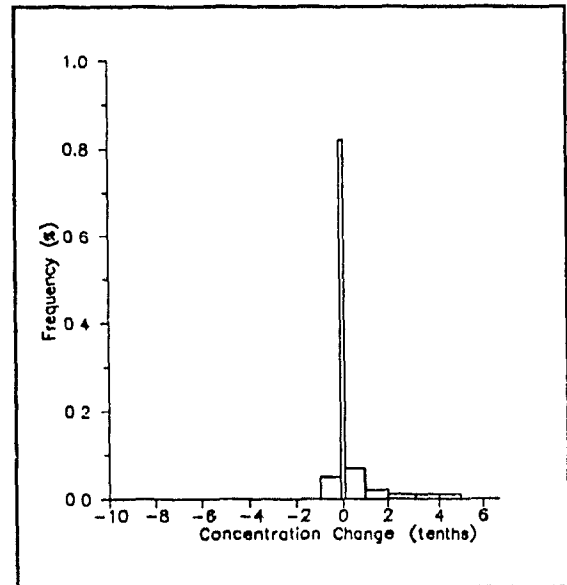
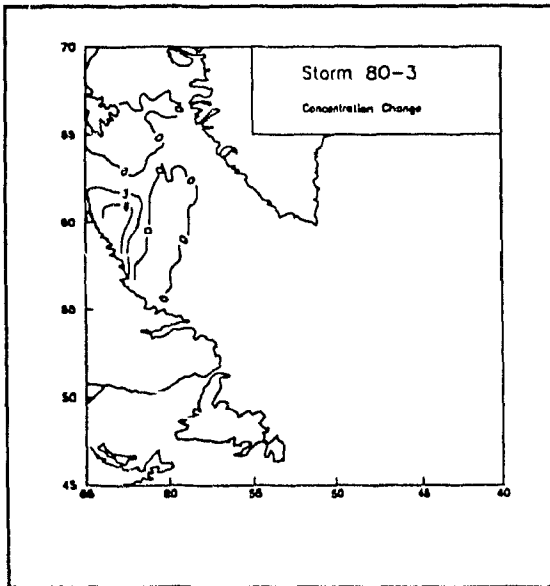
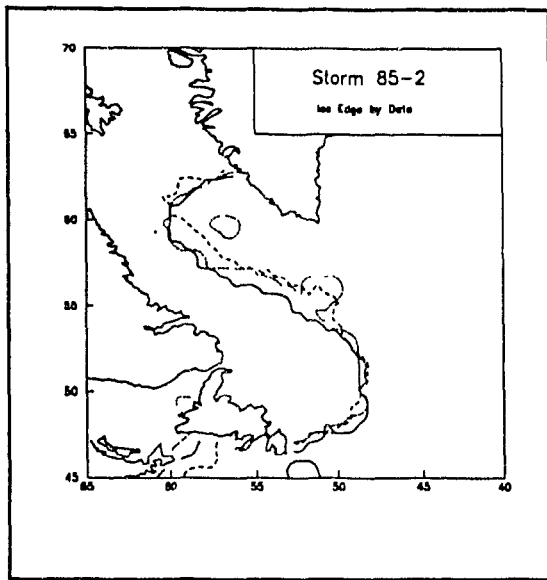


Figure 5.2 Example of Ice Dynamics During Early to Mid-Season - Storm 80-3
 (Line patterns for the ice edge plots progress by orbit from solid to coarse, medium and fine dashes)



Storm 85-2	
Minimum Pressure:	949.6 hPa
Pressure Range:	36.0 hPa
Storm Bearing:	19.0°T
Entry Latitude:	47.2°N
Entry Longitude:	57.3°W
Duration:	19 Obs
Ice Map/SMMR Dates:	01/20,01/23,01/26
Cells Increasing in Concentration:	25%
Cells Decreasing in Concentration:	14%

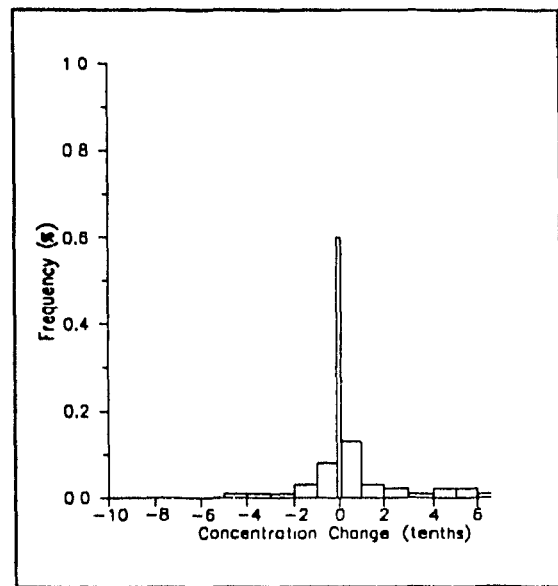
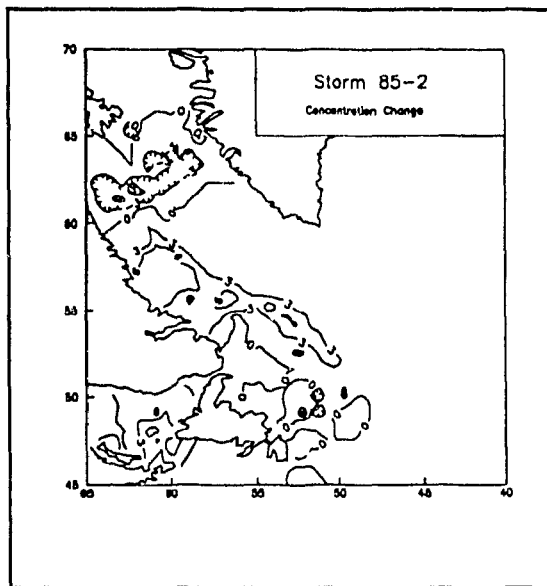
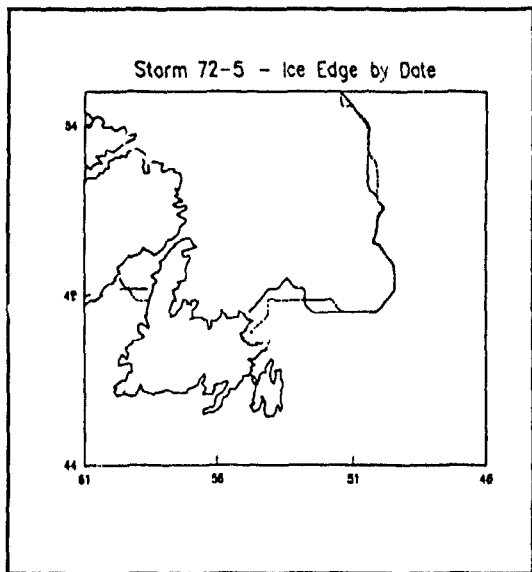


Figure 5.3 Example of Ice Dynamics During Mid-season - Storm 85-2
 (Line patterns for the ice edge plots progress by orbit from solid to coarse, medium and fine dashes)



Storm 72-4

Minimum Pressure: 980.4 hPa
 Pressure Range: 21.0 hPa
 Storm Bearing: 74.0°T
 Entry Latitude: 54.9°N
 Entry Longitude: 55.4°W
 Duration: 12 Obs

Ice Map/SMMR Dates: 05/01,05/03

Cells Increasing in Concentration: 16%
 Cells Decreasing in Concentration: 23%

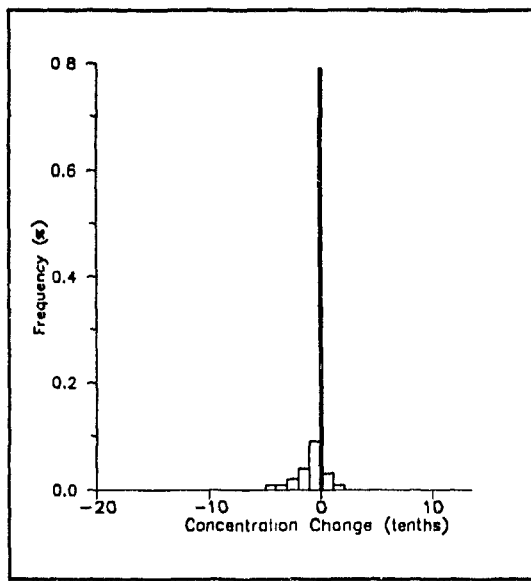
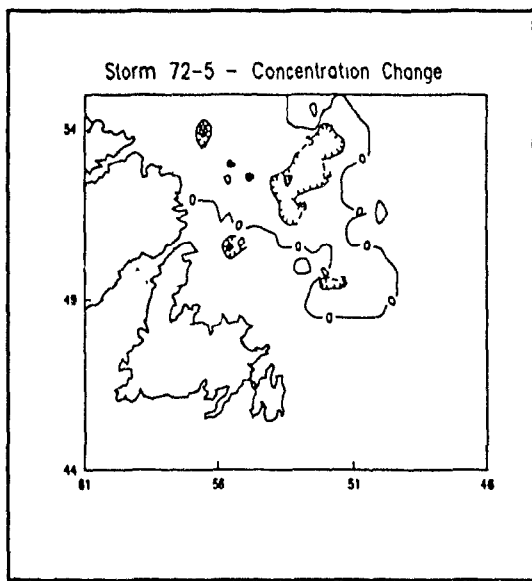


Figure 5.4 Example of Ice Dynamics During Late Season - Storm 72-5
 (Line patterns for the ice edge plots progress by orbit from solid to coarse, medium and fine dashes)

For a given storm, areas of both convergence and divergence can be observed, especially during mid-season when the ice cover is near its maximum extent. With expansion of the ice edge, there is a frequent occurrence of ice divergence inshore which can lead to reduced ice concentrations.

In order to evaluate these apparent relationships, a simple method was developed to measure changes in the ice edge position. The approach entailed measuring the direction of edge movement between the first and last SMMR-derived maps. Movement was noted to be positive if the edge advanced offshore, negative if it retreated shoreward and stationary if the net change was zero. This was done for each storm, one row of the gridded ice cover at a time. For the 1972 storms there were 33 rows and for the remainder, 50 rows. The number of rows showing advancing, retreating or steady edge position were accumulated for each storm, providing a rough indication of overall ice edge movement.

Table 5.4 shows both the proportion of grid cells experiencing concentration increases and decreases and the results of the ice edge evaluation for each storm period. Consistently, the pattern is, through early season and into mid-season, cells showing concentration increases are higher than those showing decreases, consistent with overall expansion of the ice cover as well as ice growth during this period. In the late season stage, the progression is to greater percentages showing concentration decreases as the ice pack deteriorates and the ice edge retreats.

A quantitative evaluation using the ice edge and concentration data in Table 5.4 indicates that the strength of the relationships between concentration and ice edge movement are weak. Figure 5.5 compares concentration increase versus edge advance

Table 5.4 Ice Concentration Changes and Edge Movement for Selected Storms

Storm	Edge Changes (number of rows)			Concentration Changes (%)	
	Advance	Steady	Retreat	Cells Increasing	Cells Decreasing
72-1	16	17	0	30	11
72-2	10	11	12	20	24
72-3	13	15	5	19	19
72-4	17	15	1	16	23
72-5	5	27	1	12	26
80-1	1	42	7	1	3
80-2	12	38	0	11	0
80-3	6	29	15	15	4
81-1	21	13	16	7	20
81-2	5	18	27	13	21
81-3	9	13	28	4	21
81-4	10	23	17	7	15
81-5	9	26	15	12	12
81-6	3	25	22	6	17
81-7	0	28	22	0	12
81-8	14	34	2	6	1
81-9	17	30	3	12	0
84-1	13	37	0	7	0
84-2	1	46	3	8	5
84-3	7	43	0	9	2
84-4	15	33	2	17	5
85-1	19	13	18	23	15
85-2	18	17	15	25	14
85-3	24	16	10	29	15
85-4	17	19	14	16	28
85-5	11	28	11	12	21
85-6	5	25	20	6	18
85-7	5	20	25	7	20
85-8	3	25	22	7	21
85-9	10	23	17	5	8
85-10	1	44	5	0	3

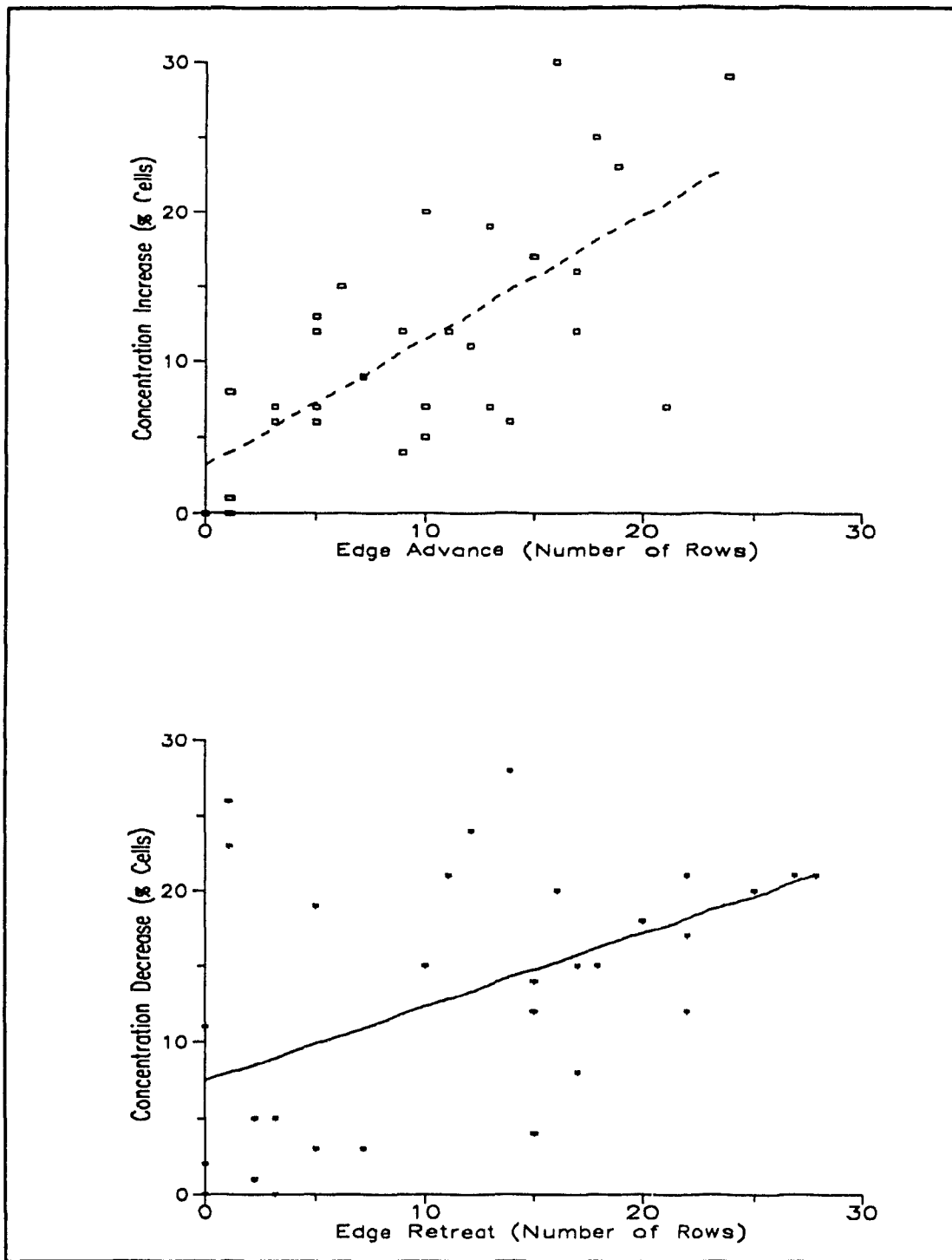


Figure 5.5 Scatter Plot Showing Concentration Increase vs. Edge Advance and Concentration Decrease vs. Edge Retreat with Least Squares Fit

Table 5.5
Results of Regression Analysis of Ice Edge Movement
on Concentration Change

1. Ice Edge Advance vs. Concentration Increase

Dependent var: Concentration Increase Independent var: Edge Advance

Parameter	Estimate	SE	T	Prob.
Intercept	3.24	1.98	1.64	.11205
Slope	0.83	0.16	5.04	.00002

Analysis of Variance

Source	Sum of Squares	Df	Mean Square	F-Ratio	Prob.
Model	868.14	1	868.14	25.36	.00002
Error	992.63	29	34.23		
Total (Corr.)	1860.77	30			

Correlation Coefficient = 0.68
 Std. Error of Est. = 5.85

$R^2 = 46.7$ percent

2. Ice Edge Retreat vs. Concentration Decrease

Dependent var: Concentration Decrease Independent var: Edge Retreat

Parameter	Estimate	SE	T	Prob.
Intercept	7.47	2.24	3.34	.00234
Slope	0.49	0.15	3.14	.00385

Analysis of Variance

Source	Sum of Squares	Df	Mean Square	F-Ratio	Prob.
Model	576.64	1	576.64	9.87	.00385
Error	1694.33	29	58.43		
Total (Corr.)	2270.97	30			

Correlation Coefficient = 0.50
 Std. Error of Est. = 7.64

$R^2 = 25.39$ percent

and concentration decrease versus ice edge retreat with the least squares linear fits also shown. An examination of the residuals indicated that in both cases the scatter about zero was quite random although there was a slight indication of non-random scatter in the case of the edge advance vs. concentration increase analysis. It would seem from the residual information that a linear fit to the data is reasonable in both cases. In both cases however, the data are widely scattered about the best fit line. Statistics for the two linear models provided in Table 5.5, confirm that the model of concentration increase versus edge advance can only account for 47% of the variance in concentration increase. In the case of concentration decrease, a retreating ice edge only accounts for 25% of the concentration variance.

It must be emphasized that in this context, use of the terms concentration increase or decrease, refers to the percentage of grid cells showing a change in concentration, either increasing or decreasing. It seems reasonable therefore, that as the ice extent increases with an advancing ice edge, more cells would show increases in concentration and vice versa. The low R^2 values suggest, either the technique for monitoring ice edge movement is not sufficiently sensitive to ice dynamics, or that perhaps internal dynamics within the ice pack are not consistent with a direct relationship between concentration increase and ice edge advance. The relatively coarse resolution of the SMMR data makes prohibits a conclusive assessment of these observations. However, the latter may be the case, as the concentration change maps in Appendix D often exhibit areas of ice divergence within the pack in association with an advancing ice edge.

5.3.2 Correlation of Ice Cover Dynamics with Storm Events

Although the ice edge and concentration change maps in Appendix D clearly indicate the dynamic nature of the ice cover, it is not immediately evident whether, or to what extent, these changes are related to the associated storms. A step-wise multiple regression was used to evaluate concentration increase and decrease and ice edge advance and retreat individually against storm duration, intensity, range in pressure, start latitude and start longitude. Trajectory was not included, instead the u (westerly) and v (southerly) velocity components of the storm track were calculated and incorporated into the model. Each storm variable was given equal weight in the model. The model results are shown in Table 5.6 for each of the four ice parameters. In all cases, highest correlations were achieved with only one or two of the storm variables. The highest R^2 value was with the model for concentration increase where R^2 was 38% using storm start longitude and the u velocity component. Storm parameters were also able to explain over 30% of the edge advance variability ($R^2 = 31\%$). Several authors have noted similar correlations between meteorological conditions and ice variability (Thorndike and Colony, 1982; Ikeda *et al.*, 1988; Nazarenko and Miller, 1986).

R^2 values for the multiple regressions were considerably lower for concentration decrease and ice edge retreat (18% and 19% respectively), suggesting that the dynamic storm parameters used here may be less important in their influence on this ice behaviour during periods of ice retreat. The role of thermodynamic effects on marginal ice cover variability has been noted previously at both seasonal (Ikeda *et al.*, 1988) and synoptic scales (Andreas, 1985) and may have some importance here as well.

Table 5.6
Multiple Regression of Storm Variables on Ice Concentration
and Edge Movement

1. Model fitting results for: Concentration Increase

Independent	Coefficient	Std. Error	t-value	Sig.Level
CONSTANT	43.01	7.81	5.50	0.0000
<i>u</i>	-0.24	0.07	-3.45	0.0018
Start Longitude	-0.59	0.14	-4.33	0.0002

Analysis of Variance for the Full Regression

Source	Sum of Squares	DF	Mean Square	F-Ratio	P
Model	790.43	2	395.22	10.34	.0004
Error	1070.34	28	38.23		
Total (Corr.)	1860.77	30			

$R^2 = 0.42$ Std. error of est. = 6.18

R^2 (Adj. for d.f.) = 0.38

2. Model fitting results for: Concentration Decrease

Independent	Coefficient	Std. Error	t-value	Sig.Level
CONSTANT	2.26	4.13	0.55	0.0588
Duration	0.85	0.31	2.77	0.0096

Analysis of Variance for the Full Regression

Source	Sum of Squares	DF	Mean Square	F-Ratio	P
Model	475.62	1	475.62	7.68	.0096
Error	1795.34	29	61.91		
Total (Corr.)	2270.97	30			

$R^2 = 0.21$ Std. error of est. = 7.86

R^2 (Adj. for d.f.) = 0.18

Table 5.6 continued

3. Model fitting results for: Ice Edge Advance

Independent	Coefficient	Std. Error	t-value	Sig.Level
CONSTANT	33.63	6.83	4.93	0.0000
u	-0.19	0.06	-3.10	0.0044
Start Longitude	-0.45	0.12	-3.72	0.0009

Analysis of Variance for the Full Regression

Source	Sum of Squares	DF	Mean Square	F-Ratio	P
Model	458.32	2	229.16	7.85	.0020
Error	817.10	28	29.18		
Total (Corr.)	1275.42	30			

$R^2 = 0.36$ Std. error of est. = 5.40

R^2 (Adj. for d.f.) = 0.31

4. Model fitting results for: Ice Edge Retreat

Independent	Coefficient	Std. Error	t-value	Sig.Level
CONSTANT	46.66	12.03	3.88	0.0006
v	-0.22	0.10	2.08	0.0472
Start Latitude	0.63	0.22	-2.85	0.0081

Analysis of Variance for the Full Regression

Source	Sum of Squares	DF	Mean Square	F-Ratio	P
Model	600.24	2	300.21	4.56	.0194
Error	1845.25	28	65.90		
Total (Corr.)	2445.68	30			

$R^2 = 0.25$ Std. error of est. = 8.12

R^2 (Adj. for d.f.) = 0.19

The low R^2 values suggest that the meteorological information obtained from the storm track data cannot, in and of itself, be used to explain with a high level of certainty, the variability in ice cover. Ideally, gridded meteorological information over the entire study area is probably necessary in order to account for more of the pack ice dynamics.

Chapter 6

CONCLUSIONS

In this thesis, the behaviour of the seasonal ice cover off Canada's east coast was examined in relation to synoptic scale atmospheric events. The overall objective was to assess the influence meteorological conditions played in the high frequency variability of the ice cover.

A prerequisite to a study of this nature was the availability of regional ice information at a suitable repetitive frequency. Ice concentration information derived from satellite passive microwave measurements of surface brightness temperatures offered a potential source for this information. The data collected by the Nimbus-7 SMMR provided coverage of the study area every second day - within the time scale of synoptic meteorological events. This information was supplemented with data derived from AES composite ice charts, providing ice documentation for the 1971/72, 1980/81 and 1984/85 ice seasons. Two of the ice seasons were selected because the annual ice extent off the east coast was greater than average and the other because ice extent was less than normal.

Atmospheric variability was monitored using the 850 hPa height at three upper air stations along the western edge of the study region. Additional information was drawn from storm track records, providing an indication of surface variability. Properties of specific storm events were obtained from the storm track data, permitting evaluation of the ice response to passing synoptic disturbances.

The results of this investigation have clarified questions raised in Chapter 1 in

several ways:

- i) Passive microwave-based ice information can be used to monitor high frequency variability in the marginal ice zone in a general manner despite noted difficulties in the ability of ice algorithms to determine the true ice edge position. The modified orbit of the more recent Special Sensor Microwave/Imager and its ability to provide daily coverage would improve this capability. The incorporation of information from the SSM/I's 85 GHz channel will also be of benefit in that it will provide finer footprint resolution.
- ii) The ability to establish periodicities in the ice cover variation is limited by the short time series for each season as well as the orbit-related data gaps in the SMMR data coverage. Band filtering can alleviate the latter problem to some extent with the result that the periodicities exhibited in the ice concentration change data appear consistent with those observed in the meteorological records of synoptic disturbances. Despite the limited record length, periodicities on the order of 7-12 days were observed; consistent with those documented in the literature.
- iii) The cross spectral relationships between ice concentration variability and 850 hPa pressure height indicate a strong association between the two at synoptic frequencies. Comparison of the two years also shows clear differences in the dominant synoptic frequency with the lighter ice year (1980/81) associated with more frequent synoptic activity. At the same time, the coherence between ice variability and pressure height was

slightly lower during this season.

- iv) The short-term advance of the seasonal sea ice zone ice edge can account for approximately 47% of the spatial increase in ice concentration, however divergent behaviour is often evidenced by reduced ice concentrations within the ice pack. Tendencies are not as strong for net area decreases in concentration with a retreating ice edge, suggesting that convergence within the ice pack offsets the net reduction in concentration along the ice edge.
- v) The relationship between ice cover variability and the passage of synoptic events, as described by the storm track data, is strongest for ice concentration increases and ice edge advance. Multiple regression of storm track parameters can account for up to 38% of the ice variability in the case of concentration increase variability and 30% of the edge advance. The results of this analysis suggest that atmospheric dynamics are not as important during periods of ice concentration decrease and when the ice edge is retreating. Ikeda *et al.* (1988) noted the importance of temperature in controlling seasonal ice flux along the Labrador coast and Andreas (1985), in analyzing heat and moisture advection over Antarctic sea ice, identified the existence of a thermodynamic relationship between sea ice extent and synoptic-scale atmospheric conditions.
- vi) Although in one context the temporal resolution of the SMMR-derived ice data is adequate, it may still be too coarse in relation to synoptic scale atmospheric variability. This would appear to be a major limitation

to further investigation of feedback effects at synoptic scales, based on the SMMR-derived ice information. In addition, an analysis of feedback relations, over spatial scales considered in this thesis, would benefit from gridded surface meteorological information.

BIBLIOGRAPHY

- Ackley, S.F. and T.E. Keliher. 1976. *Antarctic sea ice dynamics and its possible climatic effects*. AIDJEX Bulletin 33, 53-76.
- Allingham, A.M., K. Hamilton and L.A. Mysak. 1987. Climatic Atlas of the North Atlantic - Seasonal Sea Level Pressures and Sea Surface Temperature Anomalies, 1919-1979. Climate Research Group Rpt. 87-4. Department of Meteorology, McGill University. 248 pp.
- Andreas, E.L. 1985. *Heat and moisture advection over Antarctic sea ice*. Mon. Wea. Rev. 113, 736-746.
- Barry, R.G. 1986. Aspects of the meteorology of the seasonal ice zone. In: The Geophysics of Sea Ice. N. Untersteiner, ed. Plenum Publishing Corporation. pp. 993-1020.
- Barry, R.G. 1980. *Meteorology and climatology of the seasonal ice zone*. Cold Regions Science and Technology 2, 133-150.
- Barry, R.G. and A.H. Perry. 1973. Synoptic Climatology: Methods and Applications. Methuen & Co., London.
- Barry, R.G., R.S. Bradley and J.D. Jacobs. 1975. *Synoptic climatological studies of the Baffin Island area*, in Climate of the Arctic. University of Alaska. pp. 82-90.
- Bendat, J.S. and A.G. Piersol. 1980. Engineering Applications of Correlation and Spectral Analysis. John Wiley and Sons. 302 pp.
- Birch, J.R., D.B. Fissel and J.R. Marko. 1983. An Analysis of Surface Drifters and Iceberg Motion off Labrador in Winter: Volume 1. Report prepared by Arctic Sciences Ltd. on behalf of the Labrador Group of Companies.
- Brown, R.D., P. Roebber and K. Walsh. 1986. Climatology of Severe Storms Affecting Coastal Areas of Eastern Canada. ESRF Report No. 020. Department of Indian and Northern Development. 233 pp.
- Budd, W.F. 1975. *Antarctic sea-ice variations from satellite sensing in relation to climate*. J. Glaciology 15(73), 417-427.
- Bursey, J.O., W.J. Snowden, A.D. Gates and C.L. Blackwood. 1977. *The climate of the Labrador Sea*. POAC-77, St. John's, Newfoundland, September 26-30, 1977. pp. 938-951.

- Cahalan, R.F. and L.G. Chiu. 1986. *Large-scale short-period sea ice interaction*. J. Geophysical Res. 91(C9), 10709-10717.
- Campbell, W.J., J. Wayenberg, J.B. Ramseyer, R.O. Ramseier, M.R. Vant, R. Weaver, A. Redmond, L. Arsenault, P. Gloersen, H.J. Zwally, T.T. Wilheit, T.C. Chang, D. Hall, L. Gray, D.C. Meeks, M.L. Bryan, F.T. Barath, C. Elachi, F. Leberl and T. Farr. 1978. *Microwave remote sensing of sea ice in the AIDJEX main experiment*. Boundary-Layer Meteorology 13, 309-337.
- Campbell, W.J., R.O. Ramseier, H.J. Zwally and P. Gloersen. 1980. *Arctic sea-ice variations from time-lapse passive microwave imagery*. Boundary-Layer Meteorology 18, 99-106.
- Campbell, W.J., P. Gloersen, H.J. Zwally, R.O. Ramseier and C. Elachi. 1977. *Simultaneous passive and active microwave observations of near-shore Beaufort Sea ice*. Proceedings, 9th Annual Offshore Technology Conference, Houston, Texas, May 2-5, 1977. pp 287-294.
- Carleton, A.M. 1981. *Ice-ocean-atmosphere interaction at high southern latitudes in winter from satellite observation*. Aust. Met. Mag. 29, 183-195.
- Carleton, A.M. 1983. *Variations in Antarctic sea ice conditions and relationships with southern hemisphere cyclonic activity, winter 1973-1977*. Arch. Met. Geoph. Biocl., Ser. B 32, 1-22.
- Carleton, A.M. 1984a. *Synoptic sea ice-atmosphere interactions in the Chukchi and Beaufort Seas from Nimbus 5 ESMR data*. J. Geophysical Res. 89(D5), 7245-7258.
- Carleton, A.M. 1984b. *Cloud-cryosphere interactions*, in, Satellite Sensing of a Cloudy Atmosphere, Observing the Third Planet. A. Henderson-Sellers (ed.). Taylor & Francis, London. pp. 239-325.
- Carleton, A.M. 1985a. *Synoptic cryosphere-atmosphere interactions in the northern hemisphere from DMSP image analysis*. Int. J. Remote Sensing 6(1), 239-261.
- Carleton, A.M. 1985b. *Satellite climatological aspects of the 'polar low' and 'instant occlusion'*. Tellus 37A, 433-450.
- Carleton, A.M. 1987. *Summer circulation climate of the American southwest*. Annals of the American Association of Geographers 77(4), 619-634.
- Carleton, A.M. 1988. *Sea ice-atmosphere signal of the Southern Oscillation in the Weddell Sea, Antarctica*. Journal of Climatology 1(4), 379-388.

- Carsey, F.D. 1982. *Arctic Sea ice distribution at end of summer 1973-1976 from satellite microwave data*. J. Geophysical Res. 87(C8), 5809-5835.
- Cavalieri, D.J., P. Gloersen and W.J. Campbell. 1984. *Determination of sea ice parameters with NIMBUS 7 SMMR*. J. Geophysical Res. 89(D4), 5355-5369.
- Cavalieri, D.J., S. Martin and P. Gloersen. 1983. *Nimbus 7 SMMR observations of the Bering Sea ice cover during March 1979*. J. Geophysical Res. 88(C5), 2743-2754.
- Cavalieri, D.J. and C.L. Parkinson. 1981. *Large scale variation in observed Antarctic sea ice extent and associated atmospheric circulation*. Mon. Wea. Rev. 109, 2323-2336.
- Cavalieri, D.J. and C.L. Parkinson. 1987. *On the relationship between atmospheric circulation and the fluctuations in the sea ice extents of the Bering and Okhotsk Seas*. J. Geophysical Res. 92(C7), 7141-7162.
- Comiso, J.C. 1983. *Sea ice effective microwave emissivities from satellite passive microwave and infrared observations*. J. Geophysical Res. 88(C12), 7686-7704.
- Comiso, J.C. and H.J. Zwally. 1982. *Antarctic sea ice concentrations inferred from Nimbus 5 ESMR and LANDSAT imagery*. J. Geophysical Res. 87(C8), 5836-5844.
- Crane, R.G. 1978. *Seasonal variations of sea ice extent in the Davis Strait - Labrador Sea area and relationships with synoptic-scale atmospheric circulation*. Arctic 31(4), 434-447.
- Crane, R.G. 1983. *Atmosphere-sea ice interactions in the Beaufort/Chukchi Sea and in the European sector of the Arctic*. J. Geophysical Res. 88(C7), 4505-4523.
- Davies, H.C. 1975. *Climatic change, orography and geostrophic motion*. Arch. Met. Geoph. Biokl. 23B, 1-12.
- Dey, B. 1980. *Sea ice cover and related atmospheric conditions in Arctic Canada during the summer of 1978*. Mon. Wea. Rev. 108, 2092-2097.
- Digby-Argus, S., F. Carsey and B. Holt. 1988. *Wind current and swell influences on the ice extent and flux in the Grand Banks-Labrador Sea area as observed in the LIMEX '87 experiment*. Second Conference on Polar Meteorology. Madison, Wisc. March 29-31, 1988. pp 11-14.
- Feldman, U., P.J. Howarth and J.A. Davies. 1979. *Estimating the surface wind speed over drifting pack ice from surface weather charts*. Boundary-Layer Meteorology 16, 421-429.

- Garrett, C., F. Moujaess and B. Toulany. 1985. *Sea level response at Nain, Labrador, to atmospheric pressure and wind*. Atmosphere-Ocean 23, 95-117.
- Gloersen, P. and F.T. Barath. 1977. *A scanning multichannel microwave radiometer for Nimbus-G and Seasat-A*. IEEE. J. Oceanic Eng. OE-2, 172-178.
- Gloersen, P. and D.J. Cavalieri. 1986. *Reduction of weather effects in the calculation of sea ice concentration from microwave radiances*. J. Geophysical Res. 91(C3), 3913-3919.
- Gloersen, P., H.J. Zwally, A.T.C. Chang, D.K. Hall, W.J. Campbell and R.O. Ramseier. 1978. *Time-dependence of sea-ice concentration and multiyear fraction in the Arctic basin*. Boundary-Layer Meteorology 13, 339-359.
- Gloersen, P., D.J. Cavalieri, A.T.C. Chang, T.T. Wilheit, W.J. Campbell, O.M. Johannessen, K.B. Katsaros, K.F. Kuzni, D.B. Ross, D. Staelin, E.P.L. Windsor, F.T. Barath, P. Gudmandsen, E. Langham and R.O. Ramseier. 1984. *A summary of results from the first NIMBUS 7 SMMR observations*. J. Geophysical Res. 89(D4), 5335-5344.
- Gordon, A.L. and H.W. Taylor. 1974. *Seasonal changes of Antarctic sea ice cover*. Science 187, 346-347.
- Hayden, B.P. 1981. *Cyclone occurrence mapping: equal area or raw frequencies?* Mon. Wea. Rev. 109, 168-172.
- Henderson, D.A. 1980. Evaluation of the Accuracy of SMMR Derived Ice Concentrations Produced for the Labrador Coast During the Operational Demonstration Period: January, 15 - March, 31, 1980. Atmospheric Environment Service, Ice Product Development Division and Ice Research and Development. pp 36.
- Herman, G.F. and W.T. Johnson. 1978. *The sensitivity of the general circulation to Arctic sea ice boundaries: a numerical experiment*. Mon. Wea. Rev. 106, 1649-1659.
- Hibler, W.D. and S.F. Ackley. 1983. *Numerical simulation of the Weddell Sea pack ice*. J. Geophysical Res. 88(C5), 2873-2887.
- Howarth, D.A. 1983. *An analysis of the variability of cyclones around Antarctica and their relationship to sea-ice extent*. Annals of the Association of American Geographers 73(4), 519-537.
- Ikeda, M., G. Symonds and T. Yao. 1988. *Simulated fluctuations in annual Labrador Sea ice cover*. Atmosphere-Ocean, 26(1), 16-39.

- Jacobs, J.D. and J.P. Newell. 1979. *Recent year-to-year variations in seasonal temperatures and sea ice conditions in the Eastern Canadian Arctic*. Arctic 32(4), 345-354.
- Jenkins, G.M. and D.G. Watts. 1968. Spectral Analysis and its Applications. Holden-Day, Inc. 525 pp.
- Johnson, C.M. 1980. *Wintertime Arctic sea ice extremes and the simultaneous atmospheric circulation*. Mon. Wea. Rev. 108, 1782-1791.
- Jordan, F. and H.J.A. Neu. 1982. *Ice drift in southern Baffin Bay and Davis Strait*. Atmosphere-Ocean 20(3), 268-275.
- Kalkstein, L.S. and P. Conigan. 1986. *A synoptic climatological approach for geographical analysis: assessment of sulphur dioxide concentrations*. Annals of the Association of American Geographers 76(3), 381-395.
- Keely, J.R. 1979. *Geostrophic calculations of the Labrador Current*. Proceedings of the Symposium on Research in the Labrador coast and offshore region, May 8-10, 1979. MUN. pp. 207-218.
- Keen, R.A. 1977. *The response of Baffin Bay ice conditions to changes in atmospheric circulation patterns*. Fourth International Conference on Port and Ocean Engineering under Arctic Conditions. Memorial University of Newfoundland, September 26-30, 1977 pp 963-971.
- Kellogg, W.W. 1975. *Climatic feedback mechanisms involving the polar regions*, in Climate of the Arctic. University of Alaska. pp. 114-129.
- Ketchum, R.D. and A.W. Lohanick. 1980. *Passive microwave imagery of sea ice at 33 GHz*. Remote Sensing of Environment 9, 211-223.
- Koch, S.E. and R.E. Gohus. 1988. *A mesoscale gravity wave event observed during CCOPE. Phase I: Multiscale statistical analysis of wave characteristics*. Mon. Wea. Rev. 116, 2527-2544.
- Kutzbach, J.E. 1967. *Empirical eigenvectors of sea-level pressure, surface temperature and precipitation complexes over North America*. J. Applied Meteorol. 6, 791-802.
- LeBlond, P.H. 1982. *Satellite observations of Labrador Current undulations*. Atmosphere-Ocean 20(2), 129-142.
- LeDrew, E.F. 1980. *Eigenvector analysis of the vertical field over the Eastern Canadian Arctic*. Mon. Wea. Rev. 108, 1992-2005.

- LeDrew, E.F. 1983. *The dynamic climatology of the Beaufort to Laptev Sea sector of the polar basin for the summers of 1975 and 1976*. Journal of Glaciology 3, 335-359.
- Lemke, P. 1986. *Stochastic description of atmosphere - sea ice - ocean interaction*. In: The Geophysics of Sea Ice. N. Untersteiner ed. Plenum Publishing Corp. pp. 785-823.
- Lemke, P., E.W. Trinkl and K. Hasselmann. 1980. *Stochastic dynamic analysis of polar sea ice variability*. J. Physical Oceanography 10, 2100-2120.
- Manak, D.K. and L.A. Mysak. 1987. Climatic atlas of Arctic sea ice extent and anomalies, 1953-1984. Climate Research Group Rpt 87-8. Department of Meteorology, McGill University. 214 pp.
- Manak, D.K. and L.A. Mysak. 1989. *On the relationship between Arctic sea ice anomalies and fluctuations in norther Canadian air temperatures and river discharge*. Atmosphere-Ocean 27(4), 682-691.
- Markham, W.E. 1978. Ice Atlas - Eastern Canadian Seaboard. Atmospheric Environment Service, Environment Canada, Toronto.
- Maykut, G.A. 1978. *Energy exchange over young sea ice in the central Arctic*. J. Geophysical Res. 83(C7), 3646-3658.
- Maykut, G.A. and D.K. Perovich. 1987. *The role of short wave radiation in the summer decay of a sea ice cover*. J. Geophysical Res. 92(C7), 7032-7044.
- McPhee, M.G. 1986. *The upper ocean*. In: The Geophysics of Sea Ice. N. Untersteiner, ed. Plenum Publishing Corp. pp 339-394.
- McPhee, M.G. 1983. *Greenland Sea ice/ocean margin*. EOS, Transactions AGU, March 1, 1983, 82-83.
- Moreau, T.A., E.L. Sudeikis, I.G. Rubinstein, F.W. Thirkettle. 1985. A Study and Report on Operational Ice Mapping, Nimbus-7, SMMR. Report prepared by Phd. Associates Inc. for AES, Ice Branch, DSS Contract No 01SE.KM147-4-0501.
- Moses, T., G.N. Kiladas, H.F. Diaz and R.G. Barry. 1987. *Characteristics and frequency of reversals in mean sea level pressure in the north Atlantic sector and their relationship to long-term temperature trends*. J. Climatology 7, 13-30.
- Mysak, L.A. and D.K. Manak. 1989. *Arctic sea ice extent and anomalies, 1953-1984*. Atmosphere-Ocean 27(2), 376-405.

- Nazarenko, D.M. and J.D. Miller. 1986. *Sea Ice Drift Measurements Using Satellite-Tracking Beacons*. Canadian East Coast Sea Ice Workshop, January, 1986. Halifax, Nova Scotia.
- Niebauer, H.J. 1980. *Sea ice and temperature variability in the Eastern Bering Sea and the relation to atmospheric fluctuations*. J. Geophysical Res. 85(C12), 7507-7515.
- Ninnis, R.M., W.J. Emery and M.J. Collins. 1986. *Automated extraction of pack ice motion from Advanced Very High Resolution Radiometer Imagery*. J. Geophysical Research 91(C9). 10725-10734.
- NORSEX Group. 1983. *Norwegian remote sensing experiment in a marginal ice zone*. Science 220(4599), 781-787.
- Overland J.E. and T.R. Heister. 1980. *Development of a synoptic climatology for the northeastern Gulf of Alaska*. J. Applied Meteorology 19, 1-14.
- Overland, J.E., R.M. Reynolds and C.H. Pease. 1983. *A model of the atmospheric boundary layer over the marginal ice zone*. J. Geophysical Res. 88(C5), 2836-2840.
- Overland, J.E. and C.H. Pease. 1982. *Cyclonic climatology of the Bering Sea and its relation to sea ice extent*. Mon. Wea. Rev. 110, 5-13.
- Overland, J.E. and R.W. Preisendorfer. 1982. *A significance test for principal components applied to a cyclone climatology*. Mon. Wea. Rev. 110, 1-4.
- Parkinson, C.L. and D.J. Cavalieri. 1982. *Interannual sea-ice variations and sea-ice/atmosphere interactions in the Southern Ocean, 1973-1975*. Annals of Glaciology 3, 249-254.
- Parkinson, C.L., J.C. Comiso, H.J. Zwally, D.J. Cavalieri, P. Gloersen and W.J. Campbell. 1987. Arctic Sea Ice, 1973-1976: Satellite Passive-Microwave Observations. NASA Scientific and Technical Branch. SP-489. 296 pp.
- Parkinson, C.L. and A.J. Gratz. 1983. *On the seasonal sea ice cover of the Sea of Okhotsk*. J. Geophysical Res. 88(C5), 2793-2802.
- Pease, C.H. 1980. *Eastern Bering Sea ice processes*. Mon. Wea. Rev. 108, 2015-2023.
- Perry, A. 1983. *Growth points in synoptic climatology*. Progress in Physical Geography 7, 90-96.
- Petrie, B. and A. Isenor. 1985. *The near-surface circulation and exchange in the Newfoundland Grand Banks region*. Atmosphere-Ocean 23(3), 209-277.

- Petrie, B. and C. Anderson. 1983. *Circulation on the Newfoundland continental shelf*. Atmosphere-Ocean 21(2), 207-226.
- Petrie, B., K. Lank and J. de Margerie. 1987. *Tides on the Newfoundland Grand Banks*. Atmosphere-Ocean, 25(1), 10-21.
- Petro-Canada Inc. 1981. Grand Banks Environmental Overview. Petro-Canada Inc., Calgary, Alberta.
- Petro-Canada Inc. 1982. Offshore Labrador Initial Environmental Assessment. Petro-Canada Inc., Calgary, Alberta.
- Phd Associates Ltd. 1987. Final Report on Sea-ice Algorithm Development, AES/Phd Temperature Independent Ice Model. Report prepared for the Atmospheric Environment Service.
- Polar Group. 1980. *Polar atmosphere-ice-ocean processes: a review of polar problems in climate research*. Review of Geophysics 18, 525-543.
- Pritchard, R.S. (ed.) 1980. Sea Ice Processes and Models. University of Washington Press. Seattle, Washington. 474 pp.
- Rodgers, J.C. 1978. *Meteorological factors affecting interannual variability of summertime ice extent in the Beaufort Sea*. Mon. Wea. Rev. 106, 890-897.
- Rodgers, J.C. 1983. *Spatial variability of Antarctic temperature anomalies and their association with the southern hemisphere atmospheric circulation*. Annals of the Association of American Geographers 73(4), 502-518.
- Rothrock, D.A., D.R. Thomas and A.S. Thorndike. 1988. *Principal component analysis of satellite passive microwave data over sea ice*. J. Geophysical Res. 93(C3), 2321-2332.
- Schwerdtfeger, W. and St. Kachelhoffer. 1973. *The frequency of cyclonic vortices over the southern ocean in relation to the extension of the pack ice belt*. Antarctic J. U.S. 8, 234.
- Seaconsult Ltd. 1980. Offshore Labrador Summary of the Physical Environment. Report to Petro-Canada Inc. 100 pp.
- Sear, C.B. 1988. *An index variation in the Nordic seas*. Journal of Climatology 8, 339-355.
- Semptner, A.J. 1984. *On modelling the seasonal thermodynamic cycle of sea ice in studies of climatic change*. Climatic Change 6, 27-37.

- Shine, K.P. and A. Henderson-Sellers. 1983. *Modelling climate and the nature of climate models: a review*. J. Climatology 3, 81-94.
- Smith, S.D. and R.J. Anderson. 1984. *Spectra of humidity, temperature, and wind over the sea at Sable Island, Nova Scotia*. J. Geophysical Res. 89(C2), 2029-2040.
- Smithson, P.A. 1986. *Synoptic and dynamic climatology*. Progress in Physical Geography 10, 100-110.
- Stewart, R.H. 1985. Methods of Satellite Oceanography. University of California, San Diego. 360 pp.
- Swift, C.T. 1980. *Passive microwave remote sensing of the ocean - a review*. Boundary Layer Meteorology 18, 25-54.
- Swift, C.T. and D.J. Cavalieri. 1985. *Passive microwave remote sensing for sea ice research*. EOS, Transactions, American Geophysical Union, December 3, 1985. pp. 1210-1212.
- Swift, C.T., L.S. Fedor and R.O. Ramseier. 1985. *An algorithm to measure sea ice concentration with microwave radiometers*. J. Geophysical Res. 90(C1), 1087-1099.
- Symonds, G. 1986. *Seasonal ice extent on the Northeast Newfoundland Shelf*. J. Geophysical Res. 91(C9), 10718-10724.
- Taylor, K.E. 1986. *An analysis of the biases in traditional cyclone frequency maps*. Mon. Wea. Rev. 114, 1481-1490.
- Thorndike, A.S. and R. Colony. 1982. *Sea ice motion in response to geostrophic winds*. J. Geophysical Res. 87(C8), 5845-5852.
- Ulaby, E.T., R.K. Moore and A.K. Fung. 1981. Microwave Remote Sensing: Active and Passive. Addison-Wesley Publishing Co. Reading, Mass. 2162 pp.
- Untersteiner, N. (ed). 1986. The Geophysics of Sea Ice. NATO ASI series. Series B, Physics; vol. 146. Plenum Publishing Corp. 1196 pp.
- Van Loon, H. and J.C. Rodgers. 1978. *The seesaw in temperatures between Greenland and Northern Europe Part I: General description*. Mon. Wea. Rev. 106, 296-310.
- Wadhams, P. 1986. *The seasonal ice zone*, in The Geophysics of Sea Ice. N. Untersteiner ed. Plenum Publishing Corp. pp. 825-991.

- Walker, A.E. 1986. A Climatological Analysis of Eastern Canadian Seaboard Maximum Ice Extent Using Passive Microwave Satellite Data (1973-1985). M.A. thesis, Carleton University. 130 pp.
- Walsh, J.E. 1978. *Temporal and spatial scales of the Arctic circulation*. Mon. Wea. Rev. 106, 1532-1544.
- Walsh, J.E. 1983. *The role of ice in climatic variability: theories and evidence*. Atmosphere-Ocean 21(3), 229-242.
- Walsh, J.E. and C.M. Johnson. 1979. *An analysis of the Arctic sea ice fluctuations, 1953-1977*. J. Physical Oceanography 9, 580-591.
- Walsh, J.E. and C.M. Johnson. 1979. *Interannual atmospheric variability and associated fluctuations in Arctic sea ice extent*. J. Geophysical Res. 84(C11), 6915-6928.
- Walters, J.M., C. Ruf and C.T. Swift. 1987. *A microwave radiometer weather-correcting sea ice algorithm*. J. Geophysical Res. 92(C6), 6521-6534.
- Weaver, R., C. Morris and R.G. Barry. 1987. *Passive microwave data for snow and ice research: planned products from the DSMP SSM/I system*. EOS, Transactions, American Geophysical Union. September 29, 1987.
- Wendland, W.M. and R.A. Bryson. 1981. *Northern hemisphere airstream regions*. Mon. Wea. Rev. 109, 255-270.
- Wendler, G. and Y. Nagashima. 1987. *Inter-relations between the Arctic Sea ice and the general circulation of the atmosphere*. J. Glaciology 33(114), 173-176.
- Wilheit, T. 1978. *A review of applications of microwave radiometry to oceanography*. Boundary Layer Meteorology 13, 277-293.
- Wilheit, T., A.T.C. Chang and A.S. Milman. 1980. *Atmospheric corrections to passive microwave observations of the ocean*. Boundary Layer Meteorology 18, 65-77.
- Williams, D.R.P. 1986. Evaluation and Applications of Sea Ice Models to Nimbus-7 Satellite Passive Microwave Observations. M.Sc. thesis CRESS, York University. 214 pp.
- Willmot, C.J. 1981. *On the validation of models*. Physical Geography 2(2), 184-194.
- Yarnal, B. 1984. *Synoptic scale atmospheric circulation over British Columbia in relation to the mass balance of Sentinel Glacier*. Annals of the Association of American Geographers 74(3), 375-392.

Yarnal, B. and D.A. White. 1987. *Subjectivity in a computer-assisted synoptic climatology I: classification results*. J. Climatology 7, 119-128.

Zwally, H.J. 1984. *Observing polar ice variability*. Annals of Glaciology 5, 191-198.

APPENDIX A

SMMR Concentration Changes

1980/81

1984/85

1980/81 Cell Count Evaluation

Date	Cb	C0	C1	C3	C6	C9	D0	D1	D3	D6	D9	D-1	D-2	D-6	D-9
1980 11 02	461	1977	62	41	0	0									
1980 11 04	461	1966	73	52	27	0	1983	50	8	0	0	6	0	0	0
1980 11 06	461	1953	86	70	47	0	1988	44	8	0	0	7	0	0	0
1980 11 08	461	1978	61	45	2	0	1969	0	0	0	0	70	25	0	0
1980 11 10	461	1981	58	46	21	0	2012	24	1	0	0	3	1	0	0
1980 11 12	461	1953	86	65	49	0	1965	72	23	7	0	2	0	0	0
1980 11 14	461	1957	82	67	55	33	1975	48	11	2	0	16	6	1	0
1980 11 16	461	1940	99	76	56	0	1965	26	9	1	0	48	3	0	0
1980 11 18	461	1920	119	100	82	1	1959	77	19	1	0	3	0	0	0
1980 11 20	461	1912	127	108	81	2	1993	24	2	0	0	22	3	0	0
1980 11 22	461	1891	148	114	89	0	1985	46	0	0	0	8	0	0	0
1980 11 24	461	1877	162	139	88	10	1946	61	8	0	0	32	1	0	0
1980 11 26	461	1855	184	158	104	2	1975	61	11	0	0	3	0	0	0
1980 11 28	461	1843	196	165	125	47	1936	93	2	0	0	10	1	0	0
1980 11 30	461	1822	217	192	166	60	1915	104	56	1	0	20	0	0	0
1980 12 02	461	1852	187	169	136	56	1930	16	0	0	0	93	26	2	0
1980 12 04	461	1825	214	185	137	50	1963	49	16	1	0	27	8	3	0
1980 12 06	461	1806	233	210	169	77	1931	104	22	4	0	4	0	0	0
1980 12 08	461	1818	221	201	170	82	1994	18	0	0	0	27	11	0	0
1980 12 10	461	1803	236	214	174	85	1950	62	14	2	0	27	1	1	0
1980 12 12	461	1774	265	227	188	110	1945	76	14	1	0	18	0	0	0
1980 12 14	461	1775	264	235	197	115	1938	70	6	0	0	31	9	3	0
1980 12 16	461	1769	270	243	199	99	1992	24	7	0	0	23	1	0	0
1980 12 18	461	1750	289	268	237	100	1939	90	35	9	0	10	0	0	0
1980 12 20	461	1781	258	220	190	116	1929	2	0	0	0	108	49	11	0
1980 12 22	461	1768	271	230	200	115	1990	41	3	0	0	8	0	0	0
1980 12 24	461	1780	259	230	206	121	1974	33	3	0	0	32	1	0	0
1980 12 26	461	1717	322	249	211	131	1943	91	18	1	0	5	1	0	0
1980 12 28	461	1686	353	278	234	89	1943	90	3	0	0	6	0	0	0
1980 12 30	461	1633	406	347	261	90	1881	145	43	0	0	13	0	0	0
1981 01 01	461	1682	357	294	257	100	1869	62	8	0	0	108	64	0	0
1981 01 03	461	1637	402	324	275	142	1902	108	40	7	0	29	9	0	0
1981 01 05	461	1670	369	248	201	100	1832	42	4	1	0	165	86	33	0
1981 01 07	461	1508	531	421	282	138	1719	317	146	8	0	3	0	0	0
1981 01 09	461	1669	370	304	260	157	1732	66	18	5	0	241	104	34	0
1981 01 11	461	1539	500	424	331	150	1757	240	137	38	3	42	8	2	0
1981 01 13	461	1531	508	460	351	116	1757	137	49	7	0	145	38	3	0
1981 01 15	461	1651	388	323	261	167	1680	148	37	2	0	211	164	111	3
1981 01 17	461	1320	719	649	554	204	1545	482	354	232	6	12	3	0	0
1981 01 19	461	1490	549	476	384	208	1523	140	83	55	0	376	273	184	0
1981 01 21	461	1585	454	391	322	174	1639	123	91	50	11	277	185	82	1
1981 01 23	461	1362	677	582	487	222	1691	337	208	123	1	11	2	1	0
1981 01 25	461	1463	576	495	448	268	1625	180	81	44	0	234	156	90	0
1981 01 27	461	1450	589	526	469	297	1744	148	110	73	1	147	78	31	0
1981 01 29	461	1449	590	515	426	275	1779	105	17	3	0	155	61	25	0
1981 01 31	461	1429	610	560	492	253	1759	181	103	52	0	99	42	14	0
1981 02 02	461	1378	661	582	501	236	1815	128	40	10	0	96	38	6	0
1981 02 04	461	1482	557	480	414	217	1720	65	13	0	0	254	120	64	0
1981 02 06	461	1564	475	421	344	189	1632	169	110	59	0	238	168	127	4
1981 02 08	461	1288	751	609	511	199	1636	377	203	137	1	26	6	0	0
1981 02 10	461	1483	556	488	407	203	1693	52	0	0	0	294	131	69	0
1981 02 12	461	1481	558	402	287	146	1591	144	90	31	0	304	192	119	0
1981 02 14	461	1268	771	637	502	170	1567	447	249	134	0	25	4	0	0
1981 02 16	461	1317	722	627	483	169	1617	157	53	11	0	265	86	8	0
1981 02 18	461	1333	706	629	535	231	1752	206	54	2	0	81	35	1	0
1981 02 20	461	1261	778	697	540	211	1749	169	85	25	0	121	33	2	0
1981 02 22	461	1359	680	512	414	193	1678	59	18	0	0	302	197	40	0
1981 02 24	461	1428	611	518	383	178	1664	112	41	4	0	263	66	3	0
1981 02 26	461	1486	553	463	321	163	1752	78	16	1	0	209	88	8	1
1981 02 28	461	1601	438	384	307	187	1715	122	29	7	0	202	106	18	0
1981 03 02	461	1520	519	435	331	212	1776	177	94	19	0	86	28	1	1
1981 03 04	461	1608	431	359	291	203	1838	41	5	2	1	160	55	7	0
1981 03 06	461	1519	520	238	211	185	1585	244	0	0	0	210	135	54	5

Cb - land blanked cells, C# - Cells with #/10 concentration, D# - Cells showing an increase in concentration \geq #/10's, D-# - Cells showing a decrease in concentration \geq #/10's

Date	Cb	C0	C1	C3	C6	C9	D0	D1	D3	D6	D9	D-1	D-3	D-6	D-9
1981 03 08	461	1645	394	325	283	191	1614	177	95	39	1	248	0	0	0
1981 03 10	461	1590	449	372	316	201	1889	142	50	1	0	8	0	0	0
1981 03 12	461	1366	673	365	292	206	1663	272	1	0	0	104	2	0	0
1981 03 14	461	1622	417	371	328	198	1654	102	11	0	0	283	1	0	0
1981 03 16	461	1361	678	365	300	186	1629	299	13	1	0	111	18	1	0
1981 03 18	461	1431	608	341	292	176	1730	49	7	0	0	260	21	3	0
1981 03 20	461	1628	411	343	265	173	1663	78	11	0	0	298	20	1	0
1981 03 22	461	1655	384	335	283	175	1904	66	7	0	0	69	18	0	0
1981 03 24	461	1646	393	339	264	170	1923	43	6	0	0	73	11	0	0
1981 03 26	461	1375	664	361	311	205	1623	414	22	1	0	2	0	0	0
1981 03 28	461	1646	393	311	286	224	1900	25	6	4	2	114	65	22	0
1981 03 30	461	1593	446	397	321	228	1841	146	81	25	0	52	5	4	2
1981 04 01	461	1582	457	396	317	222	1962	35	0	0	0	42	1	0	0
1981 04 03	461	1669	370	313	255	216	1877	16	1	0	0	146	75	40	1
1981 04 05	461	1551	488	430	363	220	1822	217	108	54	0	0	0	0	0
1981 04 07	461	1557	482	423	357	239	1922	62	5	0	0	55	25	2	0
1981 04 09	461	1587	452	392	347	187	1895	28	3	0	0	116	19	0	0
1981 04 11	461	1581	458	411	356	212	1954	77	9	0	0	8	1	0	0
1981 04 13	461	1616	423	383	342	217	1889	44	7	0	0	106	42	15	0
1981 04 15	461	1598	441	386	350	207	1907	72	27	10	0	60	14	0	J
1981 04 17	461	1545	494	434	347	187	1851	117	53	0	0	71	6	0	0
1981 04 19	461	1615	424	345	317	223	1823	74	11	3	0	142	87	16	0
1981 04 21	461	1615	424	382	329	180	1856	80	57	19	0	103	30	7	0
1981 04 23	461	1598	441	372	312	194	1904	63	3	0	0	72	20	0	0
1981 04 25	461	1707	332	281	240	183	1821	15	4	2	0	203	84	36	1
1981 04 27	461	1663	376	338	274	155	1857	114	76	20	0	68	27	2	0
1981 04 29	461	1655	384	284	222	167	1860	59	5	0	0	120	67	7	0
1981 05 01	461	1469	570	297	236	172	1878	89	36	0	0	72	23	3	0
1981 05 03	461	1627	412	359	284	200	1653	52	64	9	0	234	1	0	0
1981 05 05	461	1668	371	292	235	177	1867	32	0	0	0	140	58	25	0
1981 05 07	461	1459	580	320	245	173	1849	110	43	11	0	80	20	2	1
1981 05 09	461	1581	458	365	263	173	1647	158	40	2	1	234	5	1	0
1981 05 11	461	1667	372	346	241	166	1795	93	37	0	0	151	81	18	0
1981 05 13	461	1624	415	360	271	152	1851	111	51	21	0	77	24	0	0
1981 05 15	461	1626	413	346	266	160	1905	66	3	0	0	68	26	1	0
1981 05 17	461	1676	363	299	242	176	1879	37	5	5	3	123	45	6	0
1981 05 19	461	1666	373	318	232	145	1901	70	24	0	0	68	12	5	3
1981 05 21	461	1733	306	278	230	156	1922	28	5	0	0	89	37	13	0
1981 05 23	461	1738	301	243	208	104	1851	49	9	0	0	139	32	0	0
1981 05 25	461	1725	314	262	198	62	1893	62	21	5	0	84	19	2	0
1981 05 27	461	1639	350	248	201	74	1875	87	10	1	0	77	8	1	0
1981 05 29	461	1733	306	269	210	77	1890	67	20	1	0	82	6	0	0
1981 05 31	461	1724	315	260	220	47	1863	72	11	1	0	104	9	0	0
1981 06 02	461	1700	339	298	243	61	1801	153	66	17	0	85	29	1	0
1981 06 04	461	1747	292	247	163	42	1840	21	1	0	0	178	89	8	1
1981 06 06	461	1742	297	270	145	60	1865	67	5	1	0	107	15	3	0
1981 06 08	461	1734	305	250	170	73	1845	144	42	1	0	50	4	0	0
1981 06 10	461	1787	252	199	134	54	1890	11	0	0	0	138	49	3	0
1981 06 12	461	1850	189	45	4	0	1817	15	3	0	0	207	141	116	8
1981 06 14	461	1891	148	26	1	0	1958	28	5	0	0	53	21	1	0
1981 06 16	461	1981	58	25	0	0	1888	31	13	0	0	120	7	1	0
1981 06 18	461	2007	32	9	0	0	1999	4	0	0	0	36	7	0	0
1981 06 20	461	2023	16	8	0	0	2023	2	1	0	0	14	0	0	0
1981 06 22	461	2015	24	7	0	0	2020	13	1	0	0	6	1	0	0
1981 06 24	461	1953	86	8	0	0	1951	75	2	0	0	13	1	0	0
1981 06 26	461	2038	1	0	0	0	1997	0	0	0	0	42	8	0	0
1981 06 28	461	1866	173	135	94	47	1867	171	134	94	46	1	0	0	0
1981 06 30	461	1877	162	125	89	15	1940	16	1	0	0	83	6	1	0
1981 07 02	461	1915	124	95	61	0	1928	12	2	0	0	99	31	6	0
1981 07 04	461	1907	132	101	66	1	1978	41	9	0	0	20	4	0	0
1981 07 06	461	1897	142	104	63	0	1988	27	3	1	0	24	4	1	0
1981 07 08	461	1957	82	66	52	0	1955	3	0	0	0	81	35	3	0
1981 07 10	461	1902	137	98	54	0	1963	71	30	1	0	5	0	0	0
1981 07 12	461	1955	84	65	48	0	1975	1	0	0	0	63	23	0	0
1981 07 14	461	1966	73	54	45	1	2006	10	0	0	0	23	4	0	0

Cb - land blanked cells, C# - Cells with #/10 concentration, D# - Cells showing an increase in concentration \geq #/10's, D-# - Cells showing a decrease in concentration \geq #/10's

Date	Cb	C0	C1	C3	C6	C9	D0	D1	D3	D6	D9	D-1	D-3	D-6	D-9
1981 07 16	461	1906	133	83	41	0	1923	76	19	1	0	40	0	0	0
1981 07 18	461	1928	111	70	37	0	1975	6	1	0	0	58	5	1	0
1981 07 20	461	1954	85	61	34	0	1973	14	2	0	0	52	8	0	0
1981 07 22	461	1950	89	57	16	0	2003	19	1	0	0	17	1	0	0
1981 07 24	461	1968	71	54	2	0	1996	5	0	0	0	38	0	0	0
1981 07 26	461	1975	64	39	4	0	1998	8	0	0	0	33	10	0	0
1981 07 28	461	1942	97	61	5	0	1993	46	9	0	0	0	0	0	0
1981 07 30	461	1977	62	42	6	0	1980	3	0	0	0	56	8	0	0

Cb - land blanked cells, C# - Cells with #/10 concentration, D# - Cells showing an increase in concentration \geq #/10's, D-# - Cells showing a decrease in concentration \geq #/10's

1984/85 Cell Count Evaluation

Date	Cb	C0	C1	C3	C6	C9	D0	D1	D3	D6	D9	D-1	D-3	D-6	D-9
1984 11 01	461	2039	0	0	0	0									
1984 11 03	461	2027	12	0	0	0	2027	12	0	0	0	0	0	0	0
1984 11 05	461	2039	0	0	0	0	2027	0	0	0	0	12	0	0	0
1984 11 07	461	2039	0	0	0	0	2039	0	0	0	0	0	0	0	0
1984 11 09	461	2039	0	0	0	0	2039	0	0	0	0	0	0	0	0
1984 11 11	461	2033	6	1	0	0	2033	6	1	0	0	0	0	0	0
1984 11 13	461	2006	33	18	0	0	2009	30	13	0	0	0	0	0	0
1984 11 15	461	1976	63	48	9	0	1978	58	26	1	0	3	0	0	0
1984 11 17	461	1946	93	74	49	0	1959	80	37	0	0	0	0	0	0
1984 11 19	461	1910	129	99	74	0	1961	78	19	2	0	0	0	0	0
1984 11 21	461	1854	185	154	111	0	1934	102	52	4	0	3	0	0	0
1984 11 23	461	1833	206	172	139	17	1938	90	25	1	0	11	0	0	0
1984 11 25	461	1845	194	170	147	26	1923	66	6	0	0	50	9	1	0
1984 11 27	461	1829	210	180	147	41	1963	48	9	0	0	28	0	0	0
1984 11 29	461	1803	236	203	172	60	1937	95	14	0	0	7	1	0	0
1984 12 01	461	1811	228	203	176	70	1985	25	4	0	0	29	1	0	0
1984 12 03	461	1783	256	218	172	56	1952	51	1	0	0	36	4	2	1
1984 12 05	461	1801	238	206	178	88	1972	37	3	2	1	30	2	0	0
1984 12 07	461	1767	272	232	173	85	1904	93	20	3	0	42	22	9	1
1984 12 09	461	1717	322	276	226	89	1885	133	57	12	0	21	0	0	0
1984 12 11	461	1719	320	292	228	102	1908	74	14	0	0	57	9	0	0
1984 12 13	461	1706	333	300	236	130	1907	101	7	0	0	31	8	0	0
1984 12 15	461	1625	414	372	332	134	1891	147	85	40	0	1	0	0	0
1984 12 17	461	1598	441	386	315	188	1907	86	16	0	0	46	9	2	0
1984 12 19	461	1534	505	451	379	149	1857	167	69	2	0	15	0	0	0
1984 12 21	461	1624	415	359	328	232	1819	70	6	4	0	150	89	36	0
1984 12 23	461	1537	502	429	375	200	1819	159	78	55	1	61	25	9	0
1984 12 25	461	1524	515	466	404	174	1821	123	54	5	0	95	3	1	0
1984 12 27	461	1535	504	372	298	159	1744	68	23	4	0	227	118	50	0
1984 12 29	461	1494	545	503	445	204	1743	255	164	53	0	41	7	3	0
1984 12 31	461	1541	498	437	384	220	1851	71	8	1	0	117	87	57	6
1985 01 02	461	1425	614	527	452	190	1749	206	120	82	0	84	40	9	0
1985 01 04	461	1209	830	676	572	309	1592	427	150	63	0	20	5	0	0
1985 01 06	461	1406	633	480	398	292	1544	95	14	0	0	400	229	120	3
1985 01 08	461	1457	582	514	466	286	1656	170	128	59	3	213	61	12	0
1985 01 10	461	1240	799	672	482	231	1640	288	161	41	0	111	32	6	0
1985 01 12	461	1285	754	649	532	291	1551	292	118	20	0	196	102	31	0
1985 01 14	461	1358	681	606	504	283	1715	77	9	0	0	247	50	5	0
1985 01 16	461	1319	720	633	446	262	1670	191	44	6	0	178	74	6	0
1985 01 18	461	1359	680	640	575	302	1608	271	119	43	0	160	75	13	1
1985 01 20	461	1382	657	566	465	262	1666	170	40	5	0	203	134	69	1
1985 01 22	461	1314	725	525	401	198	1494	291	77	6	1	254	137	86	9
1985 01 24	461	1468	571	482	393	187	1458	201	134	80	6	380	173	85	1
1985 01 26	461	1286	753	668	567	279	1610	370	208	130	17	59	19	5	0
1985 01 28	461	1379	660	520	445	247	1631	125	25	1	0	283	177	104	6
1985 01 30	461	1284	755	474	406	261	1565	224	154	86	0	250	202	140	14
1985 02 01	461	1150	889	740	534	289	1313	425	293	125	5	301	23	1	0
1985 02 03	461	1334	705	628	474	282	1601	113	38	0	0	325	192	12	0
1985 02 05	461	1332	707	632	539	272	1657	243	117	17	0	139	90	44	4
1985 02 07	461	917	1122	975	806	302	1300	589	390	219	77	150	26	3	0
1985 02 09	461	1209	830	725	546	224	1261	178	64	3	0	600	342	182	71
1985 02 11	461	1318	721	599	433	208	1647	42	2	0	0	350	137	13	0
1985 02 13	461	1195	844	734	631	271	1539	433	201	68	0	67	22	2	0
1985 02 15	461	1295	744	642	562	230	1638	128	36	1	0	273	146	52	0
1985 02 17	461	1330	709	642	566	197	1690	130	67	20	0	219	72	6	0
1985 02 19	461	1073	966	841	705	299	1415	531	255	110	0	93	52	25	0
1985 02 21	461	1285	754	692	609	226	1458	165	73	22	0	416	228	80	0
1985 02 23	461	1161	878	742	626	218	1472	329	169	69	0	238	133	54	4
1985 02 25	461	1305	734	638	536	328	1367	293	130	54	8	379	242	136	21
1985 02 27	461	1286	753	671	539	247	1600	226	116	59	6	213	138	41	2
1985 03 01	461	1092	947	767	687	381	1564	412	183	54	8	63	17	1	0
1985 03 03	461	1240	799	716	584	349	1629	49	3	0	0	361	97	20	0
1985 03 05	461	1247	792	548	426	212	1586	109	63	10	0	344	226	101	9

Cb - land blanked cells, C# - Cells with #/10 concentration, D# - Cells showing an increase in concentration \geq #/10's, D-# - Cells showing a decrease in concentration \geq #/10's

Date	Cb	C0	C1	C3	C6	C9	D0	D1	D3	D6	D9	D-1	D-3	D-6	D-#
1985 03 07	461	1035	1004	848	678	276	1432	555	325	133	1	52	0	0	0
1985 03 09	461	1131	908	760	630	335	1566	174	26	0	0	299	144	15	0
1985 03 11	461	1182	857	758	630	382	1557	246	86	28	0	236	92	31	0
1985 03 13	461	859	1180	1062	931	366	1323	546	378	244	21	170	35	3	0
1985 03 15	461	1275	764	681	585	299	1353	54	4	0	0	632	425	279	33
1985 03 17	461	1250	789	710	601	227	1651	153	84	17	0	235	47	6	0
1985 03 19	461	1062	977	846	745	372	1527	463	172	91	9	49	15	4	0
1985 03 21	461	1201	838	763	687	325	1551	182	82	28	0	306	172	97	11
1985 03 23	461	1221	818	721	580	324	1710	109	40	2	0	220	131	24	0
1985 03 25	461	1212	827	687	577	288	1645	157	58	35	0	237	61	4	0
1985 03 27	461	1285	754	630	503	313	1659	134	53	4	0	246	141	49	0
1985 03 29	461	1342	697	602	489	294	1694	127	46	2	0	218	68	16	0
1985 03 31	461	1401	638	544	456	297	1643	190	54	3	0	206	103	54	12
1985 04 02	461	1458	581	508	428	298	1640	171	92	32	1	228	139	62	10
1985 04 04	461	1374	665	583	493	316	1784	193	109	40	3	62	14	1	0
1985 04 06	461	1468	571	512	449	308	1783	64	9	0	0	192	99	36	0
1985 04 08	461	1430	609	446	372	265	1659	172	61	33	6	208	144	61	16
1985 04 10	461	1429	610	535	475	293	1720	194	123	74	21	125	10	5	3
1985 04 12	461	1479	560	493	408	306	1775	97	13	2	0	167	98	32	0
1985 04 14	461	1431	608	456	342	250	1668	201	81	10	0	170	125	73	26
1985 04 16	461	1335	704	549	482	321	1559	363	149	83	30	117	32	14	0
1985 04 18	461	1336	703	433	384	285	1463	244	20	3	0	332	140	51	1
1985 04 20	461	1529	510	446	335	176	1482	154	102	16	0	403	127	57	15
1985 04 22	461	1343	696	549	400	191	1616	322	159	41	0	101	22	0	0
1985 04 24	461	1498	541	466	333	212	1652	99	39	6	1	288	138	28	0
1985 04 26	461	1341	698	436	339	210	1637	266	19	6	0	136	32	3	0
1985 04 28	461	1378	661	533	361	264	1524	275	108	11	0	240	5	1	0
1985 04 30	461	1546	493	430	345	247	1678	92	39	21	0	269	144	39	7
1985 05 02	461	1515	524	450	375	283	1789	160	71	41	1	90	39	13	0
1985 05 04	461	1494	545	466	401	280	1838	114	64	12	0	87	41	0	0
1985 05 06	461	1543	496	420	307	240	1792	57	11	0	0	190	115	29	2
1985 05 08	461	1520	519	458	403	295	1825	181	88	13	1	33	0	0	0
1985 05 10	461	1574	465	402	345	260	1862	24	1	0	0	153	75	10	0
1985 05 12	461	1575	464	396	326	247	1828	109	58	7	3	102	67	33	12
1985 05 14	461	1555	484	419	371	230	1823	110	69	37	15	106	24	8	3
1985 05 16	461	1601	438	391	334	215	1805	81	16	4	0	153	59	24	7
1985 05 18	461	1604	435	348	282	215	1738	132	69	34	1	169	102	60	27
1985 05 20	461	1580	459	406	333	106	1598	158	129	72	18	283	93	7	1
1985 05 22	461	1653	386	358	296	92	1806	84	11	3	0	149	73	25	2
1985 05 24	461	1649	390	316	245	67	1705	166	72	33	0	168	116	75	3
1985 05 26	461	1578	461	393	324	56	1790	153	100	61	0	96	8	2	0
1985 05 28	461	1679	360	328	275	103	1815	58	20	3	0	166	82	40	0
1985 05 30	461	1602	437	378	304	78	1786	136	78	49	0	117	20	1	0
1985 06 01	461	1506	533	414	298	66	1696		57	0	0	119	32	1	0
1985 06 03	461	1685	354	296	214	86	1673		10	0	0	311	115	22	0
1985 06 05	461	1640	399	322	230	37	1751	15	50	2	0	129	29	2	0
1985 06 07	461	1559	480	311	218	56	1789	152	12	1	0	98	21	1	0
1985 06 09	461	1720	319	270	206	69	1777	46	2	0	0	216	42	0	0
1985 06 11	461	1696	343	208	212	45	1866	88	33	1	0	85	15	1	0
1985 06 13	461	1667	372	260	174	34	1796	102	9	2	0	141	32	0	0
1985 06 15	461	1794	245	179	134	52	1752	76	7	4	3	211	87	31	0
1985 06 17	461	1702	337	229	137	25	1810	159	60	14	0	70	20	6	0
1985 06 19	461	1723	316	240	132	68	1843	108	13	2	0	88	4	1	0
1985 06 21	461	1811	228	193	144	50	1812	60	31	5	0	167	64	3	0
1985 06 23	461	1784	255	169	79	0	1753	94	43	3	0	192	80	9	1
1985 06 25	461	1752	287	170	84	1	1868	99	23	0	0	72	19	0	0
1985 06 27	461	1867	172	138	89	0	1866	39	0	0	0	134	30	1	0
1985 06 29	461	1822	217	98	59	0	1862	81	5	0	0	96	31	4	0
1985 07 01	461	1804	235	124	75	7	1899	101	11	0	0	39	1	0	0
1985 07 03	461	1929	110	75	52	0	1842	2	0	0	0	195	25	14	0
1985 07 05	461	1868	171	98	33	0	1909	87	35	4	0	43	14	0	0
1985 07 07	461	1873	166	67	35	0	1925	46	3	0	0	68	17	0	0
1985 07 09	461	1921	118	60	38	0	1901	51	4	0	0	87	15	0	0
1985 07 11	461	1917	122	66	6	0	1952	30	12	0	0	57	8	0	0
1985 07 13	461	1882	157	80	3	0	1921	85	4	0	0	33	1	0	0

Cb - land blanked cells, C# - Cells with #/10 concentration, D# - Cells showing an increase in concentration \geq #/10's, D-# - Cells showing a decrease in concentration \geq #/10's

Date	Cb	C0	C1	C3	C6	C9	D0	D1	D3	D6	D9	D-1	D-3	D-6	D-9
1985 07 15	461	1950	89	53	0	0	1923	16	4	0	0	100	10	0	0
1985 07 17	461	1954	85	58	0	0	1976	21	0	0	0	42	3	0	0
1985 07 19	461	1807	232	57	2	1	1870	157	11	2	1	12	0	0	0
1985 07 21	461	1989	50	15	0	0	1814	0	0	0	0	225	15	2	1
1985 07 23	461	2008	31	1	0	0	2000	3	0	0	0	36	4	0	0
1985 07 25	461	2025	14	0	0	0	2023	0	0	0	0	16	0	0	0
1985 07 27	461	2024	15	0	0	0	2024	10	0	0	0	5	0	0	0
1985 07 29	461	2030	9	0	0	0	2033	0	0	0	0	6	0	0	0
1985 07 31	461	2039	0	0	0	0	2037	0	0	0	0	2	0	0	0

Cb - land blanked cells, C# - Cells with #/10 concentration, D# - Cells showing an increase in concentration \geq #/10's, D-# - Cells showing a decrease in concentration \geq #/10's

APPENDIX B

SMMR Concentration Changes - 60-70°N

1980/81

1984/85

1980/81 Time Series of Ice Concentrations and Changes for 60-70°N

Date	Cb	C0	C1	C3	C6	C9	D0	D1	D3	D6	D9	D-1	D-3	D-6	D-9
1980 11 02	83	261	56	41	0	0									
1980 11 04	83	244	73	52	27	0	267	50	8	0	0	0	0	0	0
1980 11 06	83	234	83	70	47	0	269	41	8	0	0	7	0	0	0
1980 11 08	83	256	61	45	2	0	250	0	0	0	0	67	25	0	0
1980 11 10	83	259	58	46	21	0	290	24	1	0	0	3	1	0	0
1980 11 12	83	236	81	65	49	0	248	67	23	7	0	2	0	0	0
1980 11 14	83	235	82	67	55	33	258	48	11	2	0	11	6	1	0
1980 11 16	83	218	99	76	56	0	243	26	9	1	0	48	3	0	0
1980 11 18	83	198	119	100	82	1	237	77	19	1	0	3	0	0	0
1980 11 20	83	190	127	108	81	2	271	24	2	0	0	22	3	0	0
1980 11 22	83	169	148	114	89	0	263	46	0	0	0	8	0	0	0
1980 11 24	83	155	162	139	88	10	224	61	8	0	0	32	1	0	0
1980 11 26	83	133	184	158	104	2	253	61	11	0	0	3	0	0	0
1980 11 28	83	131	186	165	125	47	224	83	2	0	0	10	1	0	0
1980 11 30	83	102	215	192	166	60	204	102	56	1	0	11	0	0	0
1980 12 02	83	130	187	169	136	56	210	16	0	0	0	91	26	2	0
1980 12 04	83	115	202	176	137	50	253	37	7	1	0	27	8	3	0
1980 12 06	83	97	220	198	169	77	212	101	22	4	0	4	0	0	0
1980 12 08	83	96	221	201	170	82	285	18	0	0	0	14	0	0	0
1980 12 10	83	94	223	202	172	85	241	49	2	0	0	27	1	1	0
1980 12 12	83	75	242	213	175	110	244	55	9	1	0	18	0	0	0
1980 12 14	83	76	241	224	192	115	242	60	6	0	0	15	2	0	0
1980 12 16	83	68	249	229	188	99	282	13	1	0	0	22	1	0	0
1980 12 18	83	66	251	234	211	100	247	60	14	0	0	10	0	0	0
1980 12 20	83	85	232	208	180	116	235	2	0	0	0	80	31	5	0
1980 12 22	83	84	233	215	188	113	289	22	3	0	0	6	0	0	0
1980 12 24	83	79	238	215	194	121	275	32	3	0	0	10	1	0	0
1980 12 26	83	76	241	218	197	128	292	21	2	0	0	4	1	0	0
1980 12 28	83	74	243	230	209	83	283	28	1	0	0	6	0	0	0
1980 12 30	83	71	246	233	214	90	298	18	0	0	0	1	0	0	0
1981 01 01	83	69	248	237	223	94	289	26	0	0	0	2	0	0	0
1981 01 03	83	73	244	225	212	131	285	7	0	0	0	25	9	0	0
1981 01 05	83	88	229	212	193	100	261	1	0	0	0	55	14	0	0
1981 01 07	83	79	238	227	213	131	263	53	15	1	0	1	0	0	0
1981 01 09	83	75	242	232	212	135	253	29	6	3	0	35	5	0	0
1981 01 11	83	68	249	235	218	136	248	55	9	0	0	14	4	0	0
1981 01 13	83	72	245	232	199	98	227	12	4	0	0	78	21	1	0
1981 01 15	83	69	248	234	215	152	217	82	25	1	0	18	6	0	0
1981 01 17	83	63	254	244	229	171	257	52	16	2	0	8	2	0	0
1981 01 19	83	64	253	247	228	177	291	16	2	0	0	10	2	1	0
1981 01 21	83	83	234	222	209	152	253	2	1	0	0	62	34	3	0
1981 01 23	83	76	241	229	219	179	275	40	5	0	0	2	1	1	0
1981 01 25	83	75	242	230	218	168	292	7	1	0	0	18	0	0	0
1981 01 27	83	79	238	223	214	185	290	8	1	0	0	19	1	0	0
1981 01 29	83	83	234	221	212	189	297	6	0	0	0	14	2	0	0
1981 01 31	83	72	245	231	222	183	290	25	11	2	0	2	1	0	0
1981 02 02	83	76	241	229	215	176	285	10	1	0	0	22	6	0	0
1981 02 04	83	69	248	235	220	187	292	20	7	0	0	5	0	0	0
1981 02 06	83	86	231	226	214	163	274	8	0	0	0	35	9	0	0
1981 02 08	83	67	250	239	225	160	281	36	14	0	0	0	0	0	0
1981 02 10	83	62	255	238	221	160	301	7	0	0	0	9	0	0	0
1981 02 12	83	72	245	229	202	137	240	7	1	0	0	70	15	3	0
1981 02 14	83	59	258	247	232	151	237	78	20	1	0	2	0	0	0
1981 02 16	83	57	260	251	238	169	278	31	2	0	0	8	1	0	0
1981 02 18	83	57	260	251	240	192	305	10	0	0	0	2	0	0	0
1981 02 20	83	55	262	252	241	198	297	18	1	0	0	2	0	0	0
1981 02 22	83	46	271	258	241	185	300	11	3	0	0	6	1	0	0
1981 02 24	83	75	242	232	218	171	253	0	0	0	0	64	26	3	0
1981 02 26	83	75	242	234	217	153	284	11	4	1	0	22	5	2	1
1981 02 28	83	73	244	237	210	161	237	41	12	4	0	39	20	2	0
1981 03 02	83	71	246	236	221	186	250	43	22	4	0	24	8	1	1
1981 03 04	83	77	240	233	221	186	272	22	3	2	1	23	3	0	0

Cb - land blanked cells, C# - Cells with #/10 concentration, D# - Cells showing an increase in concentration \geq #/10's, D-# - Cells showing a decrease in concentration \geq #/10's

Date	Cb	C0	C1	C3	C6	C9	D0	D1	D3	D6	D9	D-1	D-3	D-6	D-9
1981 03 06	83	87	230	215	195	172	263	0	0	0	0	54	30	6	0
1981 03 08	83	73	244	235	221	183	256	61	27	2	0	0	0	0	0
1981 03 10	83	60	257	242	230	192	278	38	5	0	0	1	0	0	0
1981 03 12	83	67	250	242	230	196	292	12	0	0	0	13	0	0	0
1981 03 14	83	73	244	239	228	178	295	2	1	0	0	20	0	0	0
1981 03 16	83	77	240	229	219	186	289	4	0	0	0	24	3	1	0
1981 03 18	83	76	241	224	201	159	255	5	1	0	0	57	18	3	0
1981 03 20	83	71	246	236	217	172	262	51	10	0	0	4	0	0	0
1981 03 22	83	62	255	240	223	175	281	28	1	0	0	8	0	0	0
1981 03 24	83	68	249	239	218	170	265	19	0	0	0	33	5	0	0
1981 03 26	83	56	261	250	234	193	251	66	11	0	0	0	0	0	0
1981 03 28	83	59	258	246	237	199	297	10	1	0	0	10	3	0	0
1981 03 30	83	51	266	256	239	199	282	31	4	0	0	4	0	0	0
1981 04 01	83	52	265	258	241	199	302	7	0	0	0	8	1	0	0
1981 04 03	83	64	253	241	224	193	275	0	0	0	0	42	13	4	0
1981 04 05	83	45	272	261	248	199	256	61	20	4	0	0	0	0	0
1981 04 07	83	40	277	268	254	212	290	26	1	0	0	1	0	0	0
1981 04 09	83	50	267	253	239	178	257	0	0	0	0	60	11	0	0
1981 04 11	83	48	269	261	250	206	277	40	5	0	0	0	0	0	0
1981 04 13	83	33	284	268	253	204	283	26	3	0	0	8	1	0	0
1981 04 15	83	40	277	265	253	198	285	14	0	0	0	18	1	0	0
1981 04 17	83	47	270	260	244	176	279	3	0	0	0	35	5	0	0
1981 04 19	83	49	268	262	253	207	275	37	6	0	0	5	0	0	0
1981 04 21	83	64	253	245	233	169	257	0	0	0	0	60	21	5	0
1981 04 23	83	61	256	246	235	181	294	15	1	0	0	8	1	0	0
1981 04 25	83	77	240	233	219	181	264	3	0	0	0	50	15	1	0
1981 04 27	83	73	244	232	210	155	269	14	1	0	0	34	8	0	0
1981 04 29	83	74	243	227	207	164	264	25	3	0	0	28	6	0	0
1981 05 01	83	72	245	232	209	172	289	22	1	0	0	6	0	0	0
1981 05 03	83	62	255	244	226	191	270	46	13	1	0	1	0	0	0
1981 05 05	83	69	248	240	219	176	279	6	0	0	0	32	2	1	0
1981 05 07	83	80	237	220	208	166	260	11	0	0	0	46	20	2	1
1981 05 09	83	66	251	229	212	167	265	36	9	2	1	16	3	1	0
1981 05 11	83	44	273	264	226	154	248	58	27	0	0	11	0	0	0
1981 05 13	83	60	257	243	217	152	258	8	0	0	0	51	16	0	0
1981 05 15	83	56	261	249	224	153	277	30	1	0	0	10	1	0	0
1981 05 17	83	73	244	230	210	160	252	7	0	0	0	58	10	0	0
1981 05 19	83	62	255	238	202	141	262	24	5	0	0	31	2	0	0
1981 05 21	83	69	248	237	212	147	287	14	4	0	0	16	0	0	0
1981 05 23	83	81	236	217	193	91	210	5	0	0	0	102	12	0	0
1981 05 25	83	74	243	228	176	62	233	27	7	0	0	57	1*	0	0
1981 05 27	83	79	238	207	176	68	262	13	1	0	0	42	6	1	0
1981 05 29	83	77	240	224	187	77	252	51	15	1	0	14	1	0	0
1981 05 31	83	86	231	217	189	40	201	26	4	1	0	90	6	0	0
1981 06 02	83	96	221	194	164	57	175	66	1	0	0	76	27	1	0
1981 06 04	83	107	210	185	141	42	226	18	1	0	0	73	19	3	1
1981 06 06	83	107	210	177	122	60	234	27	5	1	0	56	9	3	0
1981 06 08	83	109	208	183	152	73	222	78	16	1	0	17	4	0	0
1981 06 10	83	109	208	168	125	54	252	6	0	0	0	59	11	1	0
1981 06 12	83	176	141	14	1	0	127	4	1	0	0	186	139	116	8
1981 06 14	83	207	110	11	1	0	302	3	0	0	0	12	3	0	0
1981 06 16	83	295	22	0	0	0	216	8	0	0	0	93	2	1	0
1981 06 18	83	307	10	0	0	0	301	4	0	0	0	12	0	0	0
1981 06 20	83	314	3	1	0	0	312	1	1	0	0	4	0	0	0
1981 06 22	83	317	0	0	0	0	314	0	0	0	0	3	1	0	0
1981 06 24	83	250	67	1	0	0	250	67	1	0	0	0	0	0	0
1981 06 26	83	317	0	0	0	0	291	0	0	0	0	26	1	0	0
1981 06 28	83	155	162	132	94	47	157	160	131	94	46	0	0	0	0
1981 06 30	83	168	149	125	89	15	229	13	1	0	0	75	6	1	0
1981 07 02	83	193	124	95	61	0	218	12	2	0	0	87	31	6	0
1981 07 04	83	188	129	101	66	1	259	38	9	0	0	20	4	0	0
1981 07 06	83	175	142	104	63	0	269	27	3	1	0	21	4	1	0
1981 07 08	83	237	80	66	52	0	235	1	0	0	0	81	35	3	0
1981 07 10	83	180	137	98	54	0	243	71	30	1	0	3	0	0	0
1981 07 12	83	234	83	65	48	0	254	0	0	0	0	63	23	0	0

Cb - land blanked cells, C# - Cells with #/10 concentration, D# - Cells showing an increase in concentration \geq #/10's, D-# - Cells showing a decrease in concentration \geq #/10's

Date	Cb	C0	C1	C3	C6	C9	D0	D1	D3	D6	D9	D-1	D-3	D-6	D-9
1981 07 14	83	249	68	54	45	1	290	5	0	0	0	22	4	0	0
1981 07 16	83	203	114	83	41	0	225	57	19	1	0	35	0	0	0
1981 07 18	83	206	111	70	37	0	272	6	1	0	0	39	5	1	0
1981 07 20	83	237	80	61	34	0	256	9	2	0	0	52	8	0	0
1981 07 22	83	230	87	57	16	0	288	17	1	0	0	12	1	0	0
1981 07 24	83	248	69	54	2	0	278	3	0	0	0	36	0	0	0
1981 07 26	83	253	64	39	4	0	278	8	0	0	0	31	10	0	0
1981 07 28	83	220	97	61	5	0	271	46	9	0	0	0	0	0	0
1981 07 30	83	257	60	42	6	0	260	1	0	0	0	56	8	0	0

Cb - land blanked cells, C# - Cells with #/10 concentration, D# - Cells showing an increase in concentration \geq #/10's, D-# - Cells showing a decrease in concentration \geq #/10's

1984/85 Time Series of Ice Concentrations and Changes for 60-70°N

Date	Cb	C0	C1	C3	C6	C9	D0	D1	D3	D6	D9	D-1	D-3	D-6	D-9
1984 11 01	83	317	0	0	0	0									
1984 11 03	83	316	1	0	0	0	316	1	0	0	0	0	0	0	0
1984 11 05	83	317	0	0	0	0	316	0	0	0	0	1	0	0	0
1984 11 07	83	317	0	0	0	0	317	0	0	0	0	0	0	0	0
1984 11 09	83	317	0	0	0	0	317	0	0	0	0	0	0	0	0
1984 11 11	83	311	6	1	0	0	311	6	1	0	0	0	0	0	0
1984 11 13	83	287	30	18	0	0	290	27	13	0	0	0	0	0	0
1984 11 15	83	254	63	48	9	0	259	58	26	1	0	0	0	0	0
1984 11 17	83	224	93	74	49	0	237	80	37	0	0	0	0	0	0
1984 11 19	83	188	129	99	74	0	239	78	19	2	0	0	0	0	0
1984 11 21	83	139	178	154	111	0	219	95	52	4	0	3	0	0	0
1984 11 23	83	114	203	172	139	17	220	87	26	1	0	10	0	0	0
1984 11 25	83	131	186	170	147	26	212	58	6	0	0	47	9	1	0
1984 11 27	83	107	210	180	147	41	249	48	9	0	0	20	0	0	0
1984 11 29	83	94	223	203	172	60	228	82	14	0	0	7	1	0	0
1984 12 01	83	95	222	203	176	70	267	25	4	0	0	25	1	0	0
1984 12 03	83	94	223	204	172	56	257	24	0	0	0	36	4	2	1
1984 12 05	83	98	219	202	178	88	264	37	3	2	1	16	2	0	0
1984 12 07	83	81	236	206	168	85	214	61	9	0	0	42	22	9	1
1984 12 09	83	61	256	243	214	89	192	106	48	12	0	19	0	0	0
1984 12 11	83	53	264	256	227	102	246	47	8	0	0	24	0	0	0
1984 12 13	83	42	275	259	224	130	225	73	0	0	0	19	7	0	0
1984 12 15	83	36	281	272	259	134	252	65	22	4	0	0	0	0	0
1984 12 17	83	32	285	273	255	188	262	37	5	0	0	18	8	2	0
1984 12 19	83	33	284	277	263	148	284	18	8	2	0	15	0	0	0
1984 12 21	83	31	286	276	265	218	282	26	0	0	0	9	0	0	0
1984 12 23	83	37	280	272	257	181	274	15	3	0	0	28	14	5	0
1984 12 25	83	33	284	273	261	169	251	21	13	5	0	45	1	1	0
1984 12 27	83	41	276	261	243	159	238	14	1	1	0	65	11	0	0
1984 12 29	83	39	278	273	257	184	252	53	6	0	0	12	3	0	0
1984 12 31	83	31	286	276	264	206	284	32	4	1	0	1	0	0	0
1985 01 02	83	20	297	288	276	177	275	41	6	0	0	1	0	0	0
1985 01 04	83	18	299	292	279	241	278	33	0	0	0	6	3	0	0
1985 01 06	83	23	294	279	270	232	270	15	3	0	0	32	12	1	0
1985 01 08	83	48	269	258	246	188	236	0	0	0	0	81	27	5	0
1985 01 10	83	38	279	267	244	195	291	25	1	0	0	1	0	0	0
1985 01 12	83	26	291	286	256	191	275	41	12	0	0	1	0	0	0
1985 01 14	83	34	283	273	260	205	248	30	1	0	0	39	15	1	0
1985 01 16	83	33	284	275	257	169	259	21	6	2	0	37	8	2	0
1985 01 18	83	43	274	269	262	229	232	63	9	2	0	22	6	0	0
1985 01 20	83	54	263	253	236	215	270	7	1	0	0	40	26	9	0
1985 01 22	83	63	254	247	232	188	261	9	2	0	0	47	8	0	0
1985 01 24	83	66	251	232	217	178	247	14	0	0	0	56	21	0	0
1985 01 26	83	67	250	239	211	164	261	22	7	0	0	34	8	1	0
1985 01 28	83	58	259	246	235	196	242	73	22	1	0	2	0	0	0
1985 01 30	83	58	259	253	243	217	266	43	10	0	0	8	2	0	0
1985 02 01	83	49	268	258	244	207	286	16	2	0	0	15	0	0	0
1985 02 03	83	50	267	257	247	218	298	14	1	0	0	5	1	0	0
1985 02 05	83	44	273	259	253	214	295	19	3	0	0	3	0	0	0
1985 02 07	83	48	269	259	241	142	215	7	2	1	0	95	14	3	0
1985 02 09	83	57	260	249	232	175	220	47	13	3	0	50	11	0	0
1985 02 11	83	56	261	243	231	175	298	5	0	0	0	14	0	0	0
1985 02 13	83	56	261	252	238	198	284	29	2	0	0	4	0	0	0
1985 02 15	83	56	261	249	241	211	305	7	0	0	0	5	0	0	0
1985 02 17	83	62	255	240	229	158	267	2	0	0	0	48	11	1	0
1985 02 19	83	47	270	255	239	198	256	54	14	1	0	7	3	2	0
1985 02 21	83	52	265	254	243	191	267	21	12	2	0	29	7	0	0
1985 02 23	83	105	212	188	161	141	198	0	0	0	0	119	97	47	4
1985 02 25	83	48	269	262	247	190	194	123	103	52	8	0	0	0	0
1985 02 27	83	40	277	265	253	188	280	36	0	0	0	1	0	0	0
1985 03 01	83	18	299	293	278	222	267	50	36	1	0	0	0	0	0
1985 03 03	83	18	299	289	276	233	310	0	0	0	0	7	0	0	0

Cb - land blanked cells, C# - Cells with #/10 concentration, D# - Cells showing an increase in concentration \geq #/10's, D-# - Cells showing a decrease in concentration \geq #/10's

Date	Cb	C0	C1	C3	C6	C9	D0	D1	D3	D6	D9	D-1	D-3	D-6	D-9
1985 03 05	83	18	299	288	269	183	275	2	0	0	0	40	3	0	0
1985 03 07	83	14	303	292	283	188	290	22	3	0	0	5	0	0	0
1985 03 09	83	9	308	296	282	222	290	24	0	0	0	3	0	0	0
1985 03 11	83	13	304	294	280	221	306	5	0	0	0	6	0	0	0
1985 03 13	83	16	301	294	284	213	298	13	0	0	0	6	0	0	0
1985 03 15	83	28	289	279	264	237	267	4	0	0	0	46	15	2	0
1985 03 17	83	36	281	271	260	212	272	3	2	1	0	42	4	0	0
1985 03 19	83	27	290	284	273	234	276	41	10	0	0	0	0	0	0
1985 03 21	83	14	303	297	294	252	279	38	18	6	0	0	0	0	0
1985 03 23	83	23	294	289	282	247	293	1	0	0	0	23	13	3	0
1985 03 25	83	24	293	286	272	213	275	1	0	0	0	41	2	0	0
1985 03 27	83	30	287	282	274	221	293	13	1	0	0	11	5	0	0
1985 03 29	83	43	274	266	256	219	279	2	0	0	0	36	17	6	0
1985 03 31	83	36	281	272	257	212	280	22	3	0	0	15	1	1	0
1985 04 02	83	18	299	289	276	246	249	67	26	3	0	1	0	0	0
1985 04 04	83	22	295	287	275	243	296	5	0	0	0	16	0	0	0
1985 04 06	83	27	290	284	272	228	288	4	0	0	0	25	4	1	0
1985 04 08	83	39	278	267	257	227	258	13	3	1	0	46	17	1	0
1985 04 10	83	42	275	266	253	197	267	11	2	0	0	39	4	1	0
1985 04 12	83	32	285	275	265	227	259	54	7	2	0	4	2	1	0
1985 04 14	83	21	296	287	273	232	273	35	10	1	0	9	2	0	0
1985 04 16	83	28	289	284	273	227	277	19	3	0	0	21	5	2	0
1985 04 18	83	35	282	274	263	214	286	6	2	2	0	25	11	1	1
1985 04 20	83	46	271	260	241	160	243	1	0	0	0	73	26	2	0
1985 04 22	83	49	268	253	234	160	275	12	2	0	0	30	2	0	0
1985 04 24	83	54	263	251	233	158	303	7	0	0	0	7	1	0	0
1985 04 26	83	62	255	243	228	169	292	3	1	0	0	22	4	0	0
1985 04 28	83	57	260	248	226	168	294	15	3	0	0	8	0	0	0
1985 04 30	83	38	279	267	248	168	259	52	19	10	0	6	0	0	0
1985 05 02	83	51	266	257	243	198	246	41	7	2	0	30	16	4	0
1985 05 04	83	54	263	257	241	188	297	4	0	0	0	16	2	0	0
1985 05 06	83	52	265	258	244	188	303	9	0	0	0	5	0	0	0
1985 05 08	83	52	265	255	242	202	287	18	2	0	0	12	0	0	0
1985 05 10	83	56	261	251	241	191	292	1	1	0	0	24	3	0	0
1985 05 12	83	63	254	243	233	202	291	9	0	0	0	17	9	1	0
1985 05 14	83	57	260	248	226	162	254	14	7	0	0	49	8	3	0
1985 05 16	83	50	267	253	232	162	226	53	12	4	0	38	9	2	0
1985 05 18	83	64	253	242	228	196	243	37	9	2	0	37	7	0	0
1985 05 20	83	76	241	227	200	33	103	7	3	0	0	207	58	2	0
1985 05 22	83	77	240	231	198	56	242	50	8	2	0	25	4	0	0
1985 05 24	83	83	234	210	188	61	188	75	1	0	0	54	24	8	1
1985 05 26	83	85	232	215	189	46	237	19	11	6	0	61	6	2	0
1985 05 28	83	89	228	212	188	58	252	25	8	3	0	40	6	0	0
1985 05 30	83	92	225	199	161	59	221	18	0	0	0	78	15	1	0
1985 06 01	83	85	232	214	183	42	181	94	20	0	0	42	10	0	0
1985 06 03	83	87	230	199	161	74	229	41	10	0	0	47	15	3	0
1985 06 05	83	105	212	179	150	37	200	23	6	0	0	94	26	2	0
1985 06 07	83	95	222	196	154	46	229	64	10	1	0	24	7	0	0
1985 06 09	83	101	216	195	152	58	258	26	1	0	0	33	3	0	0
1985 06 11	83	102	215	193	146	45	254	27	4	0	0	36	6	1	0
1985 06 13	83	103	214	178	128	27	209	25	7	1	0	83	18	0	0
1985 06 15	83	127	190	159	117	41	204	44	2	0	0	69	24	4	0
1985 06 17	83	121	196	156	104	25	217	45	7	0	0	55	15	2	0
1985 06 19	83	124	193	155	117	64	209	76	8	1	0	32	3	1	0
1985 06 21	93	123	194	165	120	33	208	42	21	2	0	67	5	0	0
1985 06 23	83	175	142	106	67	0	144	7	1	0	0	166	65	4	0
1985 06 25	83	145	172	131	72	1	227	69	22	0	0	21	1	0	0
1985 06 27	83	161	156	125	77	0	236	32	0	0	0	49	4	0	0
1985 06 29	83	189	128	79	50	0	221	11	0	0	0	85	30	4	0
1985 07 01	83	167	150	110	63	2	221	85	11	0	0	11	1	0	0
1985 07 03	83	211	106	75	52	0	199	1	0	0	0	117	11	2	0
1985 07 05	83	202	115	74	27	0	244	31	12	0	0	42	14	0	0
1985 07 07	83	239	78	54	25	0	253	9	3	0	0	55	17	0	0
1985 07 09	83	227	90	59	38	0	260	44	4	0	0	13	3	0	0
1985 07 11	83	223	94	56	3	0	253	15	5	0	0	49	7	0	0

Cb - land blanked cells, C# - Cells with #/10 concentration, D# - Cells showing an increase in concentration \geq #/10's, D-# - Cells showing a decrease in concentration \geq #/10's

Date	Cb	C0	C1	C3	C6	C9	D0	D1	D3	D6	D9	D-1	D-3	D-6	D-9
1985 07 13	83	244	73	52	3	0	273	11	3	0	0	33	1	0	0
1985 07 15	83	255	62	46	0	0	297	2	1	0	0	18	1	0	0
1985 07 17	83	245	72	47	0	0	281	11	0	0	0	25	0	0	0
1985 07 19	83	246	71	46	0	0	302	10	0	0	0	5	0	0	0
1985 07 21	83	273	44	15	0	0	252	0	0	0	0	65	4	0	0
1985 07 23	83	300	17	1	0	0	281	0	0	0	0	36	4	0	0
1985 07 25	83	303	14	0	0	0	314	0	0	0	0	3	0	0	0
1985 07 27	83	314	3	0	0	0	312	0	0	0	0	5	0	0	0
1985 07 29	83	315	2	0	0	0	316	0	0	0	0	1	0	0	0
1985 07 31	83	317	0	0	0	0	315	0	0	0	0	2	0	0	0

Cb - blank cells, C# - Cells with #/10 concentration, D# - Cells showing an increase in concentration \geq #/10's, D-# - Cells showing a decrease in concentration \geq #/10's

APPENDIX C

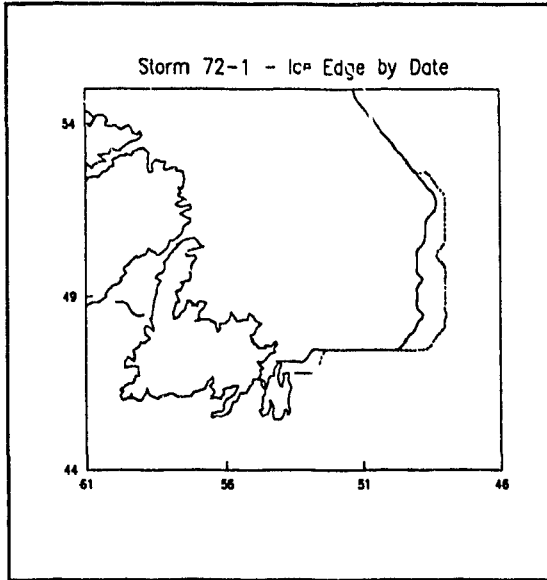
**Selected Synoptic Events and
Dates of Corresponding
Ice Information**

Appendix C
Synoptic Events Selected for Analysis

Storm	Start Date	Synoptic Observations	Ice Chart/SMMR Coverage
72-1	02/07	7	02/07,02/09
72-2	02/26	10	02/25/03/01
72-3	04/19	17	04/19,04/21,04/24
72-4	04/30	12	05/01,05/03
72-5	06/06	20	06/07,06/09
80-1	11/05	12	11/04,11/06,11/08,11/10
80-2	11/24	7	11/24,11/26,11/28
80-3	12/12	11	12/12,12/14,12/16,12/18
81-1	02/02	10	01/01,01/03,01/05
81-2	02/24	27	02/24,02/26,02/28,03/02
81-3	03/14	12	03/14,03/16,03/18
81-4	04/18	13	04/17,04/19,04/21
81-5	05/14	8	05/13,05/15
81-6	06/06	15	06/06,06/08,06/10
81-7	06/13	16	06/12,06/14,06/16,06/18
81-8	06/20	27	06/20,06/22,06/24
81-9	06/26	11	06/26,06/28
84-1	11/16	10	11/15,11/17,11/19
84-2	12/03	9	12/03,12/05
84-3	12/05	9	12/05,12/07
84-4	12/15	7	12/15,12/17
85-1	01/17	11	01/16,01/18,01/20
85-2	01/21	19	01/20,01/22,01/24,01/26
85-3	02/26	9	02/25,02/27,03/01
85-4	03/14	14	03/13,03/15,03/17
85-5	04/20	11	04/20,04/22,04/24
85-6	05/03	13	05/02,05/04,05/06
85-7	06/02	13	06/01,06/03,06/05
85-8	06/08	24	06/07,06/09,06/11,06,13
85-9	07/07	11	07/07,07/09,07/11
85-10	07/22	12	07/21,07/23,07/25

APPENDIX D

Ice Maps

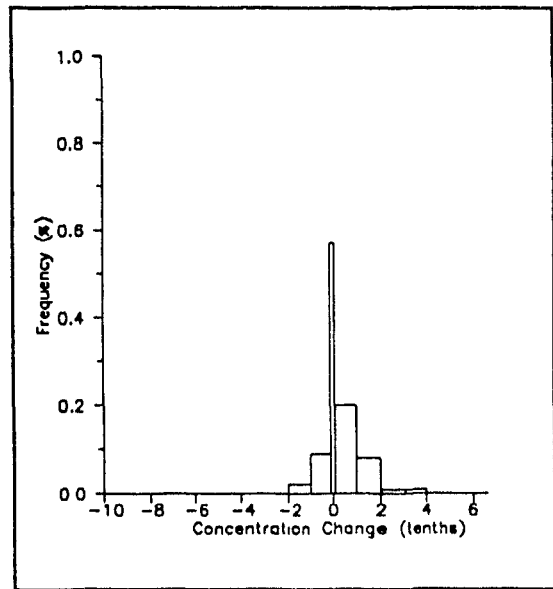
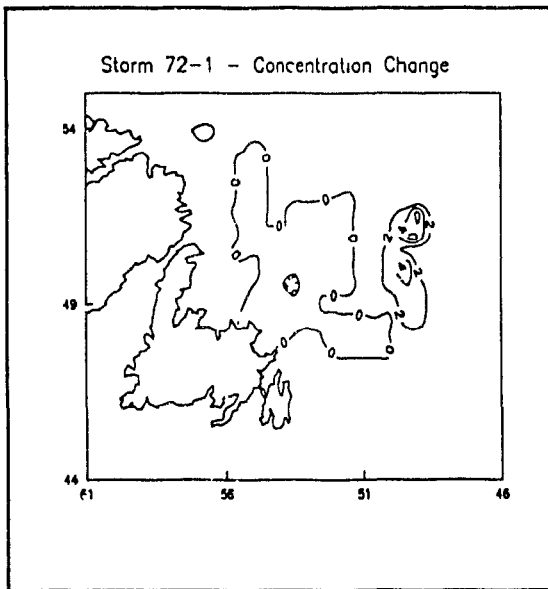


Storm 72-1

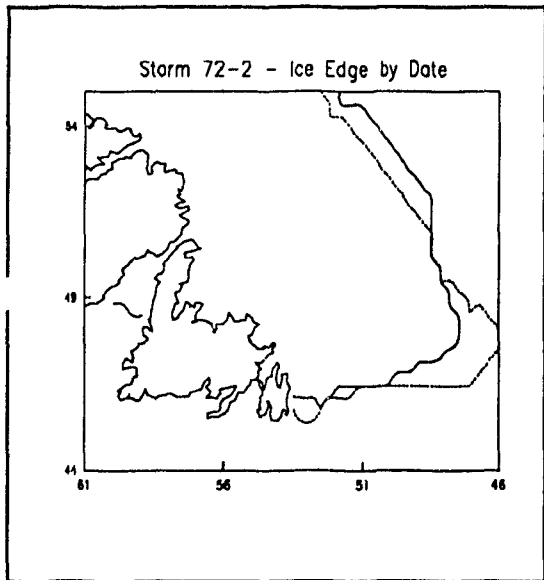
Minimum Pressure:	975.1 hPa
Pressure Range:	22.2 hPa
Storm Bearing:	45.0°T
Entry Latitude:	57.9°N
Entry Longitude:	43.2°W
Duration:	12 Obs

Ice Map/SMMR Dates:	02/07,02/09
---------------------	-------------

Cells Increasing in Concentration:	12%
Cells Decreasing in Concentration:	10%



(Line patterns for the ice edge plots progress by orbit from solid to coarse, medium and fine dashes)

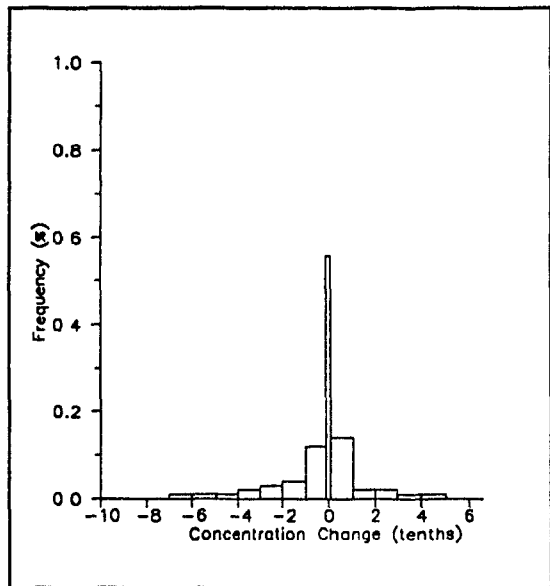
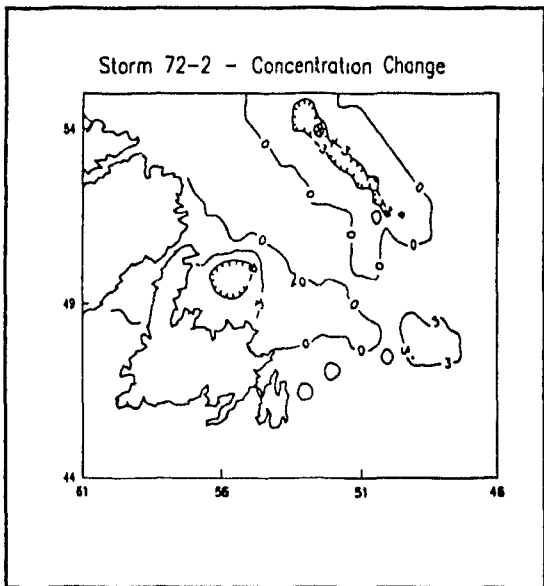


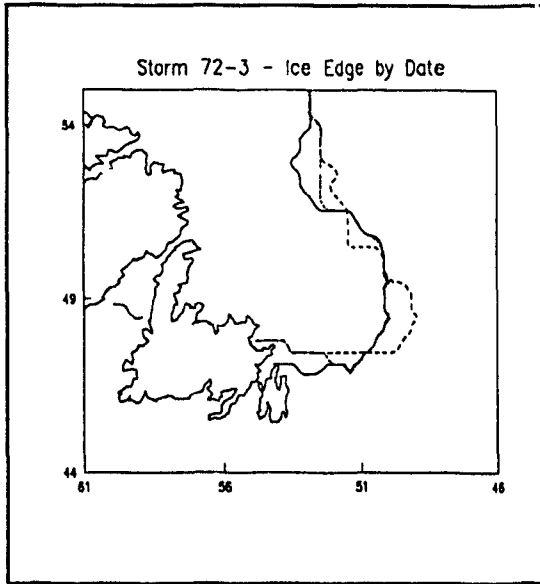
Storm 72-2

Minimum Pressure: 973.2 hPa
 Pressure Range: 29.3 hPa
 Storm Bearing: 61.0°T
 Entry Latitude: 47.3°N
 Entry Longitude: 68.5°W
 Duration: 10 Obs

Ice Map/SMMR Dates: 02/25,03/01

Cells Increasing in Concentration: 20%
 Cells Decreasing in Concentration: 24%



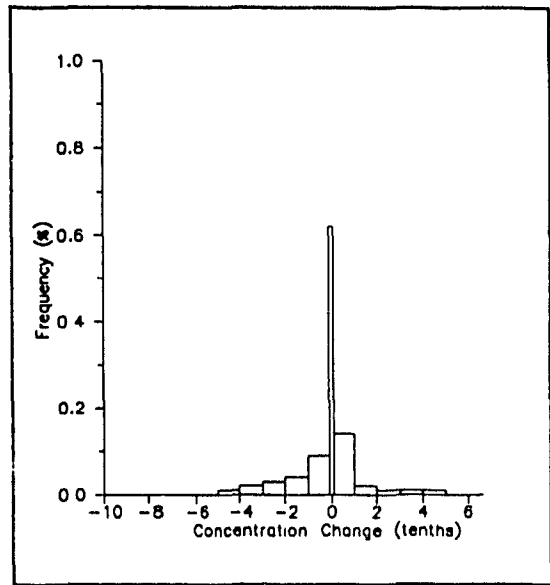
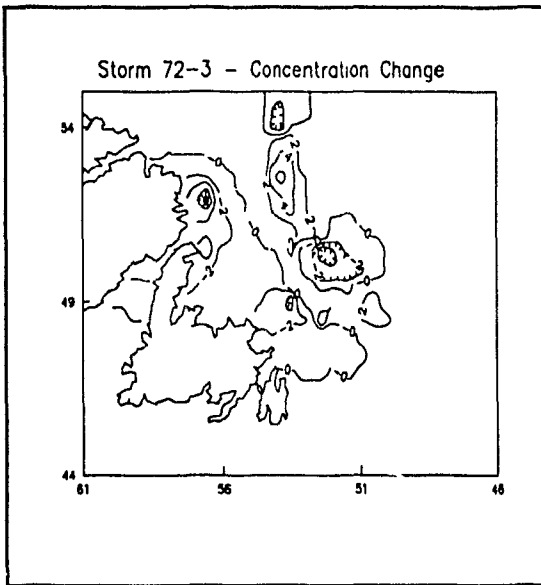


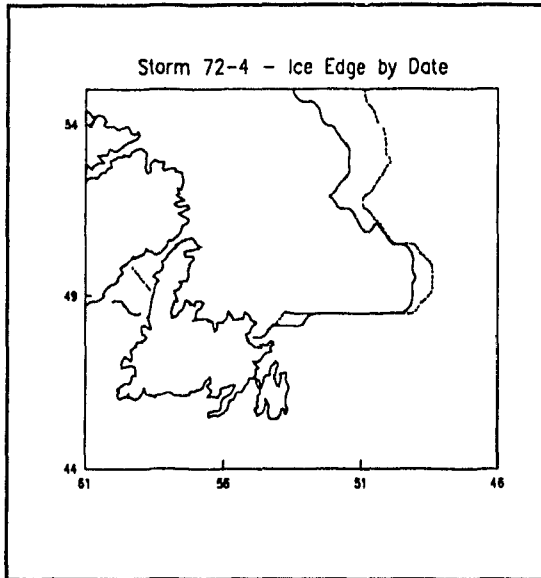
Storm 72-3

Minimum Pressure:	967.9 hPa
Pressure Range:	45.8 hPa
Storm Bearing:	2.0°T
Entry Latitude:	43.3°N
Entry Longitude:	42.8°W
Duration:	17 Obs

Ice Map/SMMR Dates:	04/19, 04/21, 04/24
---------------------	---------------------

Cells Increasing in Concentration:	19%
Cells Decreasing in Concentration:	19%



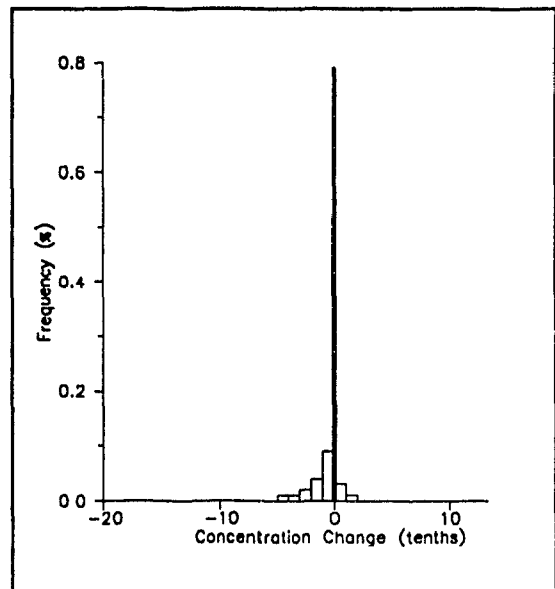
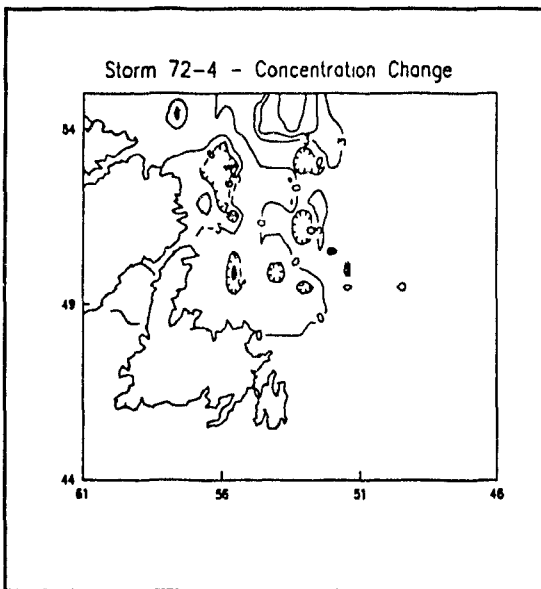


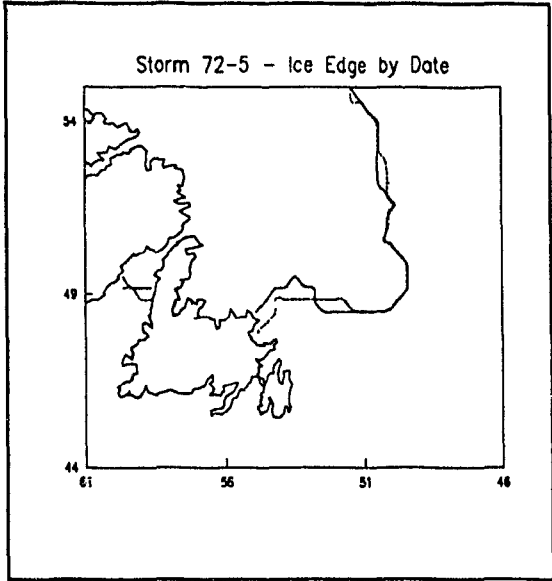
storm 72-4

Minimum Pressure:	980.4 hPa
Pressure Range:	21.0 hPa
Storm Bearing:	74.0°T
Entry Latitude:	54.9°N
Entry Longitude:	55.4°W
Duration:	12 Obs

Ice Map/SMMR Dates:	05/01,05/03
---------------------	-------------

Cells Increasing in Concentration:	16%
Cells Decreasing in Concentration:	23%



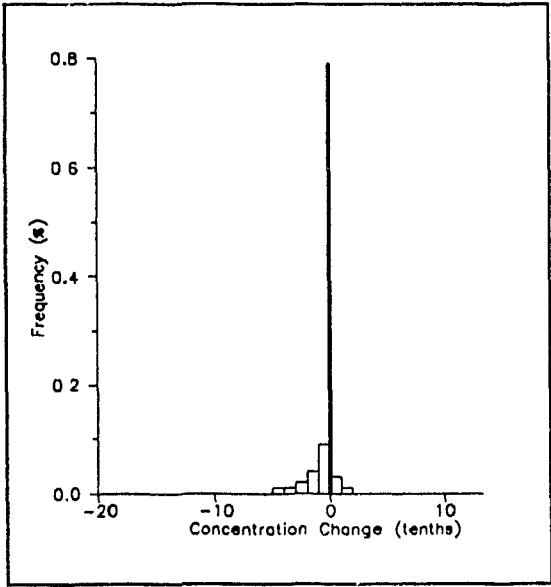
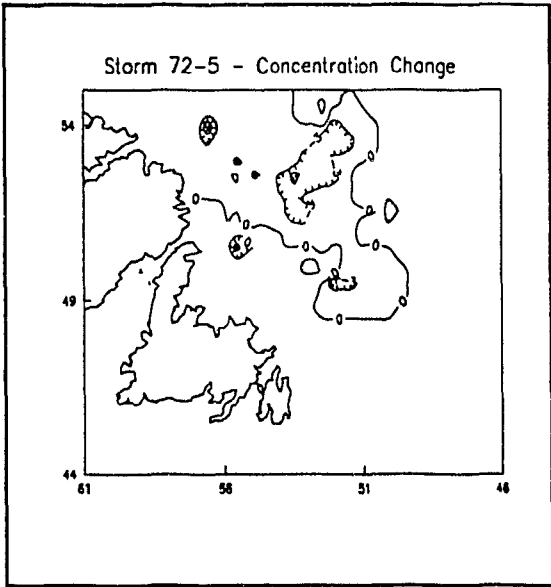


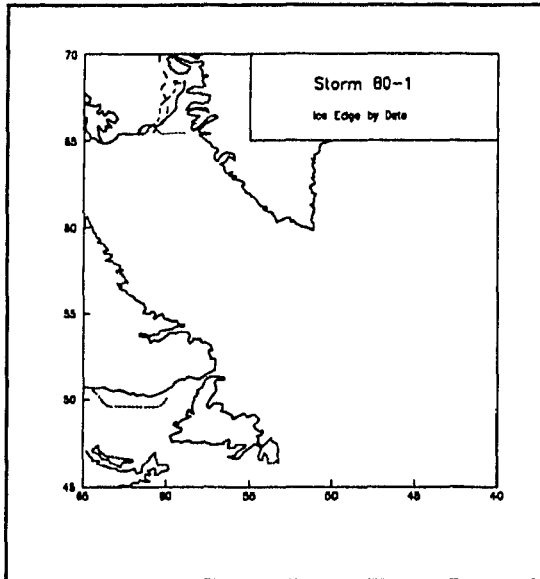
Storm 72-4

Minimum Pressure:	980.4 hPa
Pressure Range:	21.0 hPa
Storm Bearing:	74.0°T
Entry Latitude:	54.9°N
Entry Longitude:	55.4°W
Duration:	12 Obs

Ice Map/SMMR Dates:	05/01,05/03
---------------------	-------------

Cells Increasing in Concentration:	16%
Cells Decreasing in Concentration:	23%



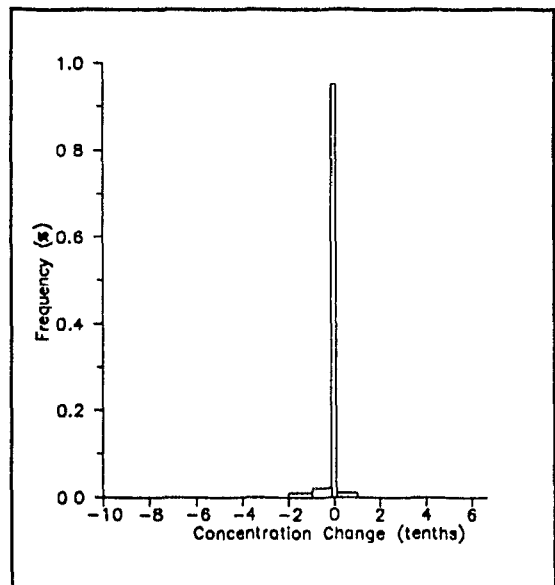
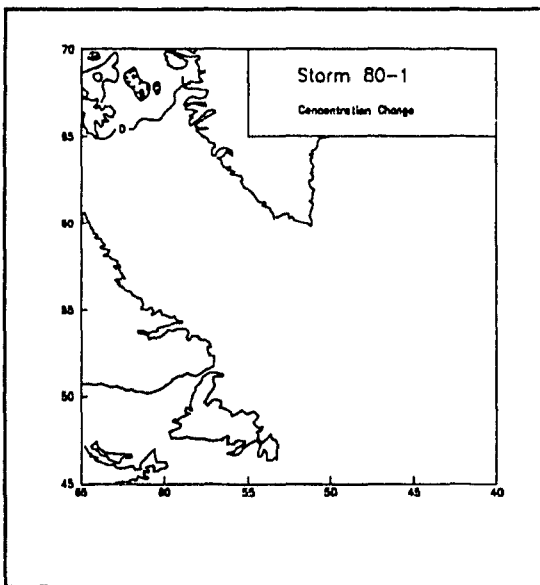


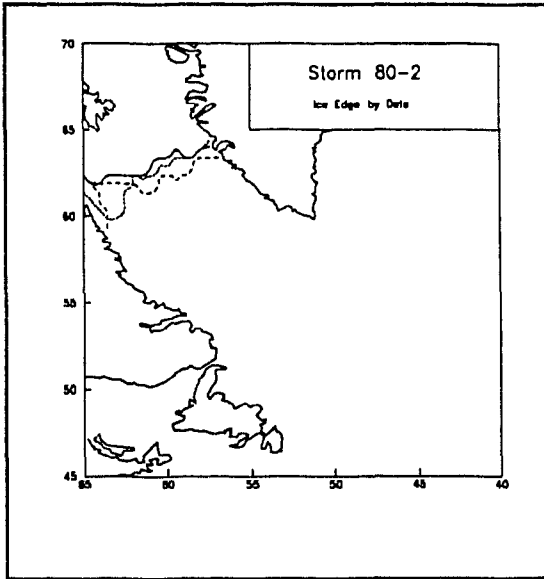
Storm 80-1

Minimum Pressure:	958.9 hPa
Pressure Range:	33.8 hPa
Storm Bearing:	320.0°T
Entry Latitude:	54.9°N
Entry Longitude:	52.3°W
Duration:	12 Obs

Ice Map/SMMR Dates:	11/04,11/06,11/08,11/10
---------------------	-------------------------

Cells Increasing in Concentration:	1%
Cells Decreasing in Concentration:	3%



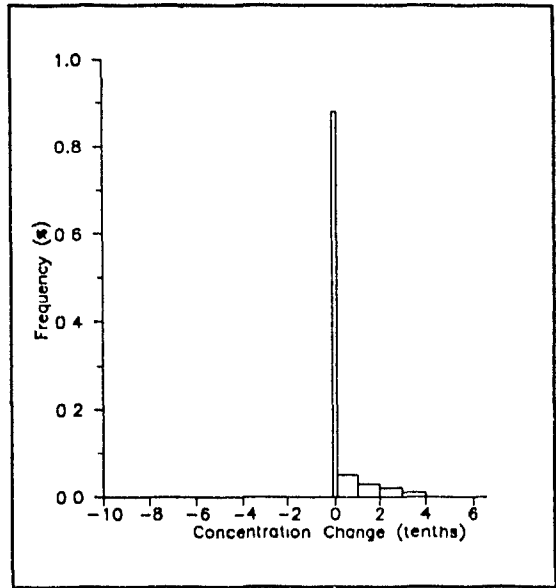
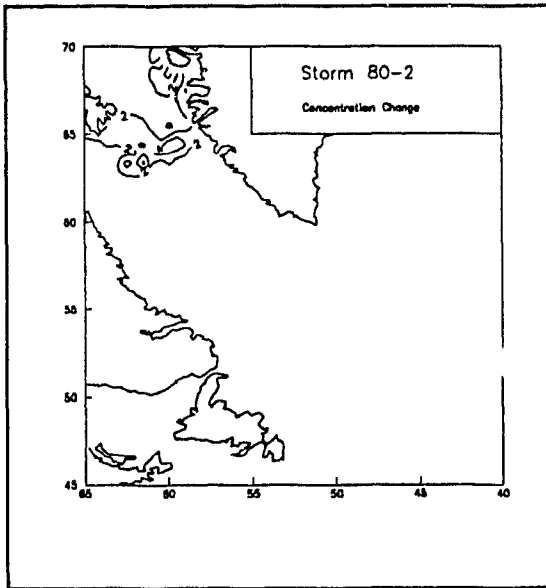


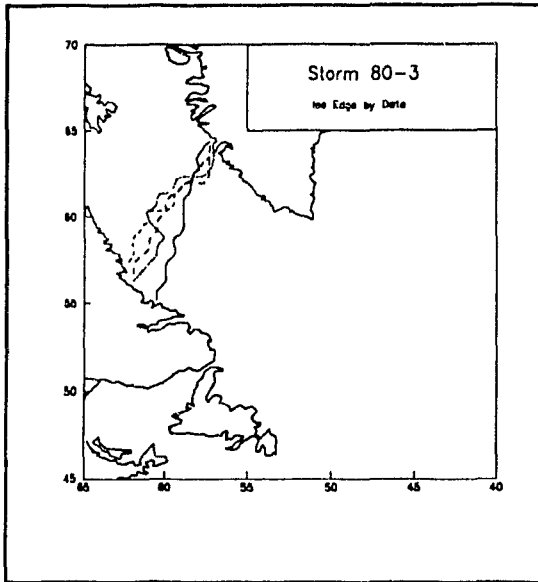
Storm 80-2

Minimum Pressure:	1005.1 hPa
Pressure Range:	14.2 hPa
Storm Bearing:	74.0°T
Entry Latitude:	65.5°N
Entry Longitude:	69.3°W
Duration:	7 Obs

Ice Map/SMPF Dates:	11/24, 11/26, 11/28
---------------------	---------------------

Cells Increasing in Concentration:	11%
Cells Decreasing in Concentration:	0%



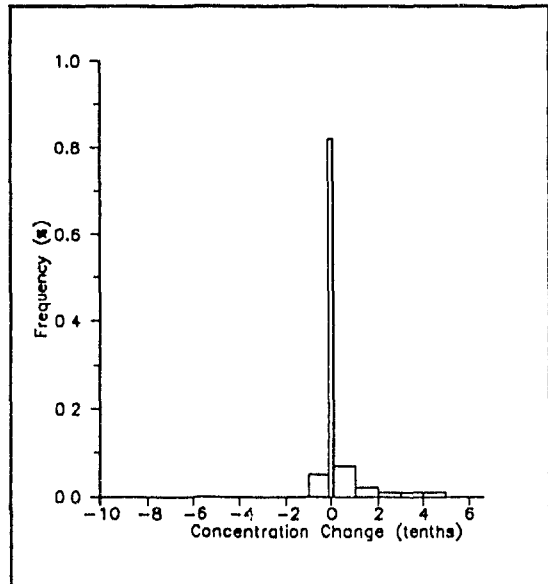
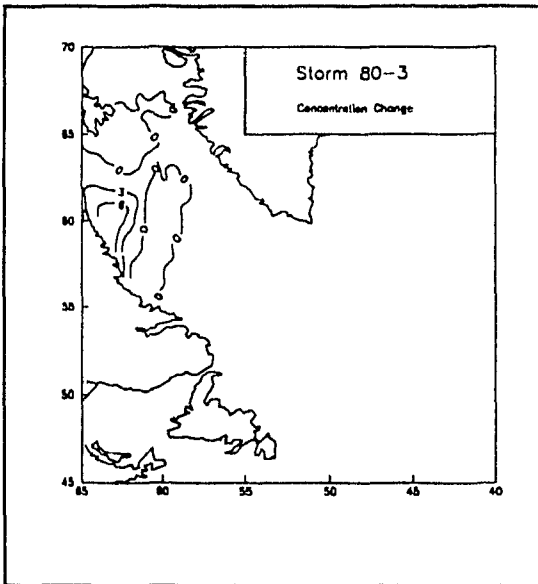


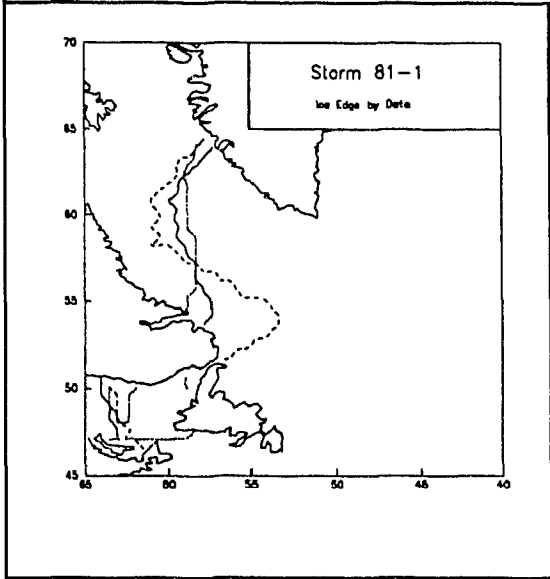
Storm 80-3

Minimum Pressure:	977.5 hPa
Pressure Range:	25.5 hPa
Storm Bearing:	59.0°T
Entry Latitude:	48.7°N
Entry Longitude:	64.9°W
Duration:	11 Obs

Ice Map/SMMR Dates:	12/12,12/14,11/ 16,12/18
---------------------	-----------------------------

Cells Increasing in Concentration:	15%
Cells Decreasing in Concentration:	4%



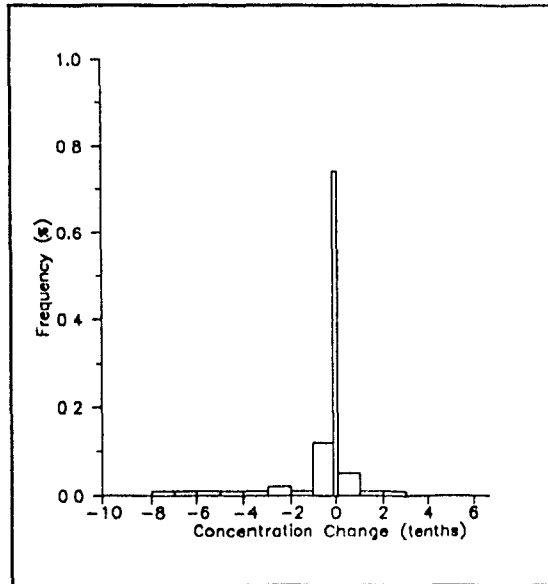
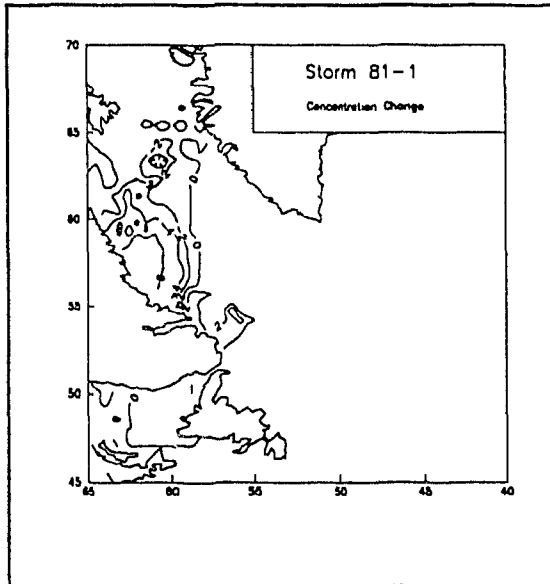


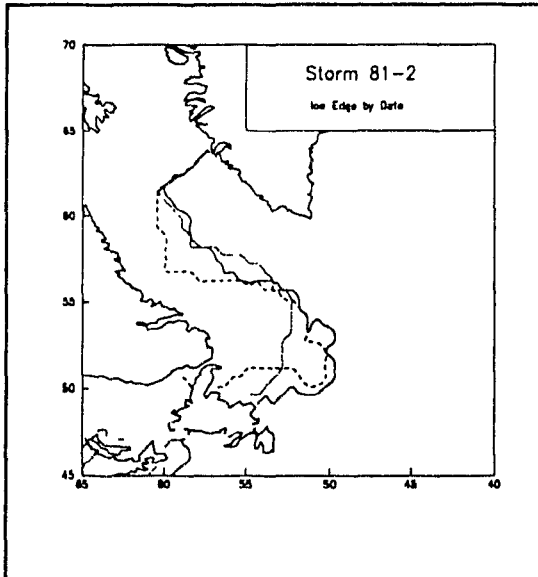
Storm 81-1

Minimum Pressure:	974.4 hPa
Pressure Range:	16.3 hPa
Storm Bearing:	58.0°T
Entry Latitude:	49.8°N
Entry Longitude:	68.1°W
Duration:	10 Obs

Ice Map/SMMR Dates:	01/01,01/03,01/05
---------------------	-------------------

Cells Increasing in Concentration:	7%
Cells Decreasing in Concentration:	20%



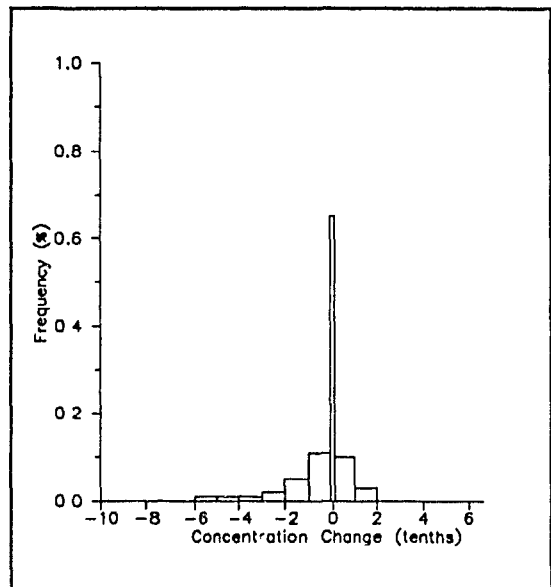
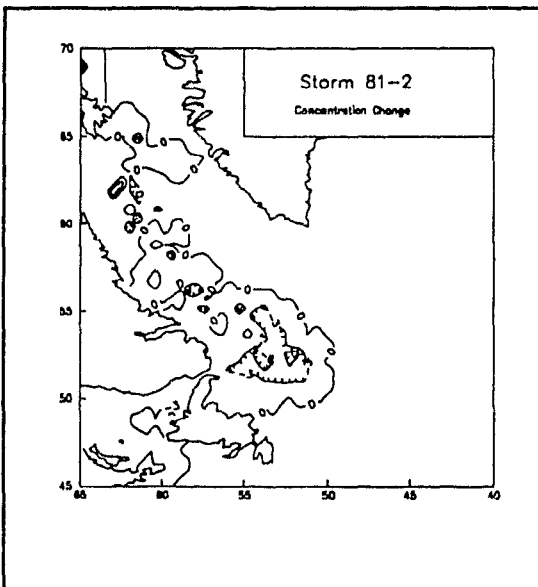


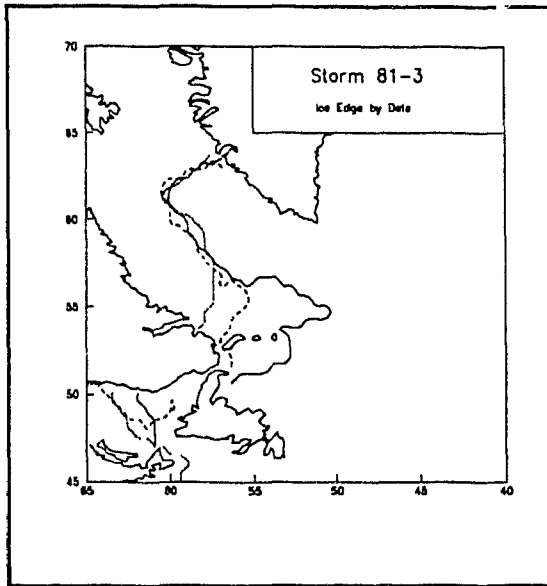
Storm 81-2

Minimum Pressure:	949.6 hPa
Pressure Range:	36.0 hPa
Storm Bearing:	19 0°T
Entry Latitude:	47.2°N
Entry Longitude:	67.6°W
Duration:	19 Obs

Ice Map/SMMR Dates:	01/20,01/23,01/26
---------------------	-------------------

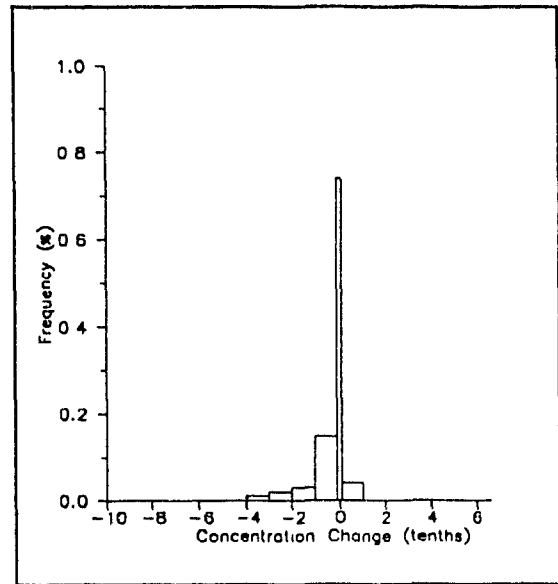
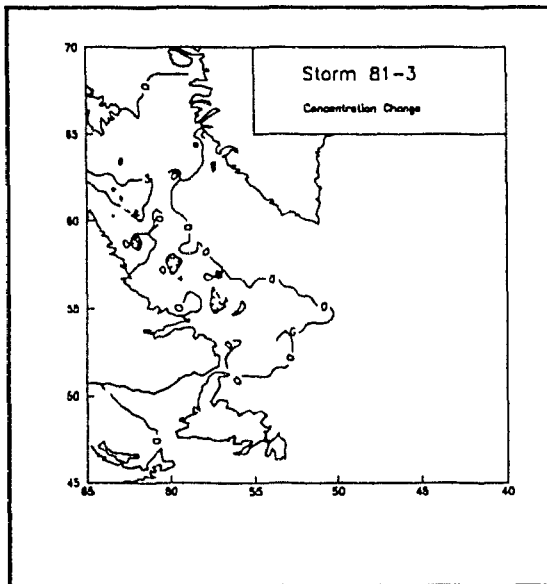
Cells Increasing in Concentration:	25%
Cells Decreasing in Concentration:	14%

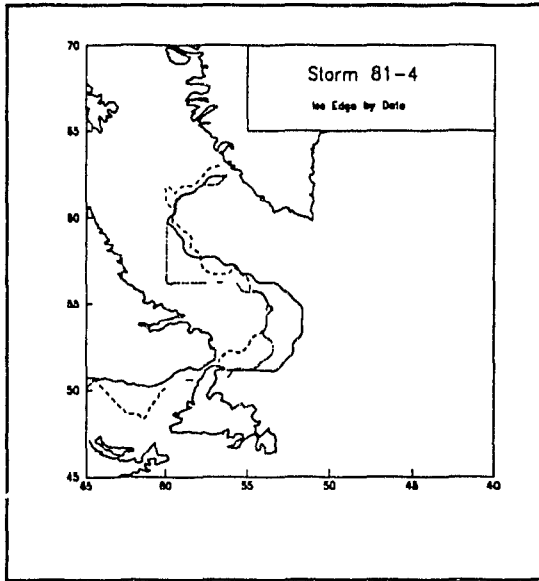




Storm 81-3

Minimum Pressure:	973.1 hPa
Pressure Range:	22.4 hPa
Storm Bearing:	11.0°T
Entry Latitude:	43.0°N
Entry Longitude:	62.5°W
Duration:	12 Obs
Ice Map/SMMR Dates:	03/14,03/16,03/18
Cells Increasing in Concentration:	4%
Cells Decreasing in Concentration:	21%



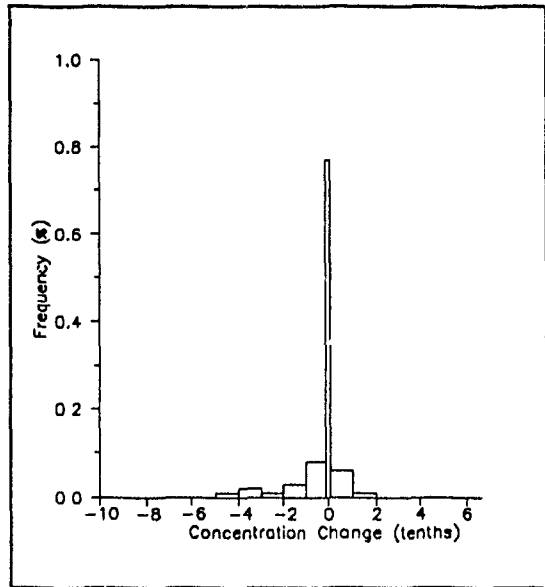
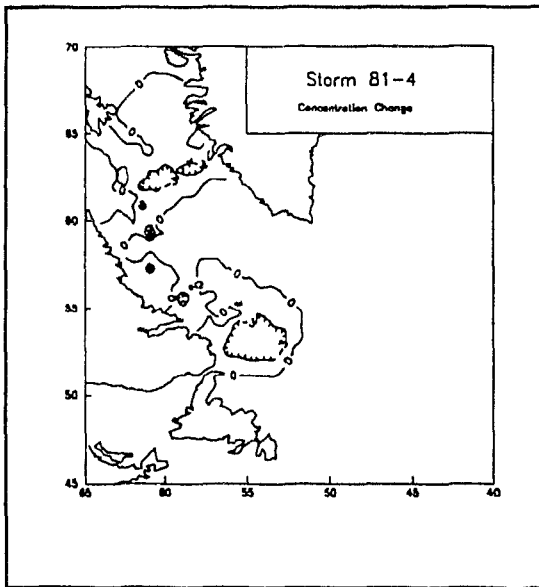


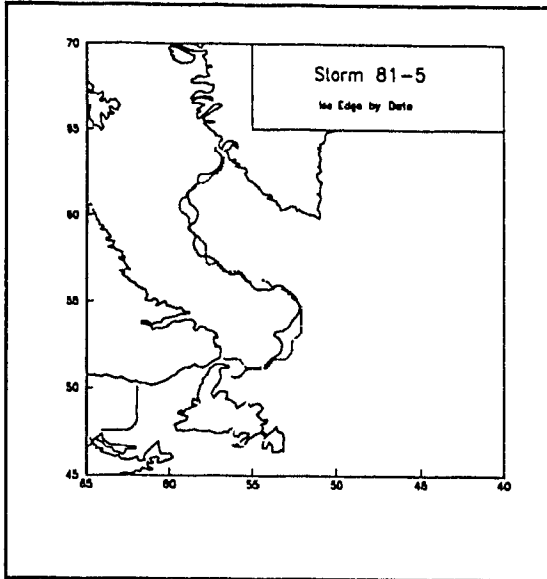
Storm 81-4

Minimum Pressure.	996.3 hPa
Pressure Range:	10.4 hPa
Storm Bearing:	105.0°T
Entry Latitude.	48.8°N
Entry Longitude:	68.0°W
Duration:	13 Obs

Ice Map/SMMR Dates:	04/17,04/19,04/21
---------------------	-------------------

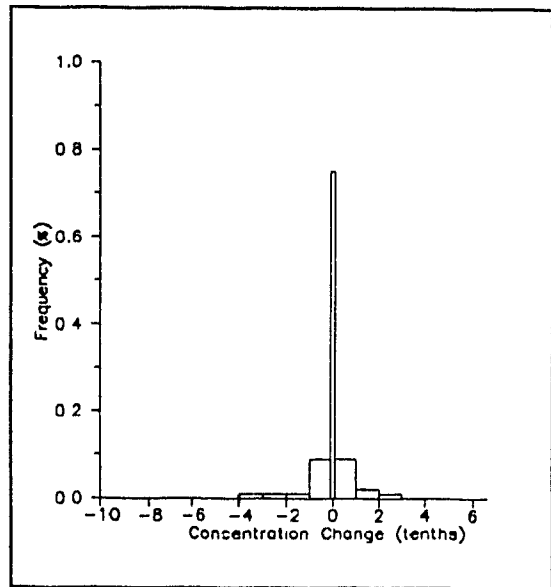
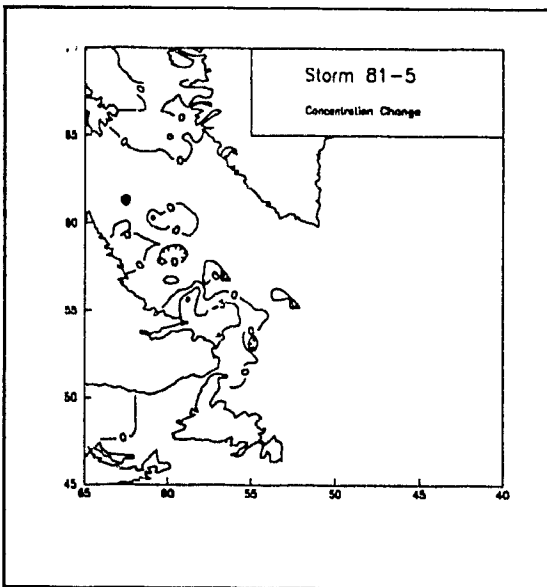
Cells Increasing in Concentration:	7%
Cells Decreasing in Concentration:	15%

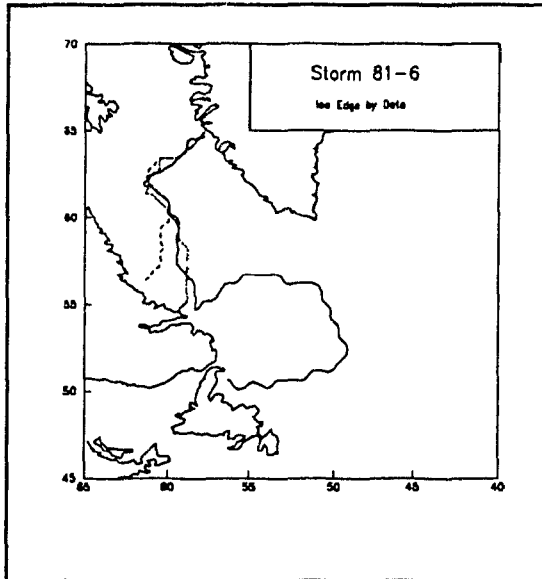




Storm 81-5

Minimum Pressure:	1002.2 hPa
Pressure Range:	11.9 hPa
Storm Bearing:	77.0°T
Entry Latitude:	52.4°N
Entry Longitude:	65.5°W
Duration:	8 Obs
Ice Map/SMMR Dates:	05/13,05/15
Cells Increasing in Concentration:	12%
Cells Decreasing in Concentration:	12%



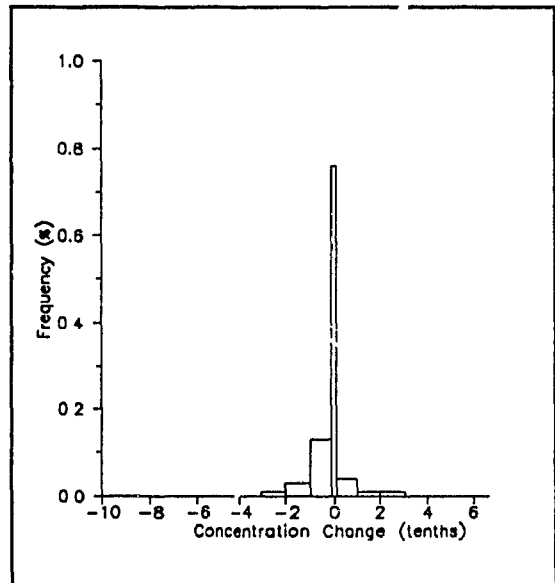
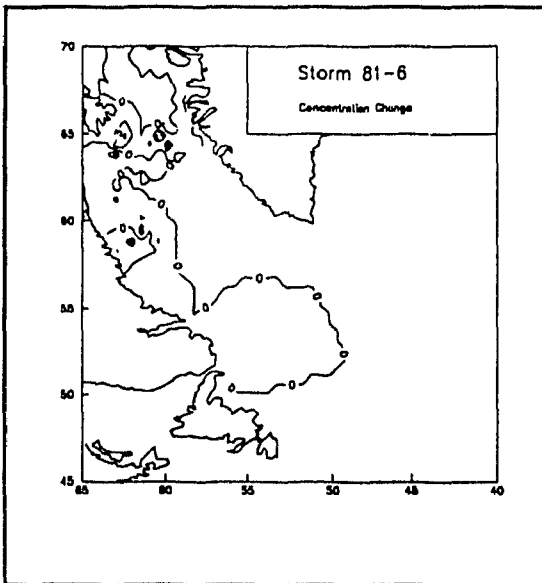


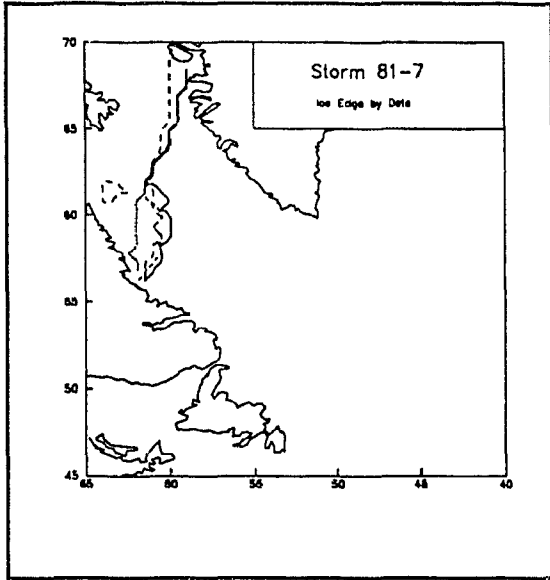
Storm 81-6

Minimum Pressure:	984.0 hPa
Pressure Range:	10.1 hPa
Storm Bearing:	97.0°T
Entry Latitude:	53.3°N
Entry Longitude:	68.0°W
Duration:	15 Obs

Ice Map/SMMR Dates:	06/06,06/08,06/10
---------------------	-------------------

Cells Increasing in Concentration:	6%
Cells Decreasing in Concentration:	17%



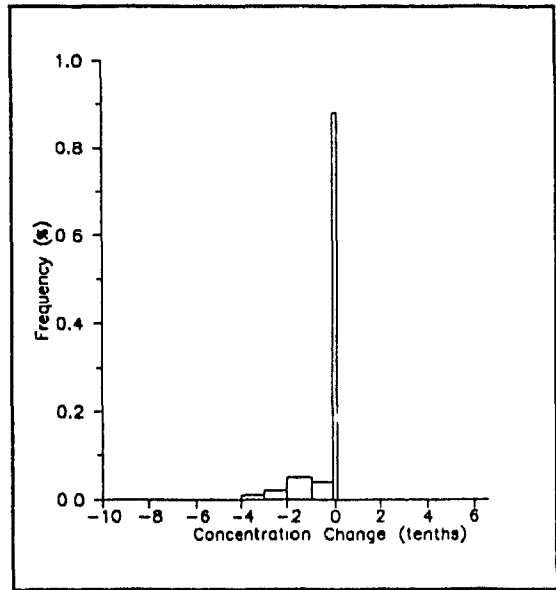
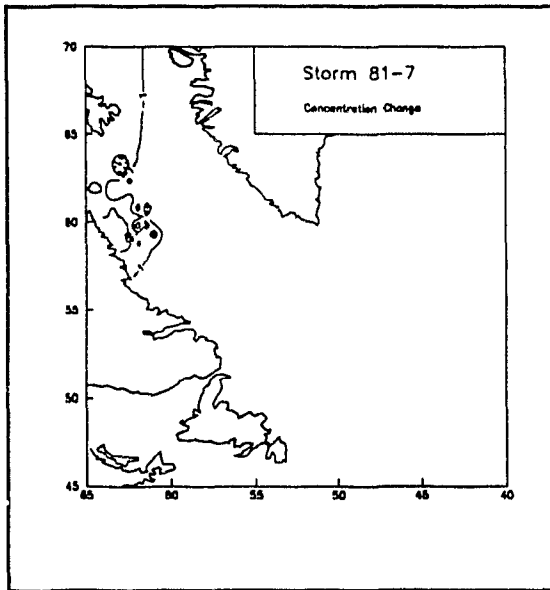


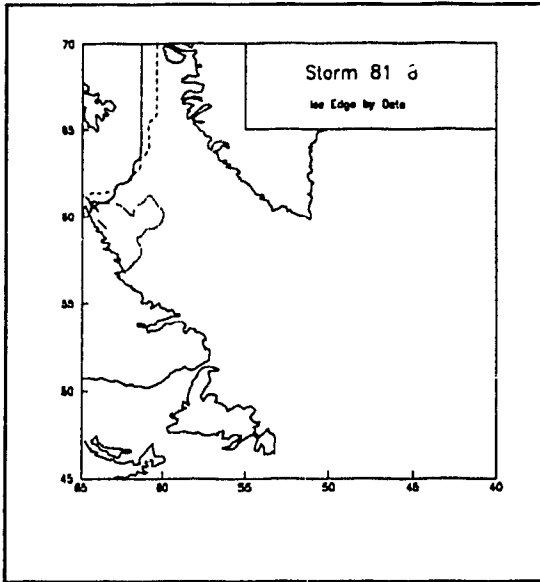
Storm 81-7

Minimum Pressure:	1004.5 hPa
Pressure Range:	5.7 hPa
Storm Bearing:	107.0°T
Entry Latitude:	64.8°N
Entry Longitude:	69.1°W
Duration:	16 Obs

Ice Map/SMMR Dates:	06/12,06/14,06/16,06/18
---------------------	-------------------------

Cells Increasing in Concentration:	0%
Cells Decreasing in Concentration:	12%



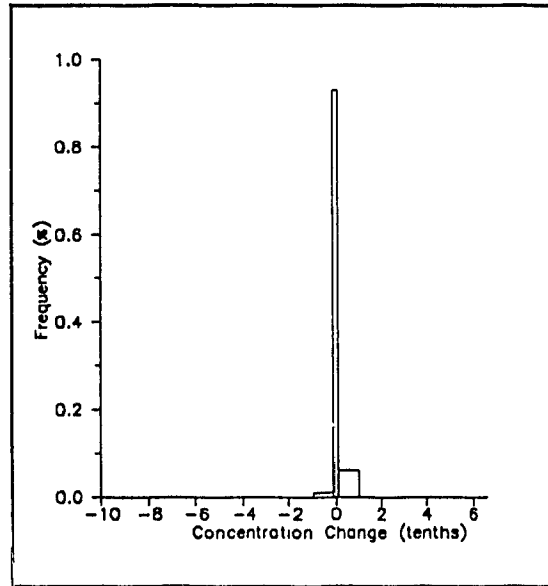
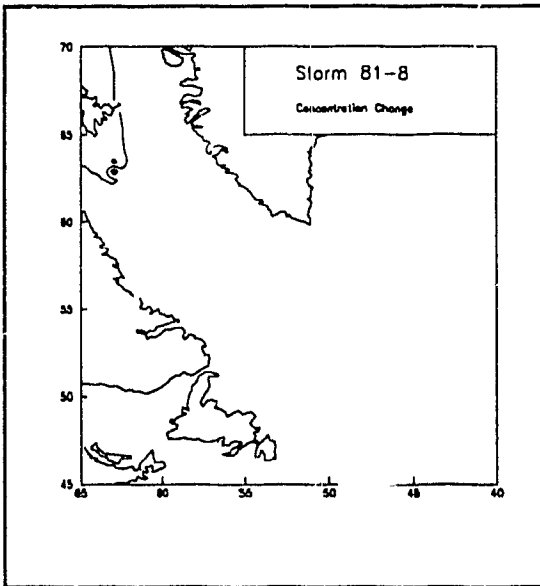


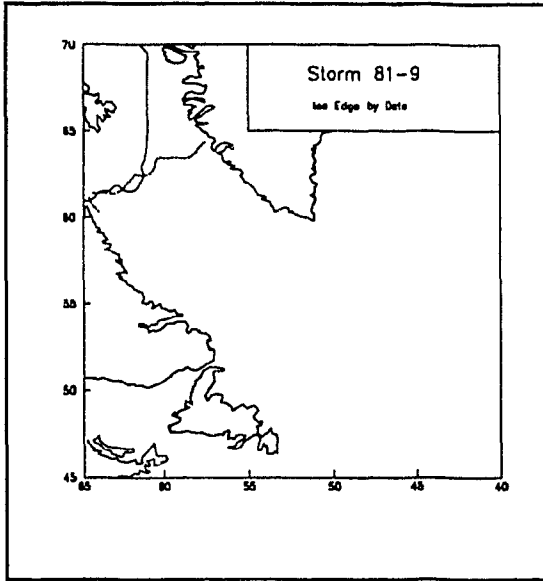
Storm 81-8

Minimum Pressure:	991.2 hPa
Pressure Range:	17.7 hPa
Storm Bearing:	27.0°T
Entry Latitude:	61.8°N
Entry Longitude:	69.3°W
Duration:	14 Obs

Ice Map/SMMR Dates:	06/20,06/22,06/24
---------------------	-------------------

Cells Increasing in Concentration:	6%
Cells Decreasing in Concentration:	1%



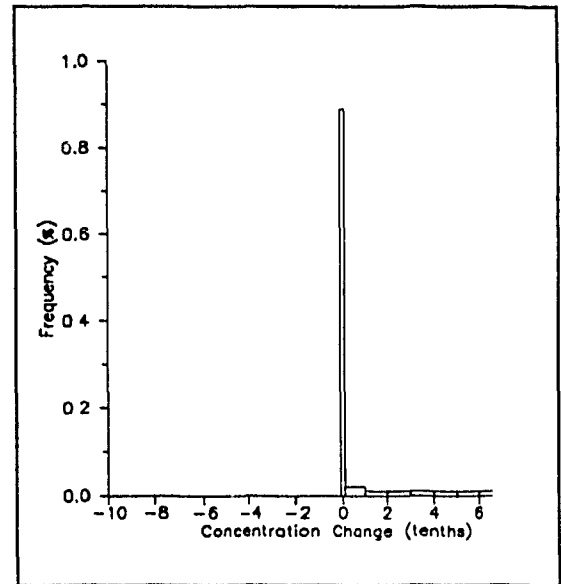
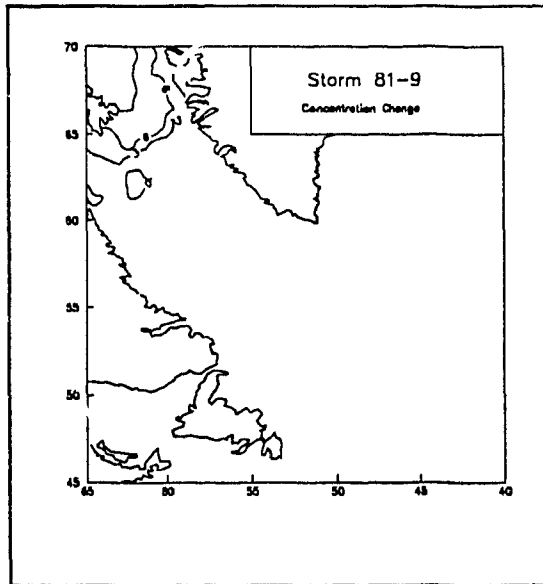


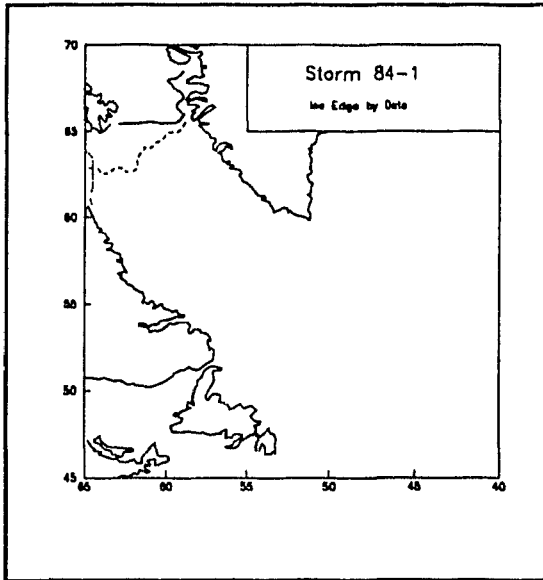
Storm 81-9

Minimum Pressure:	1000.6 hPa
Pressure Range:	4.2 hPa
Storm Bearing:	64.0°T
Entry Latitude:	47.8°N
Entry Longitude:	68.5°W
Duration:	11 Obs

Ice Map/SMMR Dates:	06/26,06/28
---------------------	-------------

Cells Increasing in Concentration:	12%
Cells Decreasing in Concentration:	0%



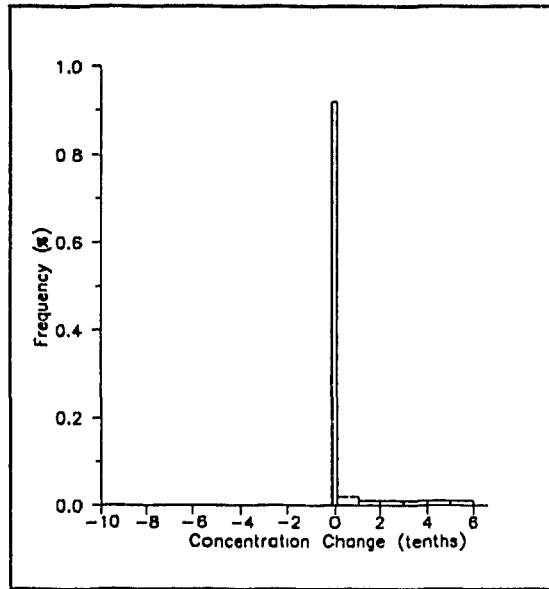
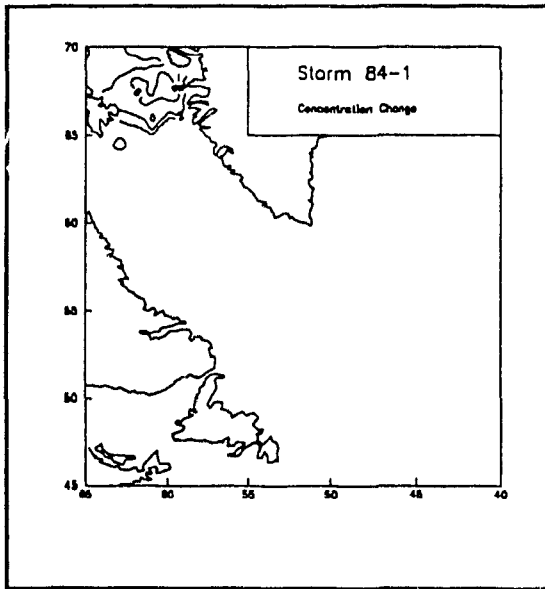


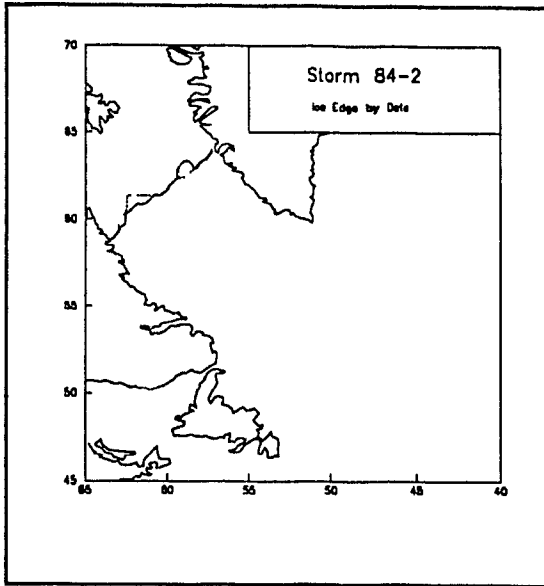
Storm 84-1

Minimum Pressure:	979.1 hPa
Pressure Range:	14.2 hPa
Storm Bearing:	284.0°T
Entry Latitude:	56.7°N
Entry Longitude:	41.3°W
Duration:	10 Obs

Ice Map/SMMR Dates:	11/15, 11/17, 11/19
---------------------	---------------------

Cells Increasing in Concentration:	7%
Cells Decreasing in Concentration:	0%



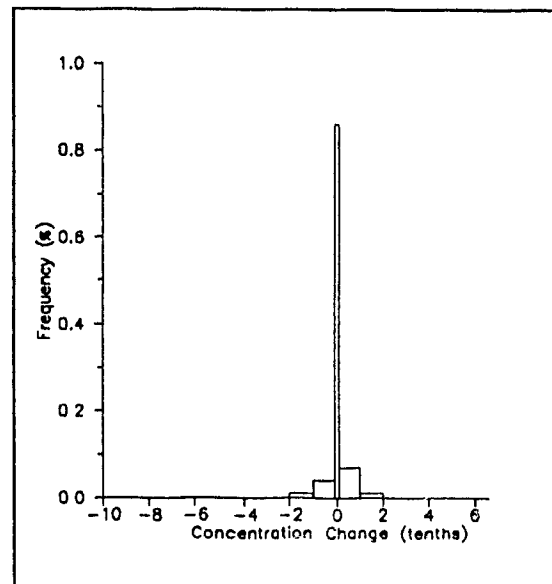
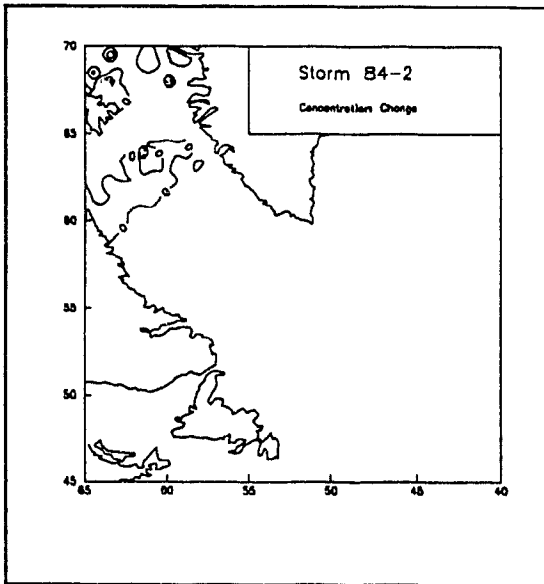


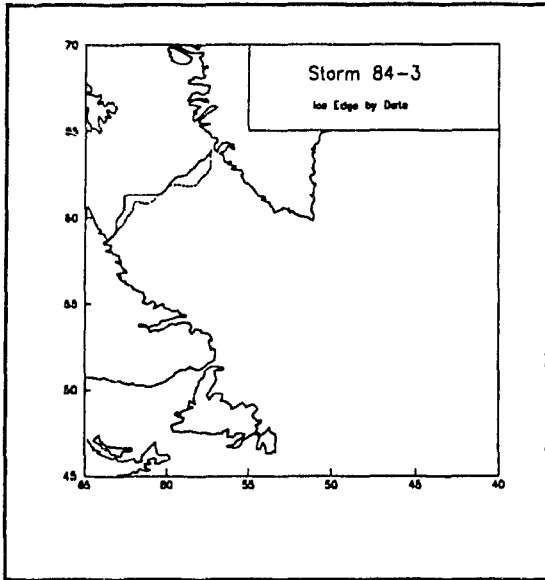
Storm 84-2

Minimum Pressure: 993.8 hPa
 Pressure Range: 6.9 hPa
 Storm Bearing: 360.0°T
 Entry Latitude: 55.9°N
 Entry Longitude: 68.1°W
 Duration: 9 Obs

Ice Map/SMMR Dates: 12/03,12/05

Cells Increasing in Concentration: 8%
 Cells Decreasing in Concentration: 5%



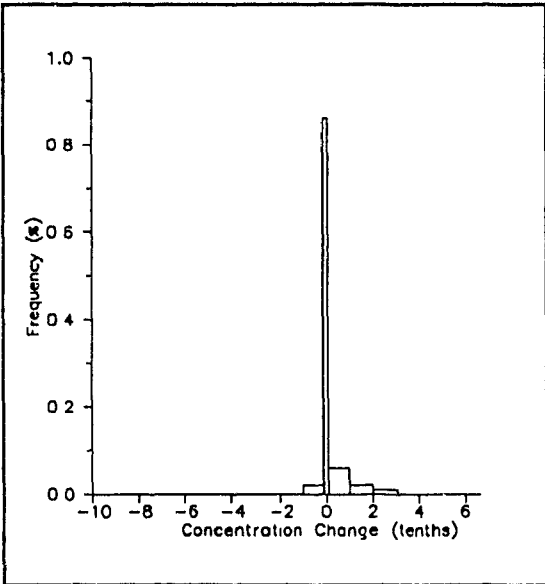
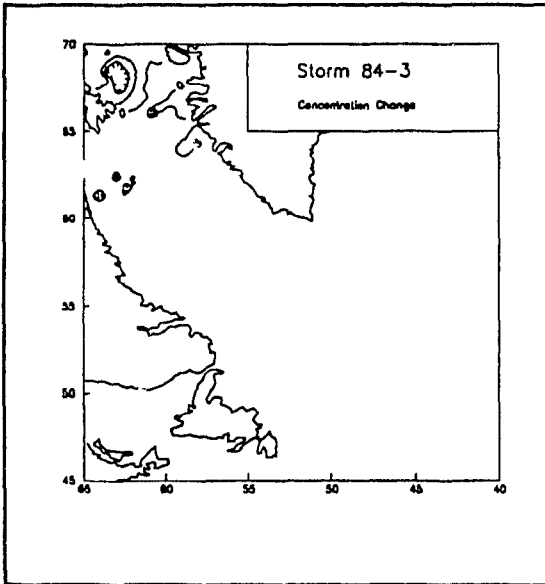


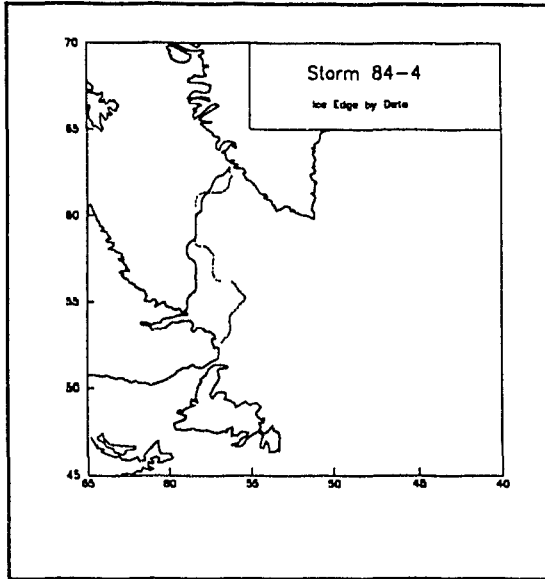
Storm 84-3

Minimum Pressure:	963.8 hPa
Pressure Range:	36.5 hPa
Storm Bearing:	54.0°T
Entry Latitude:	42.6°N
Entry Longitude:	68.3°W
Duration:	9 Obs

Ice Map/SMMR Dates:	12/05,12/07
---------------------	-------------

Cells Increasing in Concentration:	9%
Cells Decreasing in Concentration:	2%



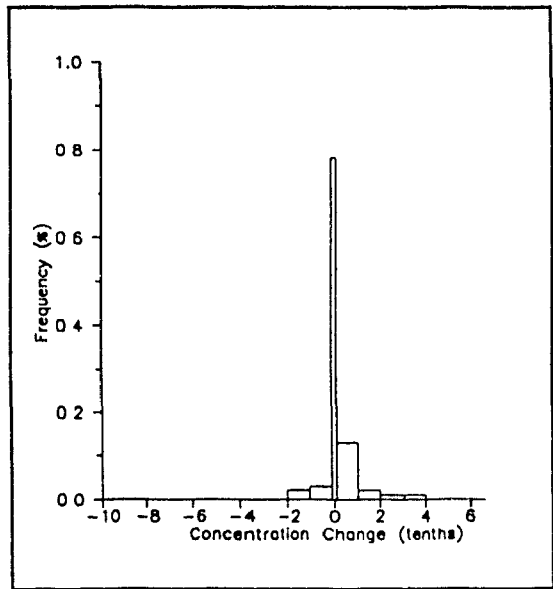
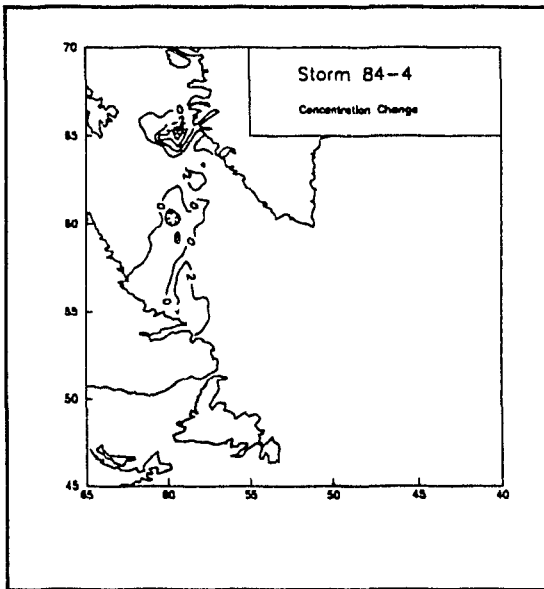


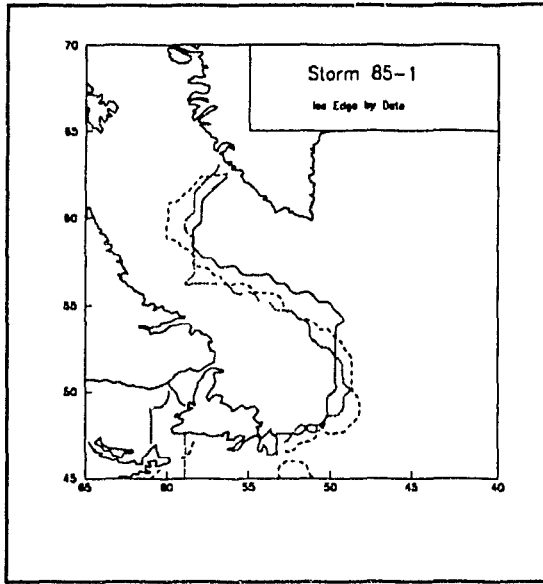
Storm 84-4

Minimum Pressure:	980.7 hPa
Pressure Range:	12.5 hPa
Storm Bearing:	82.0°T
Entry Latitude:	64.4°N
Entry Longitude:	62.4°W
Duration:	7 Obs

Ice Map/SMMR Dates:	12/15, 12/17
---------------------	--------------

Cells Increasing in Concentration:	17%
Cells Decreasing in Concentration:	5%



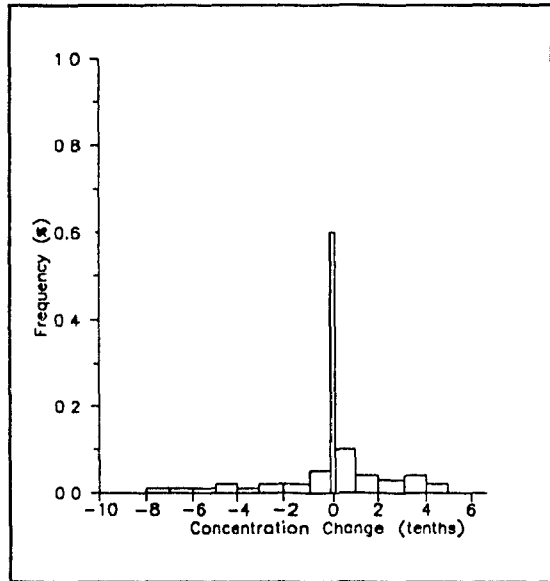
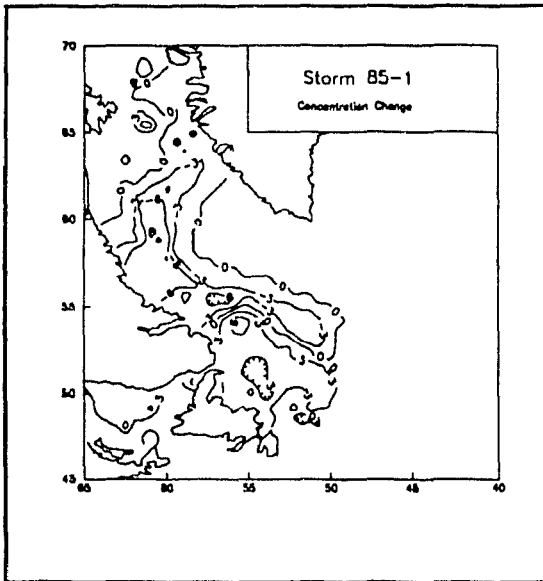


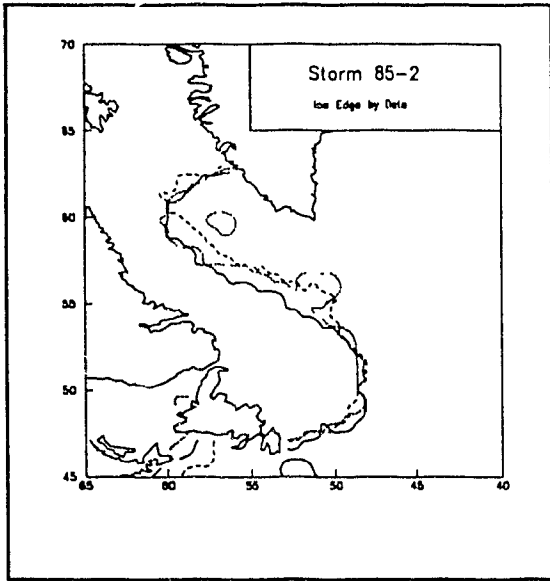
Storm 85-1

Minimum Pressure:	979.3 hPa
Pressure Range:	12.9 hPa
Storm Bearing:	298.0°T
Entry Latitude:	44.8°N
Entry Longitude:	42.0°W
Duration:	11 Obs

Ice Map/SMMR Dates:	01/16,01/18,01/20
---------------------	-------------------

Cells Increasing in Concentration:	23%
Cells Decreasing in Concentration:	15%



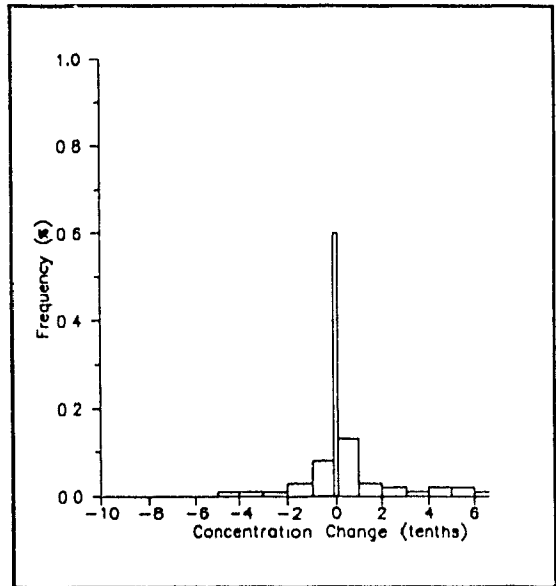
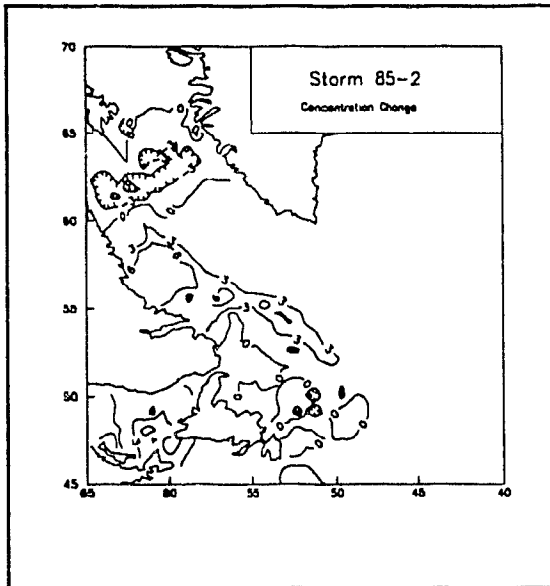


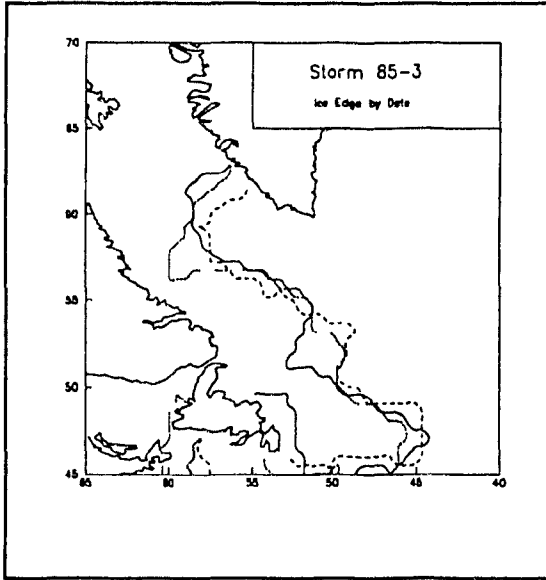
Storm 85-2

Minimum Pressure:	949.6 hPa
Pressure Range:	36.0 hPa
Storm Bearing:	19.0°T
Entry Latitude:	47.2°N
Entry Longitude:	57.3°W
Duration:	19 Obs

Ice Max./SMMR Dates:	01/20,01/23,01/26
----------------------	-------------------

Cells Increasing in Concentration:	25%
Cells Decreasing in Concentration:	14%



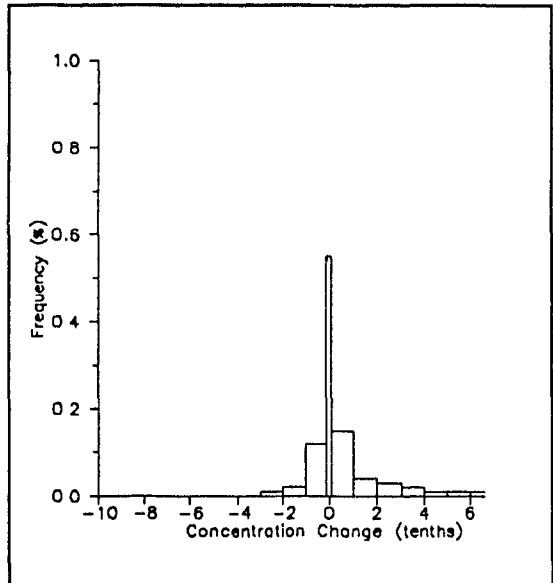
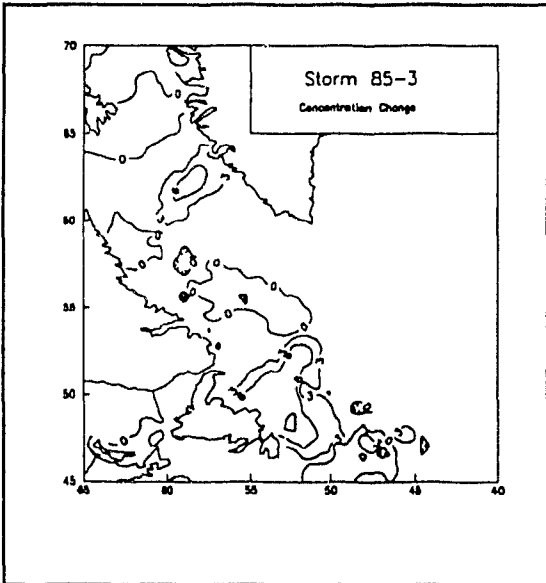


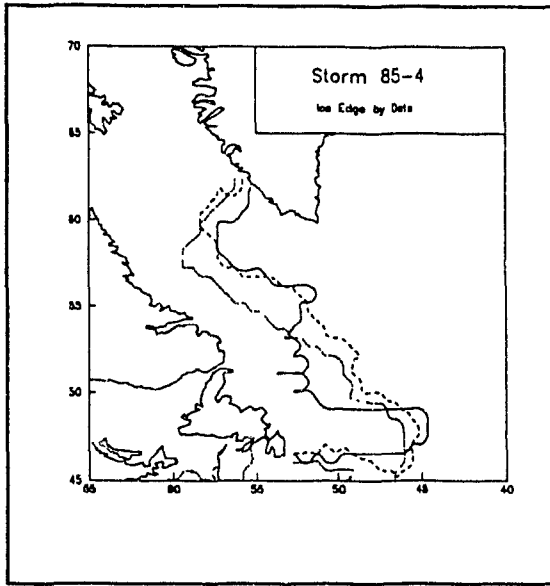
Storm 85-3

Minimum Pressure:	978.0 hPa
Pressure Range:	30.7 hPa
Storm Bearing:	101.0°T
Entry Latitude:	56.3°N
Entry Longitude:	62.0°W
Duration:	9 Obs

Ice Map/SMMR Dates:	02/25,02/27,03/01
---------------------	-------------------

Cells Increasing in Concentration:	29%
Cells Decreasing in Concentration:	15%



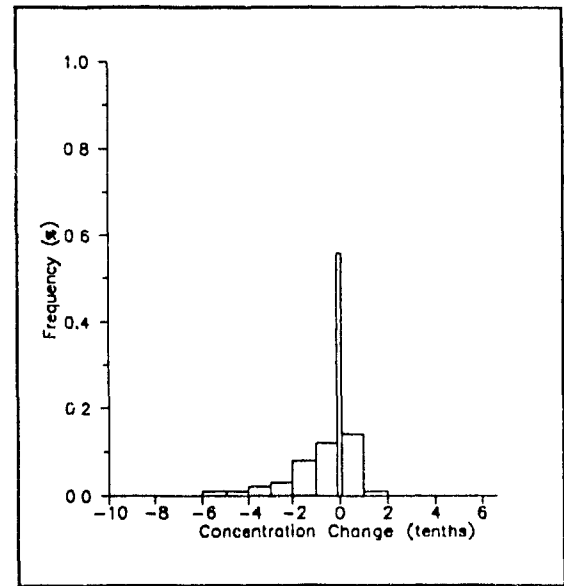
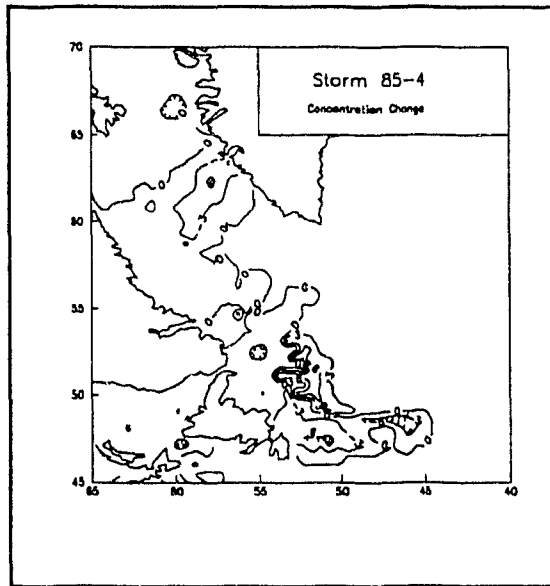


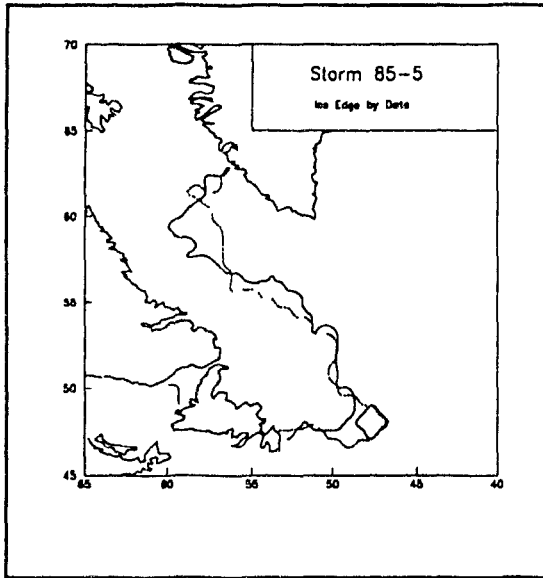
Storm 85-4

Minimum Pressure:	968.6 hPa
Pressure Range:	29.0 hPa
Storm Bearing:	65.0°T
Entry Latitude:	52.0°N
Entry Longitude:	62.5°W
Duration:	14 Obs

Ice Map/SMMR Dates:	03/13,03/15,03/17
---------------------	-------------------

Cells Increasing in Concentration:	16%
Cells Decreasing in Concentration:	28%



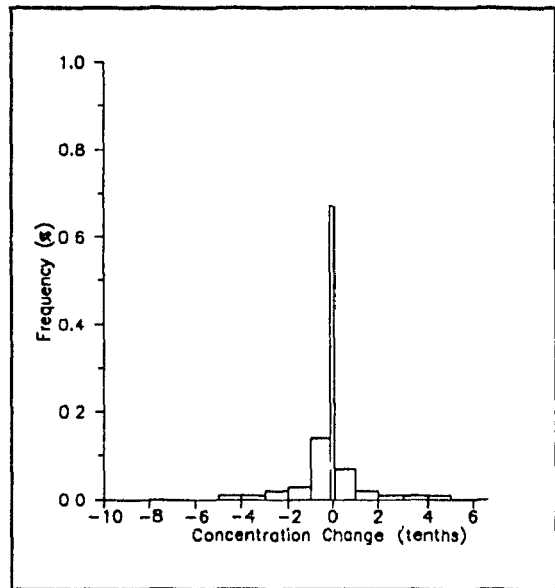
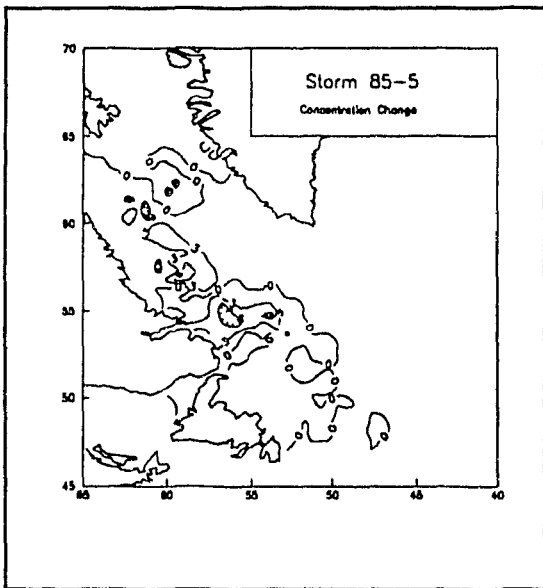


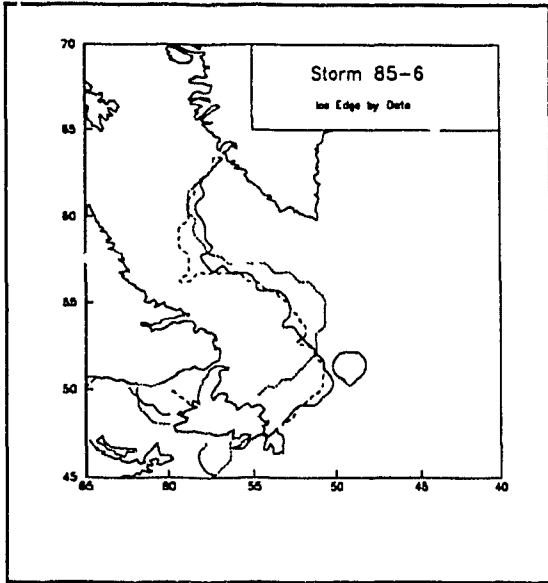
Storm 85-5

Minimum Pressure:	993.7 hPa
Pressure Range:	15.9 hPa
Storm Bearing:	214.0°T
Entry Latitude:	50.1°N
Entry Longitude:	40.4°W
Duration:	11 Obs

Ice Map/SMMR Dates:	04/20,04/24
---------------------	-------------

Cells Increasing in Concentration:	12%
Cells Decreasing in Concentration:	21%



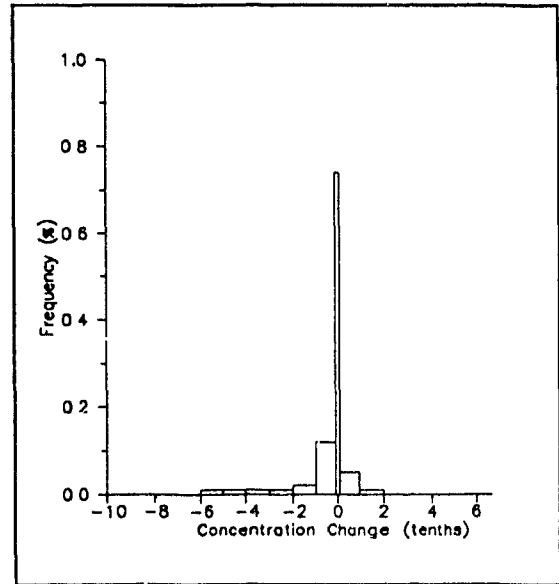
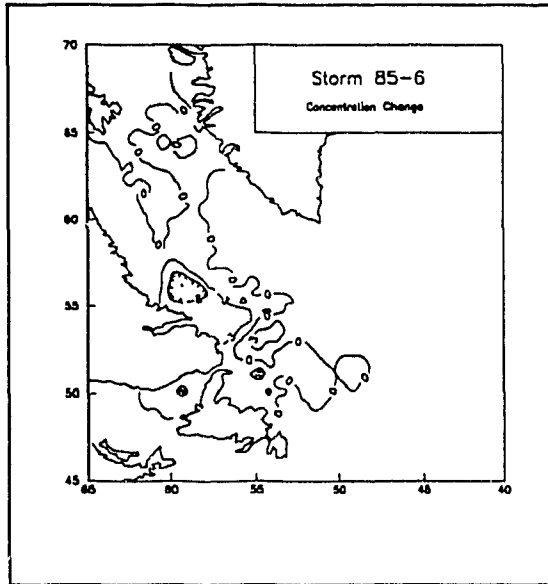


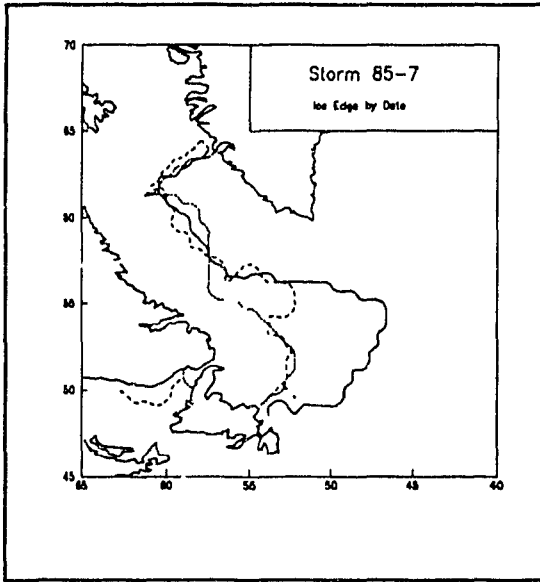
Storm 85-6

Minimum Pressure:	977.7 hPa
Pressure Range:	27.7 hPa
Storm Bearing:	53.0°T
Entry Latitude:	40.2°N
Entry Longitude:	66.5°W
Duration:	13 Obs

Ice Map/SMMR Dates:	05/02,05/04,05/06
---------------------	-------------------

Cells Increasing in Concentration:	6%
Cells Decreasing in Concentration:	18%



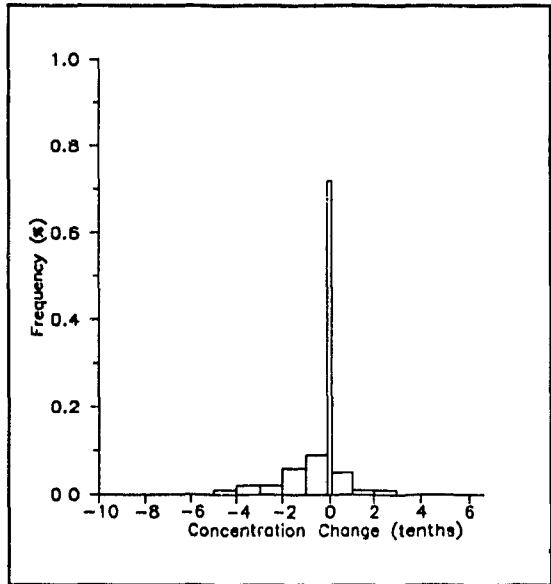
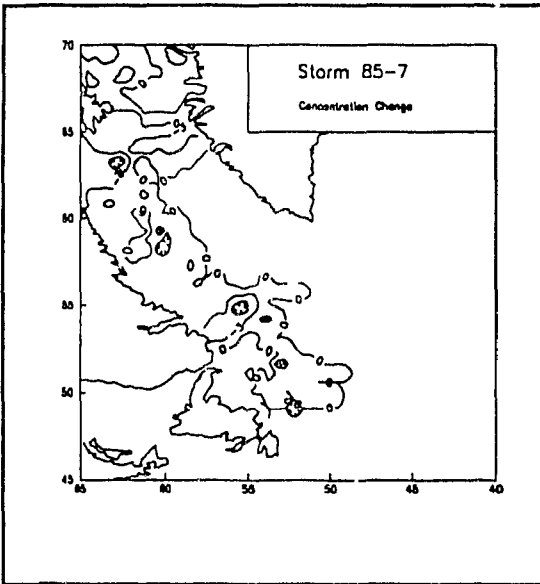


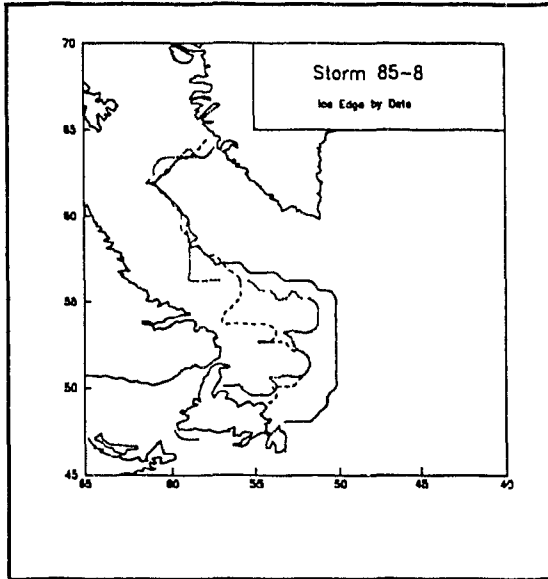
Storm 85-7

Minimum Pressure:	988.5 hPa
Pressure Range:	17.6 hPa
Storm Bearing:	52.0°T
Entry Latitude:	56.1°N
Entry Longitude:	66.1°W
Duration:	13 Obs

Ice Map/SMMR Dates:	06/01,06/03,06/05
---------------------	-------------------

Cells Increasing in Concentration:	7%
Cells Decreasing in Concentration:	20%



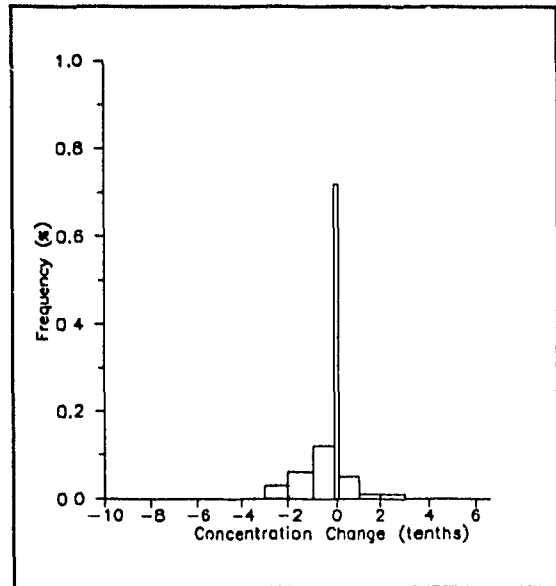
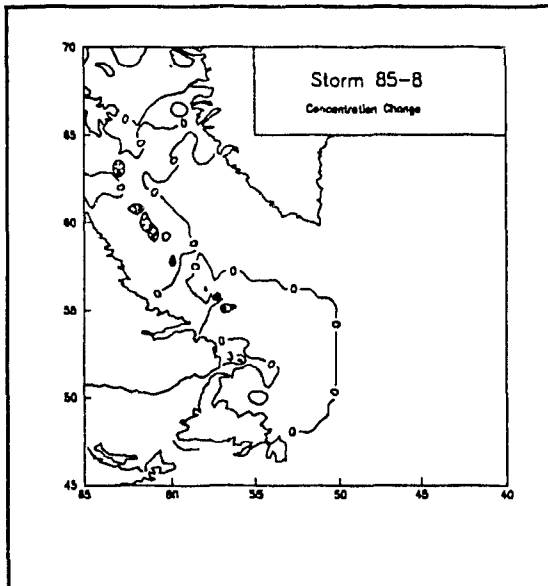


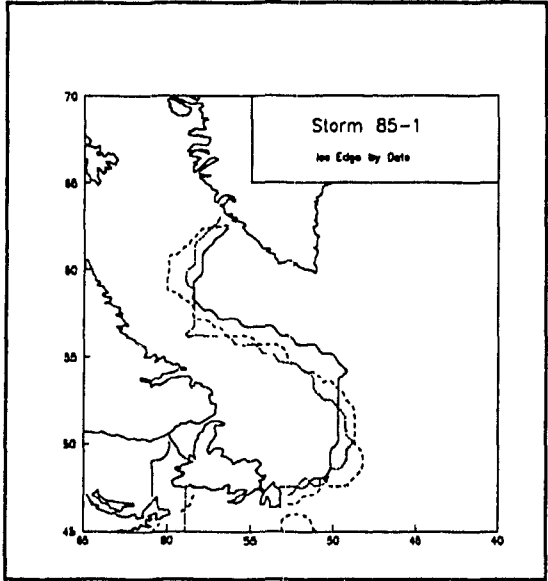
Storm 85-8

Minimum Pressure:	986.2 hPa
Pressure Range:	22.3 hPa
Storm Bearing:	62.0°T
Entry Latitude:	40.1°N
Entry Longitude:	69.8°W
Duration:	24 Obs

Ice Map/SMMR Dates:	06/07,06/09,06/11
---------------------	-------------------

Cells Increasing in Concentration:	7%
Cells Decreasing in Concentration:	21%



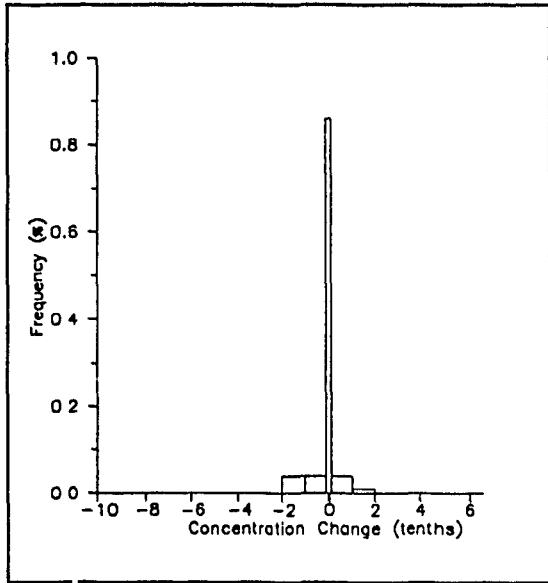
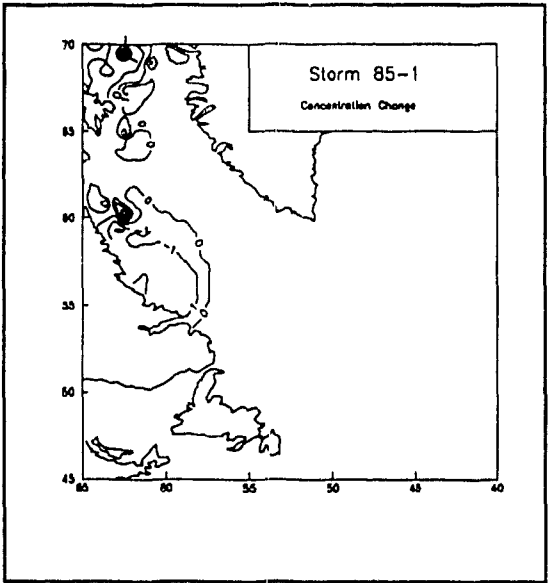


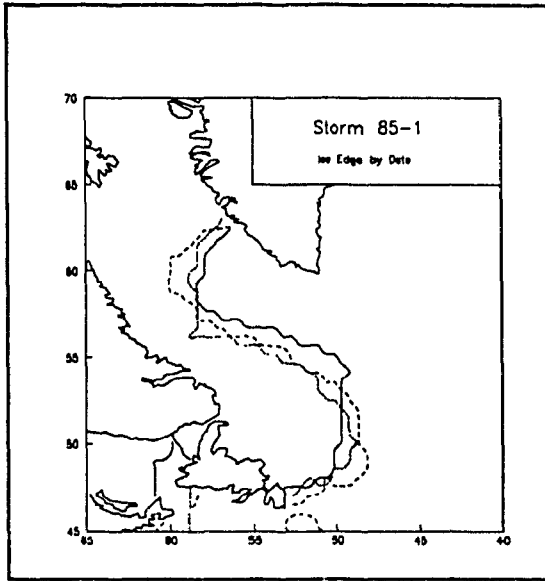
Storm 85-9

Minimum Pressure: 1003.5 hPa
 Pressure Range: 3.1 hPa
 Storm Bearing: 69.0°T
 Entry Latitude: 48.8°N
 Entry Longitude: 67.1°W
 Duration: 11 Obs

Ice Map/SMMR Dates: 07/07,07/09,07/11

Cells Increasing in Concentration: 5%
 Cells Decreasing in Concentration: 8%





Storm 85-10

Minimum Pressure:	992.2 hPa
Pressure Range:	6.5 hPa
Storm Bearing:	55.0°T
Entry Latitude:	52.3°N
Entry Longitude:	69.6°W
Duration:	12 Obs

Ice Map/SMMR Dates:	07/21,07/23,07/25
---------------------	-------------------

Cells Increasing in Concentration:	0%
Cells Decreasing in Concentration:	3%

